Mechanisms and conditions that affect phase inversion processes. A review.

Juan M. Maffi[1,2], Gregorio R. Meira[3], Diana A. Estenoz[3,4]

[1]Departamento de Ingeniería Química, Instituto Tecnológico de Buenos Aires (ITBA), Av. Madero 399, C.P. C1106ACD, Buenos Aires, Argentina.

[2]Consejo Nacional de Investigaciones Científicas y Técnicas (CONICET), Godoy Cruz 2290, C.P. C1425FQB, Buenos Aires, Argentina.

[3]Instituto de Desarrollo Tecnológico para la Industria Química, INTEC (Universidad Nacional del Litoral - CONICET), Güemes 3450, C.P. 3000, Santa Fe, Argentina.

[4]Facultad de Ingeniería Química, FIQ (Universidad Nacional del Litoral - CONICET), Santiago del Estero 2829, C.P. 3000, Santa Fe, Argentina.

Correspondence

Diana A. Estenoz

Instituto de Desarrollo Tecnológico para la Industria Química, INTEC (Universidad Nacional del Litoral - CONICET), Güemes 3450, C.P. 3000, Santa Fe, Argentina.

Facultad de Ingeniería Química, FIQ (Universidad Nacional del Litoral - CONICET), Santiago del Estero 2829, C.P. 3000, Santa Fe, Argentina.

Email: destenoz@santafe-conicet.gov.ar

Abstract

The phenomenon of phase inversion occurs in liquid-liquid dispersions found in a variety of chemical engineering fields. From simple oil-water mixtures to complex polymeric systems, the operating variables that affect this physical phenomenon are discussed in this work. The contribution on this matter by a large number of researchers is critically assessed, outlining both coherent and conflicting results. A detailed review of the mechanisms by which phase inversion takes place is also provided. While this subject has been studied for the past fifty years, this multivariate nonlinear process is

This article has been accepted for publication and undergone full peer review but has not been through the copyediting, typesetting, pagination and proofreading process which may lead to differences between this version and the Version of Record. Please cite this article as doi: 10.1002/cjce.23853

not yet comprehensively understood, and this review article aims to describe the conclusions so far reached to provide insight for future research.

KEYWORDS: phase inversion, multiple emulsions, dispersion, mixing

1 INTRODUCTION

Any physical system consisting of two immiscible phases subject to constant stirring will form a dispersion. That is, one phase will be suspended in the continuous medium of the other. Dispersions and emulsions are frequently used interchangeably, but they do refer to slightly different systems. In general, an emulsion requires the presence of a surface-active component that is usually soluble in one of the phases or locates itself at the interfaces so that it may interact with both simultaneously. If agitation is stopped, this agent will be able to stabilize the dispersed phase at a given particle size and a matrix/dispersed system will not be lost at a short time scale (it will eventually unmix, as it is kinetically but not thermodynamically stable). A dispersion, on the other hand, is usually used to refer to systems that will separate into two continuous phases immediately after stirring is ceased.[1]

Determining which phase will disperse in the other is not straightforward, since it is not always the one of which there is a smaller proportion. It depends on several interacting variables: physical properties (density, viscosity, interfacial tension), volume fraction, phase chemical composition, stirring speed, particle size and/or particle size distribution, and, in some cases, the geometry of the vessel where the dispersion is produced. This implies that, for any emulsion or dispersion, changing one or more variables may result in a phase inversion process, that is, a mechanism by which the continuous phase becomes the dispersed phase and vice versa.[2]

The phenomenon of phase inversion (PI) has been reported and studied over the past 70 years and holds a significant industrial importance in several fields, such as liquid-liquid extraction, heat control operations, polymeric reactors, micro and nano-emulsion manufacturing for controlled drug release and heavy oil transport in pipelines.[3,4] Yet, it is not a fully understood process and most of the published results are

phenomenological and qualitative, especially in polymeric systems, where PI is essential to guarantee a desired morphology (examples are from the renowned high-impact polystyrene (HIPS)[5] to blends like nylon 6-poly(methyl methacrylate)[6]). Few mathematical models exist that may predict phase inversion accurately in a given physical system.[4,7,8]

The goal of this review is to present the most important aspects that can explain the phase inversion phenomenon in stirred systems, from the effects of the operating variables to the suggested physical mechanisms and the associated mathematical models, both for traditional oil/water and polymer-polymer systems. The approach is based on the physical understanding of this complicated process and not specifically on its applications (which have been dealt with some years ago[9]) with the aim of encouraging future research that can produce a comprehensive model for its accurate prediction.

The paper is divided into three main sections. The first concerns the general aspects of the PI phenomenon and deals with the most important properties that are a part of it. The second discusses the physical mechanisms by which inversion may be achieved (with special emphasis on break-up and coalescence models) and the final section is about the formation of multiple emulsions (which are either a result of, or a prerequisite for, an inversion process).

2 GENERAL ASPECTS OF PHASE INVERSION

The phase inversion point usually refers to the volume fraction of a given phase above which it can no longer be dispersed.[10] Since this phenomenon was studied at first mainly for oil-in-water systems (or rather organic-in-aqueous), a large number of results were presented using the organic phase volume fraction, even when the aqueous phase is the dispersed one.

Increasing the dispersed volume fraction (φ_d) at a constant stirring speed may result firstly in a co-continuous system and eventually in a phase inversion point, above which the reversed system is obtained. This is especially the case of polymer blends and

mixtures.[11] Most O/W emulsions, conversely, do not present such a behavior and proceed to invert almost instantaneously when reaching a critical φ_d.[12] In both cases the PI is achieved by varying the phase volume ratios, which is known as a catastrophic inversion, due to a suggestion by Dickinson.[13] It is important to note that there are two ways of varying such volume ratios: in a gradual, dynamic way (adding dispersed phase aliquots to an existing mixture) or in separate steady-state batches. Some of the experiments conducted in the former way try to keep the total volume constant (by subtracting aliquots of the mixture) and others do not. Care should be taken when comparing results among different authors since they may refer to completely different scenarios. Comparing dynamic with steady-state experiments should also be done carefully since the effects present in the former may significantly differ from the ones present in the latter.[14] In this review, whose goal is to analyze the mechanisms by which PI occurs, both type of inversions will be presented and discussed.

If surfactants are present in the system, there exists a different way to induce phase inversion that does not involve changing the volume fraction of the dispersed phase: it consists of modifying the affinity of the surface-active component for each phase. The idea behind this type of inversion is based on Bancroft's rule, which suggests that the continuous phase is the one in which the surface-active component is more soluble. Then, a given emulsified dispersion would prefer a certain morphology according to the affinity of its emulsifier; if changed, this affinity would induce a transition to a non-preferred morphology, which is why this type of PI is named transitional.[15]

Phase inversion also occurs in systems other than O/W or W/O. Polymeric (oil-in-oil or water-in-oil) emulsions also present this phenomenon, and some work has been developed to address it.[11,16–18] The physics that govern its dynamics are equivalent to those of traditional aqueous-organic systems.

2.1. The ambivalent range

In any emulsion there is a range of volume fractions for which either one of the two phases may be dispersed and stable,[10] depending on how the mixture is prepared or

initiated. This is known as the ambivalent range, and much work has been developed to predict its limits, ie, the highest φ_d for each phase that may be obtained before inversion. This hysteresis effect is characteristic of all emulsions reported in literature.

Figure 1 shows typical ambivalence ranges, plotting the organic (or dispersed, depending on the author) volume fraction at the threshold of phase inversion as a function of stirring speed. Zone A is identified with oil-continuous systems, zone B with water-continuous, while zone C represents the operating conditions where either phase may be the dispersed one depending on how the process was started. While being the most widely spread range, authors like McClarey and Mansoori[19] have also found an intermediate inversion curve by preparing mixtures in a very specific manner. In general, the limits and span of this ambivalent range are influenced by the size, shape and material of the vessel, physical fluid properties (density and viscosity), stirring speed and interfacial tension.[20] These variables are discussed in the following sections.

2.1.1. Viscosity ratio

One of the most important variables that greatly influence the PI point is the viscosity of each phase. A general rule found by several researchers states that the tendency to remain as the dispersed phase increases with viscosity.[4,10,22–24] This is probably explained by the attenuation of coalescence probability with increasing viscosity.[25] Coalescence and break-up of dispersed particles are crucial aspects in determining the phase inversion hold-up and will be discussed in more detail in Section 3.4.

As an example, Figure 2 plotted with the data in Selker and Sleicher[10] shows how much more difficult (higher φ_d) it is for a given phase to become continuous as its viscosity increases. In most cases the absolute value of phase viscosity is not as important as the ratio of phase viscosities $r = \frac{\eta_d}{\eta_c}$ since this addresses the difference in viscous stresses developed at the interface, which represent interface mobility under a given shear condition and thus impact the inversion process directly.

By applying momentum balances to a planar interphase of two immiscible liquids, Yeh et al[22] suggested one of the first phase fraction relationships at the PI point:

$$\frac{\phi_d}{1-\phi_d} = \sqrt{\frac{\eta_d}{\eta_c}} \quad (1)$$

Yet, they specified that a more accurate relation would require finding the exact plane near the interface at which shear would occur. Given a difference in surface tensions in each phase, the shear plane would shift towards the interface and a correction was suggested to replace the viscosity of the phase of higher σ by the viscosity at the interface. For example, if the continuous phase has a stronger surface tension than the disperse one, then Equation (1) would turn into the following:

$$\frac{\phi_d}{1-\phi_d} = \sqrt{\frac{\eta_d}{\eta_{int}}} \quad (2)$$

Note that the dependence of φ_d with r in Equation (1) reproduces satisfactorily the shape of the upper limit of the ambivalent range in Figure 2 but predicts an equivolume inversion for phases with equal viscosity. This is not always the case, as observed, for example, in data from Selker and Sleicher, who informed an equivolume inversion for a mixture with a viscosity ratio of 2 (although their experiments do not keep total volume constant and are thus not directly comparable). On this same line, McClarey and Mansoori[19] prepared a mixture with equal phase viscosity and noted not the upper nor the lower but the intermediate inversion boundary was located at the equivolume conditions for all stirring speeds. This suggests that in the absence of phase viscosity difference, other effects play a part in determining the maximum dispersed volume fraction of a given system. Early authors had ruled out interfacial tension, but later work proved that it may be of considerable importance as it is discussed in Section 2.1.4.[10,19]

In a theoretical investigation, Yeo et al[23] found similar results with binary systems; yet, they suggested that surfactant-coated interfaces in systems with $r < 1$ may suppress the viscosity ratio effect on phase inversion due to Marangoni stresses. In the absence of viscous effects, all emulsions with low viscosity ratios and sufficiently laden interfaces

would invert almost at equal phase volumes. For higher values of r, the authors predict similar trends to other researchers.[10,22]

In polymeric systems, in which viscosity depends on the molecular weight distribution of each species, several phase volume and viscosity ratio relations have been suggested at the inversion point, or at least at the beginning of co-continuity. In such systems it is common to observe a co-continuous transition before phase inversion takes place.[26] In polymer blends (ie, not in the presence of monomer or solvent and in a non-reactive system) at low shear rate, the work by Jordhamo et al[11] suggests the following relationship for predicting the onset of a co-continuous system:

$$\frac{\phi_d}{1-\phi_d} = \frac{\eta_d}{\eta_c} \tag{3}$$

This expression has been evaluated successfully in some polymeric two-phase systems with a minimum grafting extent (polyester-urethane/polystyrene, polyamide/polypropylene, polystyrene/polybutadiene) under low shear conditions, but has failed to produce accurate results in other blends, such as the propylene/ethylene-propylene rubber and the polystyrene/styrene-butadiene rubber prepared by Ho et al[27] at higher torques. These authors suggested a modified version of Jordhamo's equation for a better fit of their results:

$$\frac{\phi_d}{1-\phi_d} = 1.22\left(\frac{\tau_d}{\tau_c}\right)^{0.29} \tag{4}$$

Note that stress ratio is preferred to viscosity, but the physical meaning still holds. The 0.29-0.3 power of the viscosity ratio has also been suggested by Chen and Su,[28] Kitayama et al[29] and Everaert et al.[30]

Miles and Zurek[26] have found good results using Jordhamo's expression, but only when evaluated at the in situ shear rate when preparing the blend. Other researchers, such as Arirachakaran et al,[31] working on other systems (such as transport pipelines), have found logarithmic dependences on the viscosity ratio. A summary of available models to calculate the PI point from viscosity ratio is shown in Table 1 and compared

in Figure 3. Some of them are empirical correlations and others are theoretical derivations or simplifications from emulsion rheological models.

Whether in polymer blends or in O/W systems, the phases that were used in the validation of these expressions consisted essentially of pure, immiscible compounds. They have not been investigated under the presence of a third substance that is miscible with both phases simultaneously, as could be the case of a solvent or of a reacting monomer in a heterogenous polymerization.

There seem to be two distinct families of curves: a log-linear and a sigmoidal type. Near the isoviscous point, all curves predict inversion points near the equivolume scenario. However, it does not seem appropriate to plot the experimental points on top of this figure, since each point is usually produced varying not only the viscosity ratio, but also (inevitably) one or more other properties that might affect the inversion process. Moreover, the inversion point as per these equations is independent of which phase is dispersed and which continuous, a fact that would yield a symmetric ambivalence range, and experimental findings have shown that this is not the case.[10] Thus, these models should be used carefully or coupled with extra terms that take into account the effect of other variables.

2.1.2. Stirring speed

For continually stirred batch vessels, agitation speed presents different effects depending on the mixture. A large number of systems are reported in literature and have been studied for several decades. Yet, it is troublesome to compare results from different authors due to the difference between the operating variables. Increasing agitation favors phase inversion (meaning that it occurs at lower values of φ_d) in many dispersions inverting from O/W to W/O, while delays it in the opposite case. However, there are several exceptions too.[35] Besides, not all organic phases present the same physical properties. In some cases, if the dispersed phase is less viscous than the continuous one, agitation helps phase inversion. However, then again, this does not hold

for all systems. Kumar[12] suggested an explanation for these discrepancies based on electrostatic repulsion forces driven by a difference in dielectric constants.

A general trend that is satisfied by all dispersions is the asymptotic value of phase volume fraction at the inversion point with increasing stirring speed. This was first observed by Quinn and Sigloh[2] and further shown in other experiments in both batch and flow vessels.[19,36–40] They suggest the following dependence with power input (W_P):

$$\phi_d = \phi_0 + \frac{k}{W_P} \tag{5}$$

where k is a constant that only depends on system properties and W_P, the power input, which may be related to the agitator speed N, in a stirred baffle tank of diameter D and power number N_p, by:

$$W_P = N_p \rho_c N^3 D^5 \tag{6}$$

The power number is a function of the Reynolds number and is characteristic of a given vessel.

This asymptotic behavior suggests that in extremely turbulent conditions there is a controlling mechanism that allows PI to take place only at a given phase fraction.

2.1.3. Phase density difference

Few studies aiming to determine the impact of the phase density difference have been developed. Some authors argue that it plays a minor role in phase inversion and it is only important at low stirring speeds, when large density differences make dispersions more difficult to achieve (ie, require higher energy inputs).[10,19,20] Some other researchers suggest that a large density difference favor phase inversion because it increases local relative velocity and, therefore, the shear stress to which the system is subject.[36,41] This, in turn, promotes droplet breakage and interfacial area is substantially increased. However, enhanced breakage is not necessarily a promoter of

phase inversion. Yeo et al[42] observed that the tendency to invert was indeed increased at higher density differences if the dispersed phase was organic but found the contrary in the opposite case.

Phase density may also affect the inversion characteristics of a system through wettability effects. For a dispersed phase to become in contact with an impeller blade, it must hold a larger density than the continuous phase.[43] Only then the droplets may reach the impeller by inertial impaction and form a thin film at its surface (rather than staying as a drop). This changes the breakage processes near the impeller region and can alter the critical φ_d for that phase.

2.1.4. Interfacial tension

At the interface of two immiscible liquids the difference in surface tension yields a stress known as interfacial tension. Surface and interfacial tension are sometimes mistaken as equal, and many empirical correlations are expressed in terms of the former, while physical evidence suggests that it is the latter that exerts a greater effect on the inversion characteristics of a given dispersion.

Particularly in oil/water and oil/water/surfactant systems (the case of emulsions), there have been reports, since the original research by Cayias et al,[44] that there exists a given composition or formulation that yields markedly low interfacial tensions. As an example, Figure 4 shows the case for a 0.2 wt% aqueous solution of Witco 10-80 petroleum sulfonate (and 1 wt% NaCl) with different organic phases. Interfacial tension reaches a minimum with n-heptane. In the emulsion world, this behavior gave rise to the so called optimum formulations,[45] in which the surfactant or surfactant mixture is chosen in both structure and concentration to provide such ultra-low tension values (of utmost interest in the enhanced oil recovery processes).

A similar trend has been reported when varying salinity[47] or temperature.[48–51] In the latter case, probably the most renowned, there exists a critical temperature at which interfacial tension reaches a low minimal value and usually occurs sharply in a range of

0.1ºC-2ºC depending on the surfactant.[49] This aspect is further discussed in Section 2.2.

Effect on phase inversion

It is generally assumed that interfacial tension is a symmetric property, in the sense that an O/W dispersion bears the same interfacial tension than a W/O. This would lead to the conclusion that for a system with phases of equal physical properties, PI occurs at the same volume fraction for both phases at a given stirring speed. This is not, unfortunately, the usual case as other factors must be considered (see Section 4.1).

Few studies have been published that aim to isolate the effect of interfacial tension on the phase inversion holdup. According to Clarke and Sawistowski,[52] and Kumar et al,[36] a system with lower interfacial tension should be less likely to invert. The span of the ambivalent region should be therefore wider. However, results by Reeve and Godfrey[38] challenge that idea. They prepared two O/W dispersions almost identical in viscosity ratio and density but with a 50% difference in interfacial tension. Their results indicate that the system with lower γ finds it easier to invert from O/W to W/O but harder in the opposite direction. The work by Norato et al[20] seems to support these findings but their systems presented a 25% disparity in phase density difference, and their batches were not performed under constant volume conditions. The theoretical model derived by Hu et al,[4] based on a population balance in a two-region vessel, agrees with those results.

If interfacial tension is associated with stress due to incompatibility, a minimization of free surface energy could be expected at the PI point. This would reflect the natural need of the system to invert. However, by measuring interfacial area, Clarke and Sawistowski[52] and Luhning and Sawistowski[53] found that a minimization of the interfacial energy happened only when inverting from W/O to O/W but not in the opposite case. Consequently, they postulate that phase energy minimization is not a criterion for phase inversion. Norato et al[20] suggests that the lowering of γ would

promote drop breakage and increase film drainage times (see Section 3.4.1), which would diminish coalescence rates and thus hinder phase inversion.

It would seem that the lowering of interfacial tension produces two opposing effects that may either delay or promote PI, depending on the emulsion type. On the one hand, the compatibility enhancement would favor the transition to the inverted system; on the other hand, the increase in particle breakage rate may stabilize the configuration and delay the inversion.

2.1.5. Geometry and vessel material

It has long been reported that the way agitation is started may affect phase inversion.[41] Researchers have reported a wide variety of, sometimes opposing, results regarding impeller design, impeller height and position, stirring speed, and vessel geometry[1,2,10,20,38,40,52,54]. For example, if the impeller is equipped with baffles, the ambivalent range widens. A given impeller type may promote PI of O/W but delay it for W/O dispersions. The impeller-to-vessel diameter ratio also presents different results on either limit: increasing the ratio may promote or delay PI, or not have a consequential effect at all. For this reason, results from different authors are sometimes difficult to analyze quantitatively. A thorough research on this subject was conducted recently by Deshpande and Kumar.[40]

In the case of the PI during the polymerization of styrene in the presence of polybutadiene (HIPS manufacturing process), Freeguard and Karmarkar[55] have outlined several criteria that should be examined when designing the agitation system.

Finally, the material of the vessel (and/or impeller) has been found to have an effect on PI due to wettability effects.[36]

2.2. Effect of surface-active components on phase inversion dynamics

In emulsified dispersions, surface active species are commonly found at the interface between the dispersed and the continuous phases. This is usually because these species

are somewhat miscible in both phases. In O/W (or W/O) emulsions, the emulsifiers usually present a hydrophilic head and a lipophilic tail, and thus making the O/W interface a suitable place for the surfactant to accumulate. Traditionally, these molecules contain a carbon chain long enough to be the oil-soluble part. However, in recent years, the use of polymers as surface-active components has increased significantly,[56–61] since their structure can be tailored to provide a target amphiphilicity.

The extent to which an emulsifier is hydrophilic and lipophilic is represented in the hydrophilic-lipophilic balance or HLB, and its effect on phase inversion is well discussed by several researchers.[23,62–66]

The role of emulsifiers in PI processes seems critical. Merely changing the affinity of an emulsifier for a given phase may lead to a phase inversion. Salager et al[67] suggested that phase behavior could be represented in a parameter coined Surfactant Affinity Difference (SAD) (a function of temperature, HLB, oil type, and salt concentration) whose value indicates the structure of the emulsion, which may be related to the Winsor classification. Modifying the SAD value for a given system may lead to an inversion process. By definition, SAD is the difference between the standard chemical potential of the surfactant in the aqueous and organic phases. Thus, positive SAD values yield W/O emulsions and the opposite is negative, provided that there is enough volume so that the continuous phase is the expected phase. The limiting case of SAD = 0 represents an unstable system that will undergo PI and is associated with an ultralow interfacial tension value.[68] A similar parameter is the hydrophilic-lipophilic deviation from the optimum formulation (HLD) and is qualitatively used as equivalent to the SAD, although Salager et al[69] have pointed out that their relationship is actually given by Equation (7) and depends on a reference state:

$$\frac{SAD}{RT} = HLD - \ln(K_{ref}) \tag{7}$$

The available calculation methods for HLD are only restricted to flexible interfacial films.[70] As an example, Figure 5 shows an inversion map for cyclohexane-water

emulsions using nonylphenol ethoxylates (NPE) as surfactants, taken from Brooks and Richmond.[62] These emulsifiers, of the form of an aromatic-organic head and a polyoxyethylene tail, may bare different HLB values depending on the length of their ethoxide chains.

In their work, these authors modified the SAD parameter by changing the HLB of the emulsifier at constant concentration (and temperature). The regions in the map show the emulsion structure (for example, W/Om denotes a Winsor II emulsion with surfactant-water micelles dispersed in an organic continuous phase) and their transition boundaries.

In a more recent work, developed by Acosta[71] and continued by others,[72] the phase inversion map for O/W/surfactant systems can be predicted by an equation of state linking the HLD with the equivalent alkane carbon number (EACN) of the surfactant, and the net-average curvature (NAC) of the interphase. This physical model can describe quite accurately the structure of O/W or W/O emulsions as a function of surfactant concentration, surfactant type and medium salinity.

Transitional inversion may also be achieved by only changing temperature, or pH if the surfactant is ionic and may be hydrolyzed (for example following Maestro et al[73]). This changes the surfactant solubility on either phase, modifies the interfacial curvature, and may induce a spontaneous inversion at a critical temperature, known as the phase inversion temperature (PIT). Some examples of this inversion type can be found in the works by Shinoda and Arai,[74] Shinoda and Saito,[75,76] Shinoda and Takeda,[77] Parkinson and Sherman,[78] Dokic and Sherman[79] and Rao and McClements.[80] Figure 6 shows a qualitative evolution of interfacial tension as temperature varies. The structural changes at the interface induce a spontaneous inversion to the reverse emulsion type, a concept that was endorsed by Kabalnov and Wennerström.[81] Usually, at temperatures below the PIT, the aqueous phase is continuous since the effect of the hydrophilic heads is stronger. For example, for ethoxylated non-ionic surfactants,

dehydration of the ethoxide chains is greater at higher temperatures, which results in an increase in the molecule's hydrophobicity.[70]

Shinoda and Saito[75] assembled the PIT equivalent of the inversion map of Figure 5, and it is included here for illustration purposes (Figure 7).

Emulsification by the PIT method has been largely used in traditional O/W systems but can also be employed as a polymerization route to produce materials of the micro- and even the nano scale (see, for example, a recent work by Boscán et al[83]).

The fact that inversion may occur by altering chemical affinity (through temperature, emulsifier structure or pH) sets the basis for a thermodynamic approach on phase inversion phenomena. It is no surprise then that several models aiming to predict PI points have been proposed on phase equilibria and energy-minimization grounds, even for catastrophic inversions.[4,22,84,85] However, dynamic effects should also be considered since the break-up and coalescence effects may change even with the emulsion preparation method.[14]

The main physical action of an emulsifier is to stabilize the dispersion, reducing its interfacial tension: by adsorbing at the interfaces, the contact surface between polar and non-polar phases is reduced/avoided. Interfacial stresses are diminished because emulsifiers share structural properties with each separate phase, and thus alleviate incompatibility forces. This effect is well known to be asymptotical with surfactant's concentration,[86–88] which is why they are only used in small amounts. Given that surfactants are usually found in the form of micelles, the highest concentration after which γ reduction is insignificant is known as the critical micelle concentration (CMC).[89]

Figure 8 shows, as an example, the interfacial tension reduction of the toluene-water system for different concentrations of sodium dodecyl sulfate (SDS) at several temperatures.[90]

Whether surfactants promote or delay phase inversion is still a matter of discussion and experimental results show different tendencies depending on the emulsifier type. On the one hand, the interfacial tension reduction would produce a more stable system, which would imply higher dispersed phase fractions to force PI. On the other hand, if the emulsifier is more soluble in the dispersed phase, an increase in concentration may favor coalescence (in an effort to balance out the surfactant's presence) and thus promote PI.

Figures 9 and 10, taken from Becher,[65] show the effect of increasing emulsifier concentration on the PI point of mineral oil-water systems. For O/W systems inverting to W/O, the use of different Spans (sorbitan esters) favored the inversion as their concentration was raised. Since these emulsifiers are oil-soluble, they seem to favor a W/O structure. In the case of water-dispersed systems, the use of Tweens (ethoxylated sorbitan esters) also seem to favor inversion as concentration is increased (although tendency is not always monotonical).

These results would indicate that increasing surfactant concentration favors PI. However, if the incorrect emulsifier is used (for instance reversing Tween and Span in Becher's experiments), the opposite trend might be found. Groeneweg et al[92] showed how increasing the concentration of an oil-soluble emulsifier (a monoglyceride) delayed PI of a water-in-triglyceride oil system.

These two sets of results would seem, at first sight, to be opposing (emulsifier promotes versus emulsifier delays PI). However, they may actually refer to the same stabilization versus compatibilization effects; the chemical structure of each surfactant favors a given emulsion structure, which may serve to either stabilize the dispersed phase or to promote an inversion, depending on which phase is the dispersed one. Then, aiming to draw absolute conclusions about the effect of the surfactant concentration on the PI point seems worthless if not coupled with a view of its chemical structure. However, if the aim is to produce a target type of emulsion, optimization of the formulation recipe may be achieved and has already been reported for ionic and non-ionic surfactants.[93,94]

These previous considerations hold the following underlying assumption: surfactants adsorb at the interface in a homogeneous way. When analyzed from a dynamic point of view this is not always the case, since surfactants may gather irregularly around a dispersed drop, thus producing a concentration gradient throughout the interface. This, in turn, generates an interfacial tension gradient and a balancing force appears to counteract this difference: a dynamic known as the Marangoni effect.[52,95] These forces may have a significant impact in the coalescence processes (see Section 3.4.1) and may substantially affect PI. A summary of the current emulsification techniques through phase inversion mechanisms (catastrophic and transitional) can be found in Kumar et al,[96] who also included the effect of solid surfactant particles (Pickering emulsions) which have been left out of this review.

Yeo et al[42] established a theoretical model that predicts a high coalescence suppression at low viscosity ratios when considering the Marangoni effect in emulsified dispersions. They show that PI occurs almost at a constant φ_d if interfaces are sufficiently laden with surfactants and $\eta_w \ll \eta_o$.

In polymer-polymer dispersions, copolymers are usually the surface-active species, since they show the same partial compatibility effect than the O/W emulsifiers. The similarity between their respective interfacial roles can help to better understand the effect that copolymers exert on PI.

Not as many examples as in O/W systems may be found in the literature; however, a few experiments on polymer blends show evidence that the presence of copolymers modify (to a greater or lesser extent) the inversion holdup, which in most cases represents the onset of the co-continuous transition. Relevant examples are those by Deng and Thomas,[97] Adedeji et al,[98] Charoensirisomboon et al,[99] Kitayama et al,[29] Zhang et al,[100] Dedecker and Groenickx,[6] Épinat et al,[101] and Bourry and Favis,[102] among others. In polymer-polymer solutions, there are articles by Díaz de Leon et al,[103] Soto et al,[104] and Fischer and Hellmann[105] on the PS-St-PB system.

If the copolymer's role is comparable to that of a traditional emulsifier/surfactant, then it would seem natural to study the effect of its structure and average molecular weight on the phase inversion dynamics, as it would appear to be the polymer equivalent of the HLB parameter in O/W emulsions. However, no advances have been reported on this matter so far, to the authors' knowledge.

The copolymers' role in the PI mechanism is further discussed in Section 4.

2.3. Emulsion rheology and phase inversion

Empirical phase inversion detection is usually achieved by monitoring a physical property that suffers a sudden change at the PI point. It is the widespread case of electrical conductivity in O/W systems. However, it is not the only one; dispersion or emulsion viscosity may also change dramatically during the inversion process.

Unlike most emulsion properties, which are in fact the continuous phase properties, emulsion viscosity is always higher than the continuous phase viscosity. This is due to the drop-drop interactions that take place when the mixture is subject to shear. Van der Waal's attractive forces become significant when drops move past each other, which is the case in any conventional rheometer. These interactions generate extra stresses that reflect on an increase in the mixture viscosity. Then, the presence of a dispersed phase always makes the emulsion more viscous.

From Einstein's theory for dilute dispersions to Mooney's equation and fractal theory, a large number of models have been suggested to explain the rheological measurements in dispersed systems. There is common ground between all these equations:

- The higher the volume fraction of the dispersed phase, the higher the emulsion viscosity.[106]
- For a given dispersed phase fraction, an increase in mean particle size results in a lower emulsion viscosity if drops are considered soft (deformable).[107] There is no particle size effect on dispersion rheology if the dispersed phase consists of hard spheres.[108]

- A widening of particle size distribution results in a reduction of the system's viscosity.[109]
- In non-dilute dispersions, a higher phase viscosity ratio ($r = \frac{\eta_d}{\eta_c}$) may result in an increase of mixture viscosity.[110]
- If either phase exhibits non-Newtonian behavior, the overall dispersion is non-Newtonian.[111]. Yet, traditional Newtonian oil-water emulsions may exhibit non-Newtonian behavior at high dispersed phase fractions.[107]
- Electrostatic forces, driven by surface charges or difference in dielectric constants, contribute to increase overall viscosity.[112]

According the available correlations, dispersion viscosity should change at the PI point since a system with a high concentration of dispersed phase is turned into one with low concentration. If inversion takes place without a co-continuous transition, then an abrupt change should be registered.[91] If a co-continuous system serves as transition from one dispersion type to the other, then the evolution of the mixture viscosity should follow a smooth transformation. This is the case of most polymeric systems, like the styrene-polystyrene-polybutadiene immiscible mixture in the manufacturing process of high-impact polystyrene (HIPS).[113] An example is shown in Figure 12, taken from the work by Freeguard and Karmarkar[114] on the HIPS bulk synthesis.

Other rheological properties also undergo similar changes at the phase inversion point. For example, Omonov et al[115] measured the storage modulus (E') and the loss factor ($\tan(\delta)$) in immiscible polypropylene-polystyrene blends with equal phase viscosity, as shown in Figure 13.

In this sense, viscosity alone is not a factor contributing to cause phase inversion; however, it serves to identify it. Then, modelling its evolution holds a significant interest as it may serve to predict this critical point.

3 THE PI MECHANISM

The physical mechanisms by which a dispersed phase may become the continuous phase are still under discussion. At least two significant approaches are found in the literature, as discussed in the following.

3.1. Coalescence versus break-up imbalance

The idea behind this mechanism is that, under constant stirring, dispersed droplets may coalesce between each other but also be broken up by different external forces. If a given volume of dispersed phase is added to a continually stirred, stable dispersion, coalescence between the dispersed elements will readily occur, forming larger droplets. This, in turn, will enhance the breakage frequency, and this coalescence-break up processes will lead to a new steady state for the increased φ_d. However, there will be a critical dispersed volume fraction at which the coalescence of large drops will occur at a much faster rate than that needed for external forces to break up those larger particles. At that point, droplets will change shape from spherical to cylindrical, lamellar, and ultimately other complex structures, trapping (in some cases) the continuous phase in the process. It is this imbalance between break-up and coalescence that makes PI possible. In non-stirred systems, the works by Bremond et al,[116] Kumar et al,[117] and Deblais et al[118] have demonstrated, in different applications, that enhanced coalescence is also the mechanism that causes phase inversion.

Research on this line has been conducted by Arashmid and Jeffreys,[21] Bouchama et al,[14] Groeneweg et al,[92] Hu et al,[4,119] and Liu et al,[37] among others, all focusing in traditional O/W dispersions. In polymeric systems, especially in the case of polymer compounding and blending, this is also the commonly suggested mechanisms as seen in the works by Shih,[120] Mekhilef and Verhoogt,[8] Sundararaj et al,[121] and Kitayama et al.[29] An example of this mechanism in polymer-aqueous emulsions is presented in Zerfa et al.[122]

As explained previously, the PI point may strongly depend on the emulsification method (gradually adding dispersed phase to a mixture is essentially different from stirring a predefined volume of two separate phases). On this matter, Bouchama et al[14]

compared a direct emulsification, in which organic and aqueous phases are mixed together at different phase ratios, with a wash-out method, by which dispersed phase is discretely added to the continuous phase until PI occurs. Their experiments, in which PI points were observed by conductivity measurements, are here reproduced in Figure 14 and show that the direct method produces a much earlier inversion than the wash-out route. Their explanation lies in a difference in the coalescence and break-up rates between each scenario, particularly affected by the formation of multiple emulsions in the direct emulsification case (see Section 4 for further details). It is important to note that most of the empirical evidence found in literature deal with either one of the two methods, and this is one of the few works that have reported the difference between each method for the same physical system.

3.2. Energy minimization

This thermodynamic approach considers that the total system energy, that is, the sum of its internal, kinetic, and surface energies, should find a minimum value at the inversion point. It originally finds its physical bases in the remarks by Luhning and Sawisotwski,[53] who consider that PI is a spontaneous process and must consequently be accompanied by a total energy decrease. Counterintuitively, they have also observed partial inversions and re-inversions in the moments prior to the PI point, as if the system needed to attain a certain energy level in order to invert. This would indicate that there exist local energy minima prior to the PI point that should not be considered as a criterion for inversion; it would rather be the minimization after inversion.

These authors have also shown that interfacial area (and thus, interfacial energy) may either increase or decrease after inversion, in contrast with the findings of Fakhr-Din,[123] who observed that it only decreases. This implies that surface energy minimization may not be a valid criterion for inversion.

In recent years, most models seeking to predict the PI point are based on a minimal total energy dissipation rather than just interfacial energy.[85] Nonetheless, Yeo et al,[42] on a

theoretical model, suggested that minimization of interfacial energy could be used as PI criterion because kinetic energy variations would be negligible compared to that of the interface. In two-phase pipe flows, Brauner and Ullmann[124] suggest an equalization of the surface energy of each phase as a criterion for PI, an idea also used in mixers by Tidhar et al.[39] This mechanism has not been suggested, at least to the authors' knowledge, for polymeric emulsions or blends undergoing PI.

In line with this energy minimization approach, some authors have suggested that it is the mechanical properties of the interphase that must play the key role in the PI process and suggested a hole nucleation model to represent the idea that continuous phase becomes entrapped at the moment of inversion.[81,125]

3.3. Interfacial zero shear

The approach in this case is to study the interface and all the acting stresses. It was postulated by Yeh et al[22] that, at the PI point, the shear stresses would balance out and the dispersed phase would overcome the continuous one. It is the dynamic forces that play a major role in this approach, which cannot unfortunately predict the hysteresis effect and, therefore, the ambivalent range.

3.4. Drop breakage and coalescence processes in liquid-liquid dispersions

While there are different approaches for identifying the PI point, a combination of the first two presented in the previous section is possibly the closest to the real one. It is thus of interest to incorporate into this review the coalescence and break-up mechanisms (as described in the literature), with the goal of presenting the most important concepts, variables, and models that arise from their study.

In the past few years, several attempts have been made to deepen the understanding of break-up and coalescence phenomena by combining computational fluid dynamics (CFD) and population balance models (PBM).[126–133] In these works, the spatial dependencies of the break-up and coalescence rates are incorporated by simulating the geometry in question with a proper mesh and solving the equations with a finite

elements method or similar. This methodology results in a greater physical accuracy but demands higher computational costs. An interesting trade-off has been recently developed by Castellano et al,[133] who solved the space-dependent equations through a probability density function of the energy dissipation rate, thus avoiding the need of a CFD computation.

3.4.1. Coalescence

Coalescence kinetics were first described by von Smoluchowski[134] and later continued by Lawrence and Mills.[135] Their work was based on the trajectories of drops and neglected particle-particle hydrodynamic interactions. They distinguished two possible regions: a rapid coagulation and an ineffective coalescence region. In the former, all collisions between droplets result in coalescence. Then, if a dispersion begins with n_0 equally sized particles, then the number of particles made up of r units of the original droplets at time t, is given by:

$$n_r = n_0 \frac{\left(4\pi R_{eq} \mathfrak{D} n_0 t\right)^{r-1}}{\left(1 + 4\pi R_{eq} \mathfrak{D} n_0 t\right)^{r+1}} \tag{8}$$

where $\mathfrak{D}$ is the diffusion coefficient of the drops in the liquid, and R_{eq} is the effective radius of the emulsion droplet.

If, on the other hand, collisions are not 100% effective, the authors suggest that a fraction $\boldsymbol{\lambda_c}$ of the form $\lambda_c = Ae^{-E/RT}$ can be used to account the portion of collisions that do result in coalesced drops. Then, Equation (8) is modified to yield the following:

$$n_r = n_0 \frac{\left(\lambda_c 4\pi R_{eq} \mathfrak{D} n_0 t\right)^{r-1}}{\left(1 + \lambda_c 4\pi R_{eq} \mathfrak{D} n_0 t\right)^{r+1}} \tag{9}$$

Based on Harper's work, Howarth[136] derived the following simplified expression for calculating the frequency of colliding drops (of equal diameter d) in a turbulent flow field, ω_{cd}:

$$\omega_{cd} = \sqrt{\frac{24\phi_d \bar{u}^2}{d^3}} \approx \sqrt{\frac{24\phi_d N^2}{d^3}} \tag{10}$$

where $\bar{u}$ is the average Eulerian or Lagrangian turbulent velocity fluctuation and may be approximated to N, the agitation speed, according to Gillespie.[137] Considering the number of collisions that result in coalescence, the $\boldsymbol{\lambda_c}$ factor was found using gas kinetic theory:

$$\lambda_c = e^{\frac{-3w^2}{4N^2}} \tag{11}$$

Thus, the overall coalescence frequency, ω_c, is given by:

$$\omega_c = \sqrt{\frac{24\phi_d N^2}{d^3}} e^{\frac{-3w^2}{4N^2}} \tag{12}$$

where $\boldsymbol{w}$ represents the critical approach velocity above which the collision of two drops will result in coalescence. Howarth[136] indicated that it should depend on the dispersed phase physical properties (surface tension, viscosity, density) and conducted a number of experiments to find the following correlation:

$$\omega_c = C_1\sqrt{\phi_d} N^{2.2} e^{-\frac{C_2}{N^2}} \tag{13}$$

which is one of the earliest expressions for drop coalescence frequency in the form of the product between collision frequency and coalescence efficiency, ie, $\omega_c = \omega_{cd}\lambda_c$. However, this critical approach velocity criterion is not the most popular for drop coalescence.

Another approach, by Shinnar,[138] is based on mechanical grounds, suggesting that coalescence could be prevented if the kinetic energy of the drops during a collision event is larger than the adhesion energy that drives drops together. Then, by performing the necessary balances, a minimum stable drop size above which coalescence is effectively prevented, can be found.

Yet, the most widely accepted theory (dating back to Allan and Mason[139] and MacKay and Mason[140]) explains that the fact that not all collisions result in coalescence is due to the continuous phase film that needs to drain between the two colliding drops before the drops interfaces collapse together. This mechanical process takes a given time, and drops may separate due to the constant energy fluctuations in the surrounding field; thus, there is a critical film thickness (h_c) below which film rupture readily occurs. In this model, the efficiency of the coalescence process (λ_c) depends on whether the particles are considered rigid or deformable, and on the mobility of the interfaces.[141] Since the work by Ross,[142] it is widely accepted that the efficiency is of the form $\lambda_c = e^{-\frac{\tau_{dr}}{\tau_a}}$, where τ_{dr} is a film drainage time and τ_a a contact/adhesion time between the drops. Experimental evidence that supports film drainage theory can be found in recent work by Liu et al.[143]

Inertial effects may also affect collision frequency depending on the phase density difference; if the drops hold a larger density than the continuous phase, collisions are favored compared to the opposite case.[144] It must be noted though that these effects only play an important role if $Re_d = \frac{\rho_c v d}{\eta_c} \gg 1$, where *v* represents particle velocity. In addition, the presence of electrolytes in the continuous phase also affects the collision rates, in particular by hindering coalescence and stabilizing particles, as recently detailed by Besagni and Inzoli.[145]

Sovová[146] combined the film drainage theory with an energy-based model, in which the kinetic and interfacial energies of the drop are taken into consideration to compute the efficiency of turbulent collisions. This was adopted by other researchers, such as Chatzi et al[147] and Simon.[148]

Several models to compute the collision frequency and the coalescence efficiency are available in the literature.[20,136,147,149–159] For the former, the dependency with particle volume is usually $\omega_{cd} \sim v^{7/9}$, although some others exist. Figure 15 shows a comparison for some of the available equations for ω_{cd} in a scenario with ρ_c=1000 kg/m^3, η_c=1 cP, N=100 rpm, Di=0.5 m, φ_d=0.1, and γ = 25 mN/m. This comparison is only illustrative as all equations contain an adjustable parameter that is used to fit experimental data.

The differences between each curve shown lie on the set of hypotheses taken by each author. The common ground between them is described in the following:

- Drop diameters (d) lie within the inertial subrange, which is defined by $L \gg d \gg \psi$, where L is the length scale of the energy-bearing eddies (usually identified with the length of the vessel or the impeller), and ψ is the Kolmogorov microscale (size of the smallest eddies), frequently calculated as $\psi = \left(\frac{\eta_c{}^3}{\rho_c{}^3 \varepsilon}\right)^{1/4}$.
- Droplets do not bear any particular electric charges that could modify coalescence rates due to electrostatic repulsion.
- Flow is isotropically turbulent.
- Energy is distributed uniformly throughout the vessel.
- Film drainage and contact times are random variables are only their average is computed in the equations.

Some models incorporate a correction factor to account for an observed increase in collision rates with an increase in dispersed phase fraction, usually explained by the loss of particle free space.[160–162]

Interface mobility and particle deformation were later incorporated in the mathematical framework by several authors. Figure 16 shows a scheme of the concept behind interface mobility and Figure 17 the idea of particle deformation, both taken from Simon.[148] An immobile interface refers to the case where the liquid immediately around the interface moves with the velocity of the surface, where as a fully mobile interface cannot compensate any shear stress and thus is allowed to move independently

of the liquid surrounding it. A partially mobile interface is naturally an intermediate case, frequently found in oil/water systems.

A detailed review on coalescence processes considering these effects is offered by Chesters[25] and, more recently, by Vakarelski et al[163] and Chan et al,[164] although their approach is fluid-mechanics-based and the set of equations become more complex to solve. The case for constant approach velocity (with both mobile and immobile interfaces) has been investigated by Klaseboer et al.[165]

For gas-liquid systems, a recent investigation by Guo et al[166] showed that decreasing both liquid density and its surface tension lead to a hampering of the coalescence process.

According to Yiantsios and Davis,[167] a particle interface will deform when the modified capillary number, $Ca^* = \frac{\eta_c a U}{\gamma h}$ is greater than unity. Here, U is a translational velocity, a is a characteristic length, and h is the film thickness. This means that the governing equations need to compute the value of the film thickness, which calls for a momentum balance at the interface and renders a more sophisticated mathematical model (although simplifications are possible, as shown by Chesters[25]).

For the immobile and partially mobile interfaces, some of the coalescence efficiency models depend on the critical film thickness h_c. This value depends on phase physical properties; however, most authors have found that it lies around $5 \cdot 10^{-8}$ m (500 Å) for O/W dispersions[168] and $5 \cdot 10^{-9}$ m (50 Å) for some polymer mixtures.[150] A theoretical value was derived by Vrij[169]:

$$h_c = \left(\frac{A}{8\pi\gamma \left(\frac{1}{d} + \frac{1}{d'} \right)} \right)^{1/3} \tag{14}$$

where A is the Hamaker constant.

Abid and Chesters[170] produced a model for a simplified case of partially-mobile films in the absence of van der Waal's forces.

While hydrodynamic interactions due to particle deformation are included in the film drainage theory, no interactions induced by particle trajectories are considered. These hydrodynamic effects were first introduced by van de Ven and Mason[171] and Zeichner and Schowalter,[172] and were later developed by several other authors in different configurations.[173–178] Further details on coalescence of liquid drops and bubbles may be found in a review by Liao and Lucas.[179]

In polymeric systems, the coalescence process is modelled by the same governing equations used in traditional liquid-liquid drops. In fact, few differences arise when comparing both systems. An interesting example is the viscosity ratio effect on

coalescence frequency found by Lyu et al[151] in HDPE/PS blends, which is not always monotonically decreasing as theory suggests. Detailed reviews on coalescence in polymer blends are offered by Utracki and Shi[180] and Lyu et al.[181]

Chesters and Bazhlekov[182] incorporated the effect of insoluble surfactants (present at the drop surface) to the coalescence process. By computing the surface diffusion (which tends to reduce Marangoni effects) through the Péclet number and van der Waal's forces through the Hamaker constant, they developed the set of conclusions that are listed below.

- For sufficiently large particles (d>>1 μm), diffusion is negligible and van der Waal's forces are a function of the critical film thickness.
- Film drainage is unaffected by surfactant concentration up to a given film thickness, at which interface becomes immobile. At that point, film drainage is a function of surfactant concentration, which must be higher than a given critical value (a function of the Hamaker constant).
- Analytical expressions for calculating drainage times may be derived for both mobile and immobile interfaces.
- If the interface is immobile, no dispersed phase viscosity effects should be observable.
- For sufficiently small particles, diffusion of surfactants is considerable and surface tensions gradients become small. Then, film drainage rates are unaffected by Marangoni effects and the coalescence proceeds like the surfactant-free system, but with a lower interfacial tension.

For a given surfactant (or surfactant pair) concentration and temperature, the coalescence rate, at least in a non-stirred system, may vary with the emulsifier's HLB as shown by Boyd et al[183] and exemplified in Figure 18 for various Span/Tween pairs in a dispersion of water and a commercial oil. Note that there is an HLB at which coalescence suppression is greatest, yielding a formulation that maximizes emulsion stability.

The effects reported for insoluble W/O surfactants were extended to copolymers in polymer-polymer mixtures by several authors.[99,114,184–189] Most authors consider that block or graft copolymers, which usually locate at the interface of immiscible polymer mixtures (blends or solutions), behave like surfactants and reduce the interfacial tension.[190,191] This translates to smaller coalescence efficiencies as per film drainage theory. However, coalescence suppression is most likely due to steric hindrance of the copolymer chains. These large molecules exert the following two effects on the coalescence process[192,193]: (a) they provide extra stresses needed to collapse the particle interface and (b) they interact with the matrix chains and defer film drainage.

Beck Tan et al[194] ran a series of experiments with polystyrene and polyamide blends and showed that the presence of graft copolymers does reduce surface tension but not enough to explain the observed extent of coalescence suppression. It is rather the repulsive forces exerted by the copolymer chains that hamper coalescence rates. Milner and Xi[195] provided the theoretical and mathematical framework to support this evidence, also in line with Sundararaj and Macosko,[196] Lyu et al,[151] Sundararaj et al[121] and more recently with Luo et al.[197]

Figure 19 shows a schematic interpretation of this copolymer role taken from Sundararaj and Macosko.[196] It should be noted, however, that these conclusions were reached for polymer blends, while nothing on this line has been reported for solutions, to the authors' knowledge.

Marangoni effects may also be considered a contributing cause of coalescence suppression,[193] as in O/W emulsions.

3.4.2. Break-up

The breakage process of a liquid drop or a gas bubble involves complicated phenomena, which has led to define different criteria to decide when and how a particle breaks up.[198] In addition, most authors deal with simple binary break-up and fail to recognize that daughter particles may continue to deform and undergo further splitting, as recently shown by Herø et al.[199] The proposed mechanisms are presented in the following.

Turbulent pressure fluctuation or particle-eddy collision

The idea behind this model is based on turbulent mixing, in which eddies constantly hit dispersed particles and cause them to deform. Pressure fluctuations caused by the same eddies can also modify particles' shape and eventually lead them to break into two or more smaller ones. Theory suggests that there is a balance between the dynamic pressure surrounding the particle, τ_c, and the surface stress, τ_s; breakage will occur depending on how different these forces are. Viscous stresses inside the particle are neglected. Different criteria were developed for deciding whether a particle may break up. At least five different cases can be found in literature; an extensive, critical analysis on the most relevant statistical models was presented by Kostoglou and Karabelas[200] and also reviewed by Lasheras et al.[201] Perhaps one of the only models that considers the intermittent characteristic of turbulence is the multifractal approach originally developed by Baldyga and Podgórksa[202] and recently assessed by other researchers.[127,128]

Viscous shear forces

The viscoelastic properties of the continuous phase may exert a deformation effect on the dispersed particles as velocity gradients around the interface are generated. This mechanism then considers a balance between a viscous stress τ_v at the interface and the restituting surface stress τ_s, usually expressed in terms of a capillary number $Ca = \frac{\tau_v}{\tau_s}$. Early work by Shinnar[138] considers that break-up due to viscous shear is achieved only when applying a critical stress, given by $\tau_{cr} = \frac{C\gamma\phi_d}{d}\frac{\eta_d}{\eta_c}$.

Wake effects are also considered as partly responsible for break-up in this model since a difference in shape in contact with the continuous phase (head-tail instability) causes necking of the particle and surface shear stress may subsequently lead to splitting. Few authors incorporate this effect into their models; a recent example is the one by Yang et al.[130]

Shearing-off process

Also coined erosive breakage, this mechanism is most commonly found in larger particles, whose surface instability is higher than smaller ones. A velocity gradient around the particle surface causes a number of smaller daughter particles to be sheared-off from its mother. Regarding this mechanism, the works of Evans et al,[203] Biń,[204] and Fu and Ishii[205] are important, but few other mathematical models are available.

Interfacial instability

Even in the absence of flow of the continuous phase (eg, gases flowing up a liquid or drops falling into an immiscible liquid), breakage can still occur due to particle surface instability. This includes both Rayleigh-Taylor (density differences) and Kelvin-Helmholtz (velocity differences across an interface) instabilities. These effects are usually neglected without justification.

Models for break-up frequency

Exhaustive work has been conducted to develop models for computing the breakage frequency.[147,158,161,202,206–211] However, the vast majority only consider eddy-particle collisions as the most important cause for burst, neglecting the other present forces without much further validation. This is most likely due to the large availability of simple turbulent flow systems (ie, continually stirred liquid-liquid tanks, air-bubble columns, etc.). In other cases, for example polymer mixtures undergoing breakage due to shearing effects, particle-eddy turbulent models would rarely apply, and other models must be used or developed.

In addition, expressions for the breakage frequencies of bubbles and of drops are often used interchangeably. Striking as it may seem, Andersson and Andersson[212] have shown that their breakage mechanisms are similar. The most important difference lays in the daughter particle size distributions; equal breakage is most likely for drops than for bubbles (due mainly to pressure-driven internal fluid distribution after break-up). It should be noted, however, that the viscosity of the dispersed phase plays a significant role in the break-up mechanism, as it is intrinsically involved in the force balances.

Therefore, expressions should be used with caution when dealing with specially viscous materials (as it is the case with polymer systems[213]).

Regarding the mathematical models available to computing such distributions, Gao et al[127] point out that their functionality, while bearing a considerable impact on the final particle size distribution, they have a little effect on the Sauter mean diameter. A summary of the available equations may be found in Liao and Lucas[198] and more recently in Chu et al[214] for bubble break-up.

Break-up mechanisms that do not consider particle-eddy collision

Exhaustive studies on drop deformation in simple and rotational shear flows were conducted by Grace[215] and by Bentley and Leal.[216] The latter authors showed that the lower the viscosity ratio the greater the extent to which the particle is stable (yielding larger critical Ca values). In rotational flows, deformation depends on the orientation angle of shear and particle viscosity may help dissipate shear-induced vorticity through internal circulation. This means that, in slightly rotational flows, the more viscous the particle, the more solid-like behavior it presents, needing greater shear rates to induce break-up. In stronger rotational flows, the authors showed that there exists a critical viscosity ratio above which break-up cannot occur (the orientation of the drop is such that the effective strain rate is very low), which was first predicted by Taylor in dilute, Newtonian dispersions.[217] Their results are also in agreement with Arai et al,[218] who particularly studied this effect (both theoretically and experimentally) in fully turbulent conditions. Figure 20 illustrates an example taken from their work, in which the dispersed phase is a solution of PS in a polystyrene-o-xylene and the continuous phase is an aqueous solution of polyvinylalcohol.

Depending on the phase properties and on the local shear conditions, the critical viscosity ratio above which break-up does not occur may widely vary. Taylor's limit for small deformation is a known value of 2.5 and some polymeric systems in simple shear exhibit a value of 4,[215] but this is by far not the case for extensional flow as shown by Wu[219] or Sundararaj and Macosko.[196]

The works by Grace,[215] Elemans et al,[220] Elmendorp,[221] de Bruijn,[222] Tomotika[223] and Hinze[224] consider the effects of different mechanisms other than eddy-particle collision for splitting. Hinze highlights that there are different types of drop deformation and that the condition at which a drop deforms may be described in terms of a general Weber number $\left(We = \frac{\tau d}{\gamma}\right)$ and a Viscosity number $\left(Vi = \frac{\eta_d}{\sqrt{\rho_d \gamma d}}\right)$ and suggests a simple model to predict drop deformation, as a function of a critical Weber number:

$$We_c = C(1 + C_2 Vi) \tag{15}$$

The critical value would depend on the deformation type (namely lenticular, elongated, or bulgy). Even if the simplicity of this model casts further validation questions, both theory and practice (in rotational shear flow) yield an interesting result: for very low and very high viscosity ratios the critical We rises to an infinitely large value, meaning that no break-up occurs, which is in line with previously stated authors.

Liquid thread break-up (Figure 21) was firstly discussed by Tomotika,[223] and later continued by Elmendorp[221] and Janssen and Meijer.[150] Polymer liquid-liquid systems, especially under extruding conditions, are examples that may be modeled following their work, which includes both Newtonian and non-Newtonian behavior. This particular process accounts for the sinusoidal reshaping of slender threads caused by shear, up to a point after which break up occurs, splitting the thread into several daughter drops. A recent investigation by Épinat et al[101] on polyamide/HDPE blends is also in line with their work and has further shown the effect of the viscosity ratio on the break-up mechanism and the yielded particle morphology.

Particularly for extruded polymer blends, Wu[219] suggested a correlation between Ca and the viscosity ratio that can predict final particle mean size considering only thread break-up:

$$d = 4\frac{\gamma}{\dot{\gamma}\eta_c}\left(\frac{\eta_d}{\eta_c}\right)^{\pm 0.84} \tag{16}$$

where the power is +0.84 when $\frac{\eta_d}{\eta_c} > 1$ and -0.84 otherwise.

In stirred dispersions, the breakage process of non-Newtonian drops was incorporated by Lagisetty et al,[225] who presented a model to predict the maximum stable size at a given shear rate. Their work was based on the theory and models developed by Hinze,[224] Coulaloglou and Tavlarides[226] and Arai et al.[218] Considering viscoelastic drops modeled by a power law equation, the maximum stable drop diameter may be calculated by computing the following non-dimensional breakage time:

$$t^* = \int_0^1 \left[\left(\theta - \frac{1}{2}\right)^2 + CWe \left(\frac{d}{D_i}\right)^{5/3} - \tau_0 \frac{d}{\gamma} - \frac{1}{4} \right]^{-1/n} d\theta \qquad (17)$$

and then solving:

$$t^* = \left(\frac{K\gamma}{d_{max}}\right)^{1/n} \frac{(d_{max} D_i)^{2/3}}{N} \qquad (18)$$

where θ is the dimensionless strain, τ_0 a yield stress (nonzero for Bingham plastics), and K and n are the power law model parameters. The authors have provided solutions of the integral for several values of n, and noted that break-up can only occur if the term $CWe \left(\frac{d}{D_i}\right)^{5/3} - \tau_0 \frac{d}{\gamma} - \frac{1}{4}$ is positive.

Koshy et al[227] studied the effects of including drag-reducing agents in the continuous phase and incorporated this feature into the model by Lagisetty et al.[225] They indicated that these species contribute to change the magnitude of the turbulent stresses (probably due to turbulent damping) and showed that the maximum stable drop size before break-up increases with the presence of such agents, as experiments confirm.

The effect of insoluble surfactants on droplet breakup was studied by Stone and Leal[228] and recently simulated by Li et al.[128] The former showed that the presence of these agents translates into a lower Ca needed for break-up since the interfacial tension reduction allows for increased drop deformation. However, they demonstrated (at least numerically) that the predictions on such critical Ca depend on the dominant flow

regime at the interface (convection or diffusion) since two opposing effects appear, as described in the following.

1. If surfactant diffusion is fast, concentration profiles along the interface are almost constant, and shear-induced drop deformation will only serve to dilute the surfactant's effect, lowering its surface concentration and thus increasing the interfacial tension compared to the saturated case.
2. If convection is dominant, drop deformation causes the surfactant to accumulate at the end of the drop (where surface curvature is greatest), leading to extra tangential stresses (Marangoni effect) but lower interfacial tension compared to the fully coated interface.

Depending on the dominating regime, the critical shear rate needed for break-up may differ substantially compared to the ideal case in which interfacial tension is held constant at an equilibrium value. Yet, compared to a clean, surfactant-free interface, the addition of surface-active species will lower interfacial tension and promote break-up.

The convection-dominant case described by Stone and Leal[228] may result in a particular break-up mode named tip-streaming, in which drops deform into a sigmoidal shape and small daughter droplets break off at the tips (see Figure 22). This case was also subject of different studies. Examples are by de Bruijn[222] and Eggleton et al[229] and show that this mode of breakage may occur at much lower shear rates than traditional binary splitting.

All the above described mechanisms are only concerned with shear-induced deformation, most often based on a single particle. In concentrated dispersions under mixing conditions it is likely that particle-particle collisions become of importance, and most available works on this matter focus mainly on the coalescence process that results (as described in Section 3.4.1). However, a thorough analysis of water drop-drop collisions in air was presented by Ashgriz and Poo,[230] who have empirically and theoretically shown that particle break-up also occurs as a result of collisions. As explained by the authors, there are four possible outcomes to drop-drop collision:

bouncing, coalescence, separation and shattering. Figure 23 shows examples of coalescence (above) and separation (below).

The mechanics of drop-drop collisions are affected by both dispersed and continuous fluid properties, the relative velocity between drops, and the contact angle before collision. Even though their work was not carried out in stirring conditions (drops were generated from jets), the conceptual conclusions that arise are of interest, since they provide a thorough explanation of some of the mechanisms that are frequently cited in literature. In the case of air drops in water, the authors found that a Weber number (defined $We = \frac{\rho_c d u_r^2}{\gamma}$), was a governing parameter together with the particle size ratio and an arbitrary dimensionless relative position. They thus produced maps like the one in Figure 24, which show clearly that: (a) not all drop-drop collisions result in coalescence nor in bouncing and (b) break-up can occur as a result of particle-particle impact, even if We increases.

4 MULTIPLE EMULSIONS

Often, the structure of an O/W or W/O emulsion is not made up of simple drops dispersed in a continuous matrix; it is also possible for some volume of the continuous phase to become entrapped in the dispersed one, giving rise to an emulsion within an emulsion (Figure 25). These kinds of structures have been observed for almost a century (perhaps since the work by Seifriz[231]) and may be either intentionally prepared or a consequence of a phase inversion process. In several cases, these structures were also observed for surfactant-free systems (dispersions), especially in the vicinity of the phase inversion threshold.[2,12,35,53,232,233]

Extensive work has been conducted since the early 1970s to describe the properties of these emulsions and their potential applications (they are of interest in the pharmaceutical, food, waste water treatment, and even upstream oil production industries, though today have limited applicability due to their inherent instability[244]).[91,235–243] These fractal-like systems are not necessarily drop-within-a-

drop structures; there have been reports of triple, quadruple and even quintuple emulsions.[91,245] Some authors refer to this type of emulsions as abnormal, as opposed to the normal emulsions that satisfy Bancroft's rule.[51,68,246]

4.1. Inclusion mechanisms

The process of continuous phase entrapment inside dispersed drops has been observed to occur both with and without emulsifiers. Examples of the former include those of Brooks and Richmond,[68] Jahanzad et al,[234] Groeneweg et al,[92], and Pal,[247] while cases of the latter are seen in Pacek et al[35,233,248] and Gilchrist et al.[232] Whichever the case, two main mechanisms have been suggested and are described as follows.

1. Deformation of dispersed drops under high shear rate. This is mostly observed with large drops and particularly enhanced in the presence of surfactants.[66,249]
2. Simultaneous coalescence of two or more drops, by which continuous phase is engulfed following film rupture.[12,250]

These mechanisms are illustrated respectively in Figures 26 and 27. The former is based on the pressure fluctuations that occur in turbulent stirred systems, which promote particle break-up (see Section 3.4.2). The restoring force in this case is the interfacial tension, which increases locally when deformation occurs, as interfacial area is created. If surfactants are present at the interface, the Marangoni effect tends to counteract such local increase. Thus, if interfacial forces are higher than pressure fluctuations, then no inclusion occurs. Conversely, if the interfacial tension is not as high and/or surfactant diffusion is rapid (so that any attempt to locally increase the interfacial tension is counteracted), then continuous phase protrusions take place and further drop sealing (inter-particle coalescence) ensures the occlusion.[249]

The latter case is believed to occur as a result of a multiple coalescence processes (two-body collision may also produce continuous phase entrapment but is highly dependent on the intensity of the collision and the interfacial properties[250,251]. In this context, film drainage occurs simultaneously between more than two drops and most of the liquid from each film is forced out to a common bulk inside the drop.

According to Sajjadi et al,[51] mechanism 1 is usually dominant at low dispersed fractions since multi-drop coalescence occurs preferably at more densely packed systems. Thus, a gradual change between mechanisms is expected when increasing the dispersed phase fraction; larger and/or more numerous drops promote coalescence, which favors continuous-phase inclusion, and finally increases the effective dispersed volume fraction. It is of no surprise, then, that the drop-in-drop structure has been observed prior to catastrophic phase inversion processes.

At intermediate values of φ_d (ie, not low enough for inclusions to be deformation-induced and not high enough for PI to occur), two conditions should be satisfied for entrapment to be possible (as explained by Pacek et al[35]):

1. Enhanced coalescence frequency, so that multiple drops may coalesce and engulf part of the continuous phase.
2. Stability of the entrapped droplet inside the drop, without which the drop-in-drop structure would only be temporary.

When surfactants are present, post-inclusion stability is naturally a function the emulsifier's structure and concentration. In the absence of any surface-active species, experimental evidence shows that occlusions are more frequently seen in O/W/O rather than the reverse dispersions.[35,252] This would seem to indicate that water-in-oil droplets are much less stable (ie, their escape processes are enhanced) than oil-in-water ones. Kumar[12] suggests that this asymmetry lies in the difference of dielectric constants (eg, 78.3 for water and 1.88 for n-hexane at 25ºC), which explains the disparity in coalescence rates between water-water and oil-oil drops, the latter being much lower due to the overlapping of the electrical double layers. In fact, this is the argument that explains the asymmetry observed in many ambivalent ranges (in the absence of emulsifiers) even with systems that hold similar physical properties.

4.2. Manufacture methods

An early procedure for the preparation of multiple emulsions (for example W/O/W) consisted in a two-step process: a first emulsification of an aqueous phase in a

continuous organic matrix (with a lipophilic surfactant), followed by the emulsification of the organic phase by the addition of water and a hydrophilic emulsifier (Figure 28). The final structure and properties of the multiple emulsion depend on surfactants concentration, their weighted HLB,[240] phase volume fractions and electrolyte concentration.[253]

The stability of the multi-emulsions produced this way has been the subject of several papers, for there are numerous mechanisms by which occluded continuous phase may escape the dispersed particle and rejoin the matrix. This is usually known as the breakdown of the multiple emulsion, and a review on the mentioned mechanisms was produced by Florence and Whitehill.[243]

Multiple emulsions may also be obtained via a one-step process, prior to or as a result of a phase inversion.[51,244,246] In this case, the procedure begins with a continuous phase in which a pair of surfactants is solubilized. Then, the dispersed phase is gradually added with sustained agitation. Depending on the average HLB of the surfactant pair and its concentration, a drop-in-drop structure may be readily obtained at low dispersed phase fraction.[51] This type of morphology is sometimes considered instable and the addition of further dispersed phase gives rise to a catastrophic phase inversion to the normal reverse emulsion. For this structure to be possible, the weighed HLB should favor the stability of the continuous phase inside the dispersed one, of which there is not enough volume become continuous and satisfy Bancroft's rule. Remarkably, Jahanzad et al[234] have shown that, for an O/W emulsion produced after the inversion of an O/W/O system, the average particle size is always lower than when produced by a direct emulsification method (and the size difference is greater as surfactant loading increases). This gives abnormal emulsions an interesting application if fine dispersions are targeted.

According to Morais et al,[246] stable multiple emulsions may be produced in one step by adding dispersed phase to a normal emulsion (continuous phase plus dissolved surfactant mixture) and subsequently crossing the PIT threshold. The combination of

both catastrophic and transitional phase inversion (at a suitable HLB) may produce a stable multi-emulsion as a result continuous phase being transferred across the interface, which is deemed possible due to the very low interfacial tension at the PIT (see section 2.1.4).

The relationship between operating conditions and the final emulsion structure obtained with the methods of Sajjadi et al[51] and Morais et al[244,246] is discussed in the next section. It should be noted, nevertheless, that the experimental procedures reported by these authors were conducted without keeping a constant total volume, which is at least questionable in stirred systems. Moreover, their manufacture procedure requires a precise mixture of two types of surfactants. In this line, the work by Hong et al[254] shows that stabilized multi-emulsions are obtained just as easily with one single surface-active species, if an amphiphilic block copolymer is used (although they only reported the preparation of 4 mL samples).

In a more targeted procedure, originally developed by Utada et al[255] and later continued by others,[242,256,257] double or multiple emulsions may also be obtained with specific inner structures, using microfluidic capillary devices. This approach generates the emulsion structure by forcing part of the continuous phase (or sometimes a third phase) directly inside the dispersed drop. Unlike the previous methods, this one enables a much precise control of inside-drop dispersity. However, it is much more goal-specific and requires expertise in microfluidic device managing.

4.3. Effects of main variables in morphology and inversion point

Sajjadi and coworkers[51] studied the influence of surfactant concentration and its HLB on the structure of the O/W/O emulsions (prior to the catastrophic inversion to O/W). The main conclusions of their work are summarized as follows:

1. Larger drops usually accommodate a higher number of internal droplets (at a given system composition). More but smaller occlusions are observed with increasing φ_d and increasing surfactant concentration.

2. For a constant drop size, the number of internal droplets increases as the surfactant concentration increases.

3. At low surfactant concentrations, the internal phase volume ratio (volume of entrapped droplet/volume of dispersed drop) does not change considerably with φ_d. Conversely, at higher surfactant loadings, more occluded droplets are found when increasing φ_d.

4. There is a minimal drop size below which little continuous phase is entrapped. This critical size decreases when increasing surfactant concentration.

5. High surfactant loading yields a bimodal size distribution of internal droplets. The work by Liu et al[258] also added that it may lead to a radical change in the emulsion structure, going from micellar to hexagonal liquid crystal.

6. Phase inversion occurs at lower values of dispersed phase fraction as surfactant loading increases (a natural consequence of conclusion 1).

7. At a high surfactant concentration, most occluded droplets remain unchanged in size after PI has occurred.

8. The number of occluded droplets increases with decreasing HLB values (at constant loading). As a natural consequence, PI occurs at lower HLB values at constant φ_d (note that the system under study is an O/W/O with HLB values always higher than the transitional threshold, where O/W is the preferred structure). This conclusion has also been reached for W/O/W emulsions by Tyrode et al[259] by clever conductimetric measurements.

9. Larger internal droplets are found with increasing HLB.

10. PI points are modified by the surfactant's chain length distribution. Their results show that a broader distribution caused a delayed PI because of the preferential solubility in the oil phase by the short-chain homologues. Yet, only two systems were compared, thus limiting the conclusion on the direction of change in the PI point.

In turn, Jahanzad et al[234] have partially proven that the inner droplet size distribution is mainly the result of a surfactant concentration gradient between oil and water phases, at least in batch systems. In continuous operation, Tyrode et al[259] showed that it also

depends on the rate at which dispersed phase is added to the emulsification vessel. Regarding the viscosity ratio, Liu et al[258] concluded that an increase in the dispersed-phase viscosity leads to fewer occlusions, which is in line with the mechanism outlined by Kumar.[12]

4.3.1. Catastrophic versus transitional inversion and the role of multiple emulsions

Sajjadi et al[260] revealed an interesting behavior of multiple emulsions when subject to a decrease of the average HLB at constant φ_d. In most inversion maps, varying the HLB parameter yields a transitional PI; however, the authors managed to track the evolution of the emulsion structure at a close range of the transitional inversion threshold and noticed that the emulsion goes through a catastrophic inversion before undergoing the expected transitional process. Path B in Figure 29, reproduced from the original paper, depicts this scenario.

The explanation is as follows: a multiple emulsion (for example O/W/O) with constant dispersed water fraction will present a number of occlusions that depend on the average HLB, being higher at lower values of this parameter.[51] This means that a decrease of HLB will produce higher effective dispersed fractions (water + occluded oil phase), which is comparable to an increase in water phase fraction at constant HLB. Hence, coalescence is expected to be stimulated and PI may occur, not as a result of affinity changes of the emulsifier but rather as an imbalance between break-up and coalescence, enhanced by the occlusion process that is a consequence of interfacial fluctuations. Yet, the W/O emulsion formed this way will present a near-ultralow interfacial tension and is prone to go through a transitional inversion at a slightly lower HLB. These studies have shown that, in fact, catastrophic phase inversion should be associated with the coalescence versus break-up rates rather than only with an increase in dispersed phase fraction.

In turn, numerous examples of a drop-in-drop structure have been reported in polymer-polymer or polymer-solvent-polymer systems. Most often, they are reported for

extruded blends, such as the SAN-PS-(PMMA-*b*-PS) by Adedeji et al,[98] a PSU-PA by Charoensirisomboon et al,[99] a PP-PA by Hietaoja et al,[16] and the PA-SAN by Kitayama et al.[29] There are also reports of a water-PU emulsion by Saw et al[261] and the well-known case of the in-situ formed occlusions in the HIPS manufacture process.

In all these cases, the particle-particle morphology holds a significant importance since many mechanical properties strongly depend on their characteristics.[262] Here, the block or graft copolymers play the role of traditional O/W emulsifiers, as described in Sections 2.2 and 3.4.1. These copolymers are either added intentionally or produced in-situ as part of the polymerization mechanism. Consequently, the concentration of such polymer species and its molecular-weight distribution affects the number of occluded particles inside the dispersed phase. For example, Leal and Asua[263] reported that the number of entrapped droplets increases when the concentration of chemical initiator increases (reproduced in Figure 30). This is because the chemical initiator used for the free-radical polymerization may induce the formation of graft-copolymers, as is the case of the polymerization of styrene in presence of polybutadiene studied by the authors.

5 CONCLUDING REMARKS

Analyzing both the physical evidence and the mathematical models presented in the previous sections, the effects of phase viscosity, phase density, interfacial tension, and surfactant properties on the phase inversion mechanism have been summarized in Table 2. Since some of the models suggest different dependencies on some of these properties, this table should serve as a general guide while the real interdependence should be assessed on a case-by-case basis.

It is clear that the phase inversion phenomenon (both in O/W and polymer-polymer systems) is a complex, multivariable, nonlinear process. Even though it has been studied in depth by many researchers, it has been mostly treated in a qualitative, descriptive way; the effect of the main operating variables on the PI point is rarely analyzed under a *ceteris paribus* condition and is therefore troublesome to understand the real output and relative weight of each parameter. Moreover, when comparing results from different

authors, care must be taken to ensure that all the operating variables in question are considered, since otherwise the resulting conclusions could be (at least partially) erroneous or misleading.

The analysis of each variable in isolation is a challenge, since it is empirically troublesome (or impossible) to generate liquid mixtures with all but one similar property. The viscosity ratio is probably the best example: changing the viscosity of one phase is usually achieved by changing its composition (or choosing an entirely new fluid), which often yields a different density, interfacial tension or electrostatic behavior. Since the most widespread mechanism that explains PI is strongly based on the interfacial interactions (particle break-up versus coalescence), an unforeseen change in one operating variable may readily introduce an effect on the dynamics of the agitated system and completely alter the inversion point. Vessel geometry is also an acceptable example: even the position of the impeller at the beginning of the experiment has proven to exert an effect on φ_d.

Regarding its mechanism, PI is most commonly explained through an imbalance between particle break-up and coalescence rates; the latter being much greater than the former at the onset of inversion. This approach has not been entirely validated since accurate measurements of these frequencies are an experimental challenge. Yet, this mechanism better explains the empirical evidence found when changing the emulsification route; the thermodynamic, energy minimization-based model does not account for dynamic nor initial-condition effects that could change the inversion point dramatically. Moreover, the conclusions of the energy-minimization model arise from theoretical considerations that lie on systems under thermodynamic equilibrium, which is not always the case, especially in polymer-polymer mixtures and in systems where PI occurs during a chemical reaction.

Interestingly, regardless of its mechanism, the PI process seems to strongly depend on one common feature: interfacial activity. The role of interfacial tension, and all the operating variables that modify it, is essential in determining which phase will invert at

a given stirring speed. The presence of surface-active agents, in the form of emulsifiers, impurities, block or graft copolymers, can change the inversion point substantially, depending on their concentration and chemical structures. The affinity of these species towards a given phase usually determines that it will be preferred as the continuous one (provided that there is enough volume of it), which can be regarded both as a thermodynamic argument but also as being the result of interfacial curvature that favors one structure over the other. Moreover, the potential formation of drop-in-drop arrangements, for which interfacial tension (and electrostatic behavior) is a key variable, may favor the occurrence of phase inversion by increasing the effective dispersed volume fraction.

The formation of a preferred structure in O/W or polymer/polymer emulsions is essential in a number of industrial applications. Therefore, a better understanding of the phase inversion process is vital. Comprehensive mathematical models capable of accurately predicting the PI point are useful tools that are still to be developed.

NOMENCLATURE

A	Hamaker constant
C, C_1, C_2	Adjustable constants
Ca	Capillary number
D	Tank diameter (m)
D_i	Impeller diameter (m)
De	Deborah number
d, d’	Average particle diameter (m)
d_e	Eddy diameter (m)
f	Fractal dimension
G’	Storage modulus (Pa)
h_c	Critical film thickness (m)
HLB	Hydrophilic-lipophilic balance
HLD	Hydrophilic-lipophilic deviation

K_{ref}	Reference value for SAD calculation
k	Adjustable constant
N	Stirring speed (1/s)
N_P	Power number
N_e	Number of eddies
P	Parachor
R	Ideal gas constant ($Pa \cdot m^3/^oK \cdot mol$)
r	Dispersed-to-continuous viscosity ratio
SAD	Surface affinity difference
T	Absolute temperature (K)
$\bar{u}$	Eulerian or Lagrangian velocity fluctuation (m/s)
u_{rel}	Relative velocity of approaching particles (m/s)
Vi	Viscosity number
v, v'	Volume of particle (m^3)
W_P	Power input to stirred tank (W)
We	Weber number
W	Volume of daughter particle (m^3)
z	Self-crowing factor
Greek letters	
Γ	Surface excess relative to a given plane (m^2)
$\Gamma_{\left(\frac{x}{2},\frac{k}{2}\right)}$	Incomplete Gamma function with k degrees of freedom
γ_{jk}	Interfacial tension between phases j and k (N/m)
$\dot{\gamma}$	Shear rate (1/s)
ε	Specific energy dissipation rate(m^2/s^3)
ϵ	Dielectric constant
ζ	Zeta potential of emulsion (V)

η	Apparent viscosity of emulsion (Pa·s)
η_c	Apparent viscosity of continuous phase (Pa·s)
η_d	Apparent viscosity of dispersed phase (Pa·s)
η_{int}	Apparent viscosity at the interphase (Pa·s)
Θ	Dimensionless strain
κ	Specific electric conductivity of emulsion
λ_b	Break-up efficiency
λ_c	Coalescence efficiency
μ_i	Chemical potential of phase i (J/mol)
ρ_c	Density of continuous phase (kg/m^3)
ρ_d	Density of dispersed phase (kg/m^3)
ρ_L	Density of liquid phase (kg/m^3)
ρ_V	Density of vapor phase (kg/m^3)
σ_i	Surface tension of phase i (N/m)
τ	Shear stress (Pa)
τ_0	Yield stress (Pa)
τ_a	Adhesion or contact time (s)
τ_c	Shear stress by continuous phase (Pa)
τ_{cr}	Critical shear stress (Pa)
τ_d	Shear stress by dispersed phase (Pa)
τ_{dr}	Drainage time (s)
τ_s	Surface restitution stress (Pa)
τ_v	Viscous stress (Pa)
φ_0	Volume fraction of dispersed phase at inversion point for very high stirring speeds
φ_c	Volume fraction of continuous phase
φ_d	Volume fraction of dispersed phase
φ_p	Maximum packing factor
Ψ	Kolmogorov's microscale length

ω_b	Break-up frequency (1/s)
ω_c	Coalescence frequency (m^3/s)
ω_{cd}	Frequency of colliding drops (m^3/s)

REFERENCES

[1] T. R. Guilinger, A. K. Grislingas, O. Erga, *Ind. Eng. Chem. Res.* **1988**, *27*, 978.

[2] J. A. Quinn, D. B. Sigloh, *Can. J. Chem. Eng.* **1963**, 15.

[3] C. Solans, I. Solé, *Curr. Opin. Colloid Interface Sci.* **2012**, *17*, 246.

[4] B. Hu, P. Angeli, O. K. Matar, G. F. Hewitt, *Chem. Eng. Sci.* **2005**, *60*, 3487.

[5] G. E. Molau, H. Keskkula, *J. Polym. Sci. Part A-1* **1966**, *4*, 1595.

[6] K. Dedecker, G. Groeninckx, *Polymer (Guildf).* **1998**, *39*, 4993.

[7] G. E. J. Vaessen, *PhD Thesis*, Technische Univesrsiteit Eindhoven, Eindhoven, The Netherland **1996**.

[8] N. Mekhilef, H. Verhoogt, *Polymer (Guildf).* **1996**, *37*, 4069.

[9] A. Perazzo, V. Preziosi, S. Guido, *Adv. Colloid Interface Sci.* **2015**, *222*, 581.

[10] A. H. Selker, C. A. Sleicher, *Can. J. Chem. Eng.* **1965**, *43*, 298.

[11] G. M. Jordhamo, J. a. Manson, L. H. Sperling, *Polym. Eng. Sci.* **1986**, *26*, 517.

[12] S. Kumar, *Chem. Eng. Sci.* **1996**, *51*, 831.

[13] E. Dickinson, *J. Colloid Interface Sci.* **1981**, *84*, 1.

[14] F. Bouchama, G. A. Van Aken, A. J. E. E. Autin, G. J. M. M. Koper, *Colloids Surfaces A Physicochem. Eng. Asp.* **2003**, *231*, 11.

[15] P. Becher, *Encyclopedia of Emulsion Technology Vol. 3*, , 1st ed., Marcel Dekker, New York, **1987**.

[16] P. Hietaoja, R. Holsti-Miettinen, J. Seppala, O. Ikkala, *J. Appl. Polym. Sci.* **1994**, *54*, 1613.

[17] G. E. Molau, *J. Polym. Sci. Part A* **1965**, *3*, 1267.

[18] C. Shih, *Adv. Polym. Technol.* **1992**, *11*, 223.

[19] M. J. McClarey, G. A. Mansoori, *AIChE Symp. Ser.* **1978**, *74*, 134.

[20] M. Norato, C. Tsouris, L. Tavlarides, *Can. J. Chem. Eng.* **1998**, *76*, 486.

[21] M. Arashmid, V. Jeffreys, *AIChE J.* **1980**, *26*, 51.

[22] G. C. Yeh, F. H. Haynie, R. E. X. A. Moses, *AIChE J.* **1964**, *10*, 260.

[23] L. Y. Yeo, O. K. Matar, E. Susana Perez de Ortiz, G. F. Hewitt, *Chem. Eng. Sci.* **2002**, *57*, 3505.

[24] A. R. A. Colmanetti, M. S. de Castro, M. C. Barbosa, O. M. H. Rodriguez, *Chem. Eng. Sci.* **2018**, *189*, 245.

[25] A. K. Chesters, *Chem. Eng. Res. Des.* **1991**, *69*, 259.

[26] I. S. Miles, A. Zurek, *Polym. Eng. Sci.* **1988**, *28*, 796.

[27] R. M. Ho, C. H. Wu, A. C. Su, *Polym. Eng. Sci.* **1990**, *30*, 511.

[28] T. H. Chen, A. C. Su, *Polymer (Guildf).* **1993**, *34*, 4826.

[29] N. Kitayama, H. Keskkula, D. R. Paul, *Polymer (Guildf).* **2001**, *42*, 3751.

[30] V. Everaert, L. Aerts, G. Groeninckx, *Polymer (Guildf).* **1999**, *40*, 6627.

[31] S. Arirachakaran, K. D. Oglesby, M. S. Malinowsky, O. Shoham, J. P. Brill, *SPE Prod. Oper. Symp.* **1989**, *18836*, 155.

[32] V. I. Metelkin, V. S. Blekht, *Colloid J. USSR* **1984**, *46*, 425.

[33] L. A. Utracki, *J. Rheol.* **1991**, *35*, 1615.

[34] S. Steinmann, W. Gronski, C. Friedrich, *Polymer (Guildf).* **2001**, *42*,

6619.

[35] A. W. Pacek, A. W. Nienow, I. P. T. Moore, *Chem. Eng. Sci.* **1994**, *49*, 3485.

[36] S. Kumar, R. Kumar, K. S. Gandhi, *Chem. Eng. Sci.* **1991**, *46*, 2365.

[37] L. Liu, O. K. Matar, E. De Susana Perez Ortiz, G. F. Hewitt, *Chem. Eng. Sci.* **2005**, *60*, 85.

[38] R. N. Reeve, J. C. Godfrey, *Chem. Eng. Res. Des*, **2002**, *80*.

[39] M. Tidhar, J. C. Merchuk, A. N. Sembira, D. Wolf, *Chem. Eng. Sci.* **1986**, *41*, 457.

[40] K. B. Deshpande, S. Kumar, *Chem. Eng. Sci.* **2003**, *58*, 3829.

[41] W. A. Rodger, V. G. Trice, J. H. Rushton, *Chem. Eng. Prog.* **1956**, *52*.

[42] L. Y. Yeo, O. K. Matar, E. S. P. de Ortiz, G. F. Hewitt, E. S. Perez De Ortiz, G. F. Hewitt, *J. Colloid Interface Sci.* **2002**, *248*, 443.

[43] L. Y. Yeo, O. K. Matar, E. S. de Perez Ortiz,G. F. Hewitt, *Multiph. Sci. Technol.* **2000**, *12*, 51–116.

[44] J. L. L. Cayias, R. S. S. Schechter, W. H. H. Wade, *Soc. Pet. Eng. J.* **1976**, *16*, 351.

[45] J. L. Salager, J. C. Morgan, R. S. Schechter, W. H. Wade, E. Vasquez, *Soc. Pet. Eng. J.* **1979**, *19*, 107.

[46] J. C. Morgan, R. S. Schechter, W. H. Wade, in *Improved Oil Recovery by Surfactant and Polymer Flooding*, (Eds: D. O. Shah, R. S. Shechter), Academic Press, Inc., New York **1977**, p. 103.

[47] J.-L. Salager, A. M. Forgiarini, J. Bullón, *J. Surfactants Deterg.* **2013**, *16*, 449.

[48] T. Sottmann, R. Strey, *J. Chem. Phys.* **1997**, *106*, 8606.

[49] H. Leitão, A. M. Somoza, M. M. Telo Da Gama, T. Sottmann, R. Strey, *J. Chem. Phys.* **1996**, *105*, 2875.

[50] R. Strey, *Colloid Polym. Sci.* **1994**, *272*, 1005.

[51] S. Sajjadi, F. Jahanzad, M. Yianneskis, B. W. Brooks, *Ind. Eng. Chem. Res.* **2002**, *41*, 6033.

[52] S. Clarke, H. Sawistowski, *Chem. Eng. Res. Des.* **1978**, *56*, 50.

[53] R. W. Luhning, H. Sawistowski, presented at International Solvent Extraction Conference, The Hague, April **1971**.

[54] S. Kato, E. Nakayama, J. Kawasaki, *Can. J. Chem. Eng.* **1991**, *69*, 222.

[55] G. F. Freeguard, M. Karmarkar, *J. Appl. Polym. Sci.* **1972**, *16*, 69.

[56] M. Homs, G. Calderó, M. Monge, D. Morales, C. Solans, *Colloids Surfaces A Physicochem. Eng. Asp.* **2018**, *536*, 204.

[57] F. Wang, Y. Ouyang, H. Zou, Z. Yang, H. Liu, *Colloids Surfaces A Physicochem. Eng. Asp.* **2017**, *535*, 274.

[58] L. Besnard, F. Marchal, J. F. Paredes, J. Daillant, N. Pantoustier, P. Perrin, P. Guenoun, *Adv. Mater.* **2013**, *25*, 2844.

[59] X. Huang, R. Fang, D. Wang, J. Wang, H. Xu, Y. Wang, X. Zhang, *Small* **2015**, *11*, 1537.

[60] X. Huang, Y. Yang, J. Shi, H. T. Ngo, C. Shen, W. Du, Y. Wang, *Small* **2015**, *11*, 4876.

[61] G. Duan, A. Kumar, S. Li, C. M. Cheng, D. Lee, *J. Colloid Interface Sci.* **2019**, *537*, 579.

[62] B. W. Brooks, H. N. Richmond *Chem. Eng. Sci.* **1994**, *49*, 1053.

[63] B. W. Brooks, H. N. Richmond, *Chem. Eng. Sci.* **1994**, *49*, 1065.

[64] A. T. Florence, J. A. Rogers, *J. Pharm. Pharmacol.* **1971**, *23*, 233.

[65] P. Becher, *J. Soc. Cosmet. Chem.* **1958**, *9*, 141.

[66] S. Sajjadi, M. Zerfa, B. W. Brooks, *Colloids Surfaces A Physicochem. Eng. Asp.* **2003**, *218*, 241.

[67] J. L. Salager, L. Márquez, A. A. Peña, M. Rondón, F. Silva, E. Tyrode, *Ind. Eng. Chem. Res.* **2000**, *39*, 2665.

[68] B. W. Brooks, H. N. Richmond, *Colloids and Surfaces* **1991**, *58*, 131.

[69] J. L. Salager, A. Forgiarini, L. Márquez, A. Peña, A. Pizzino, M. P. Rodriguez, M. Rondón-González, *Adv. Colloid Interface Sci.* **2004**, *108–109*, 259.

[70] S. Queste, J. L. Salager, R. Strey, J. M. Aubry, *J. Colloid Interface Sci.* **2007**, *312*, 98.

[71] E. J. Acosta, *Colloids Surfaces A Physicochem. Eng. Asp.* **2008**, *320*, 193.

[72] L. Jin, A. Jamili, Z. Li, J. Lu, H. Luo, B. J. Ben Shiau, M. Delshad, J. H. Harwell, *J. Pet. Sci. Eng.* **2015**, *136*, 68.

[73] A. Maestro, I. Solè, C. González, C. Solans, J. M. Gutiérrez, *J. Colloid Interface Sci.* **2008**, *327*, 433.

[74] H. Shinoda, K. Arai, *J. Phisical Chem.* **1964**, *68*, 3485.

[75] K. Shinoda, H. Saito, *J. Colloid Interface Sci.* **1968**, *26*, 70.

[76] K. Shinoda, H. Saito, *J. Colloid Interface Sci.* **1969**, *30*, 258.

[77] K. Shinoda, H. Takeda, *J. Colloid Interface Sci.* **1970**, *32*, 642.

[78] C. Parkinson, P. Sherman, *J. Colloid Interface Sci.* **1972**, *41*, 328.

[79] P. Dokic, P. Sherman, *Colloid Polym. Sci.* **1980**, *258*, 1159.

[80] J. Rao, D. J. McClements, *J. Agric. Food Chem.* **2010**, *58*, 7059.

[81] A. Kabalnov, H. Wennerström, *Langmuir* **1996**, *12*, 276.

[82] H. Kunieda, K. Shinoda, *Bull. Chem. Soc. Jpn.* **1982**, *55*, 1777–1781.

[83] F. Boscán, M. J. Barandiaran, M. Paulis, *J. Ind. Eng. Chem.* **2018**, *58*, 1.

[84] E. Dickinson, *J. Colloid Interface Sci.* **1982**, *87*, 416.

[85] P. Poesio, G. P. Beretta, *Int. J. Multiph. Flow* **2008**, *34*, 684.

[86] T. Al-Sahhaf, A. Elkamel, A. S. Ahmed, A. R. Khan, *Chem. Eng. Commun.* **2005**, *192*, 667.

[87] L. H. Chen, Y. L. Lee, *AIChE J.* **2000**, *46*, 160.

[88] A. Bąk, W. Podgórska, *Colloids Surfaces A Physicochem. Eng. Asp.* **2016**, *504*, 414.

[89] A. Domínguez, A. Fernández, N. González, E. Iglesias, L. Montenegro, *J. Chem. Educ.* **1997**, *74*, 1227.

[90] J. Saien, S. Akbari, *J. Chem. Eng. Data* **2006**, *51*, 1832.

[91] P. Becher, *Emulsions: theory and practice*, 2nd ed, Reinhold Publishing Corporation, New York, **1965**.

[92] F. Groeneweg, W. G. M. Agterof, P. Jaeger, J. J. M. Janssen, J. A. Wieringa, J. K. Klahn, *Chem. Eng. Res. Des.* **1998**, *76*, 55.

[93] I. Sole, A. Maestro, C. Gonza, C. Solans, M. Gutie, *Langmui* **2006**, *22*, 8326.

[94] E. Assadpour, Y. Maghsoudlou, S. M. Jafari, M. Ghorbani, M. Aalami, *Int. J. Biol. Macromol.* **2016**, *86*, 197.

[95] C. V Sternling, L. E. Scriven, *AIChE J.* **1959**, *5*, 514.

[96] A. Kumar, S. Li, C. M. Cheng, D. Lee, *Ind. Eng. Chem. Res.* **2015**, *54*, 8375.

[97] Y. Deng, N. L. Thomas, *Eur. Polym. J.* **2015**, *71*, 534.

[98] A. Adedeji, A. M. Jamieson, S. D. Hudson, *Macromolecules* **1995**, *28*, 5255.

[99] P. Charoensirisomboon, T. Chiba, T. Inoue, M. Weber, *Polymer (Guildf).* **2000**, *41*, 5977.

[100] X. Zhang, Z. Yin, J. Yin, *J. Appl. Polym. Sci.* **1996**, *62*, 893.

[101] C. Épinat, L. Trouillet-Fonti, P. Sotta, *Polymer (Guildf).* **2018**, *137*, 132.

[102] D. Bourry, B. D. Favis, *J. Polym. Sci. Part B Polym. Phys.* **1998**, *36*, 1889.

[103] R. Díaz de León, G. Morales, P. Acuña, F. Soriano, *Polym. Eng. Sci.* **2010**, *50*, 373.

[104] G. Soto, E. Nava, M. Rosas, M. Fuenmayor, I. M. González, G. R. Meira, H. M. Oliva, *J. Appl. Polym. Sci.* **2004**, *92*, 1397.

[105] M. Fischer, G. P. Hellmann, *Macromolecules* **1996**, *29*, 2498.

[106] D. B. Genovese, *Adv. Colloid Interface Sci.* **2012**, *171–172*, 1.

[107] C. Liu, M. Li, R. Han, J. Li, C. Liu, *J. Dispers. Sci. Technol.* **2016**, *37*, 333.

[108] R. Pal, *AIChE J.* **1996**, *42*, 3181.

[109] J. Bałdyga, M. Jasińska, A. J. Kowalski, *Chem. Eng. Res. Des.* **2016**, *108*, 3.

[110] P. Sherman, *J. Colloid Sci.* **1955**, *10*, 63.

[111] P. Snabre, P. Mills, *Colloids Surfaces A Physicochem. Eng. Asp.* **1999**, *152*, 79.

[112] P. Kundu, V. Kumar, I. M. Mishra, *J. Dispers. Sci. Technol.* **2018**, *39*, 384.

[113] J. M. Maffi, N. Casis, P. Acuña, G. Morales, D. A. Estenoz, *Polym. Eng. Sci.* **2020**, *60*, 491

[114] G. F. Freeguard, M. Karmarkar, *J. Appl. Polym. Sci.* **1971**, *15*, 1649.

[115] T. S. Omonov, C. Harrats, P. Moldenaers, G. Groeninckx, *Polymer (Guildf).* **2007**, *48*, 5917.

[116] N. Bremond, H. Doméjean, J. Bibette, *Phys. Rev. Lett.* **2011**, *106*, 1.

[117] A. Kumar, S. Li, C. M. Cheng, D. Lee, *Lab Chip* **2016**, *16*, 4173.

[118] A. Deblais, R. Harich, D. Bonn, A. Colin, H. Kellay, *Langmuir* **2015**, *31*, 5971.

[119] B. Hu, O. K. Matar, G. F. Hewitt, P. Angeli, *Chem. Eng. Sci.* **2006**, *61*, 4994.

[120] C. Shih, *Polym. Eng. Sci.* **1995**, *35*, 1688.

[121] U. Sundararaj, C. W. Macosko, C. K. Shih, *Polym. Eng. Sci.* **1996**, *36*, 1769.

[122] M. Zerfa, S. Sajjadi, B. W. Brooks, *Colloids Surfaces A Physicochem. Eng. Asp.* **2001**, *178*, 41.

[123] S. M. Fakhr-Din, *PhD Thesis*, University of Manchester, Manchester **1973**.

[124] N. Brauner, A. Ullmann, *Int. J. Multiph. Flow* **2002**, *28*, 1177.

[125] A. Kabalnov, J. Weers, *Langmuir* **1996**, *12*, 1931.

[126] L. M. Oshinowo, C. G. Quintero, R. D. Vilagines, *J. Dispers. Sci. Technol.* **2016**, *37*, 665.

[127] Z. Gao, D. Li, A. Buffo, W. Podgórska, D. L. Marchisio, *Chem. Eng. Sci.* **2016**, *142*, 277.

[128] D. Li, A. Buffo, W. Podgórska, D. L. Marchisio, Z. Gao, *Chinese J. Chem. Eng.* **2017**, *25*, 1369.

[129] S. Aryafar, N. Sheibat-Othman, T. F. L. McKenna, *Macromol. React. Eng.* **2017**, *11*, 1.

[130] G. Yang, H. Zhang, J. Luo, T. Wang, *Chem. Eng. Sci.* **2018**, *192*, 714.

[131] C. Qin, C. Chen, Q. Xiao, N. Yang, C. Yuan, C. Kunkelmann, M. Cetinkaya, K. Mülheims, *Chem. Eng. Sci.* **2016**, *155*, 16.

[132] L. Xie, Q. Liu, Z. H. Luo, *Chem. Eng. Res. Des.* **2018**, *130*, 1.

[133] S. Castellano, N. Sheibat-Othman, D. Marchisio, A. Buffo, S. Charton, *Chem. Eng. J.* **2018**, *354*, 1197.

[134] M. v. Smoluchowski, *Kolloid-Zeitschrift* **1916**, *18*, 190.

[135] A. S. C. Lawrence, O. S. Mills, *Discuss. Faraday Soc.* **1954**, *18*, 98.

[136] W. J. J. Howarth, *Chem. Eng. Sci.* **1964**, *19*, 33.

[137] T. Gillespie, *J. Colloid Sci.* **1962**, *17*, 290.

[138] R. Shinnar, *J. Fluid Mech.* **1961**, *10*, 259.

[139] R. S. Allan, S. G. Mason, *J. Colloid Sci.* **1962**, *17*, 383.

[140] G. D. M. Mackay, S. G. Mason, *Can. J. Chem. Eng.* **1963**, *41*, 203.

[141] J. C. Lee, T. D. Hodgson, *Chem. Eng. Sci.* **1968**, *23*, 1375.

[142] S. L. Ross, *PhD Thesis*, The University of Michigan, Ann Arbor, **1971**.

[143] B. Liu, R. Manica, Q. Liu, E. Klaseboer, Z. Xu, G. Xie, *Phys. Rev. Lett.* **2019**, *122*, 194501.

[144] A. K. Chesters, *Chem. Eng. Res. Des.* **1991**, *69*, 259.

[145] G. Besagni, F. Inzoli, *Chem. Eng. Res. Des.* **2017**, *118*, 170.

[146] H. Sovová, *Chem. Eng. Sci.* **1981**, *36*, 1567.

[147] E. G. Chatzi, C. Kiparissides, E. Details, A. D. Gavrielides, C. Kiparissides, *Ind. Eng. Chem. Res.* **1989**, *28*, 1704.

[148] M. Simon, *PhD Thesis*, Techinsche Universität Kaiserslautern, Kaiserslautern **2004**.

[149] H. Sovová, J. Prochazka, *Chem. Eng. Sci.* **1981**, *36*, 163.

[150] J. M. H. Janssen, H. E. Meijer, *Polym. Eng. Sci.* **1995**, *35*, 1766.

[151] S. P. Lyu, F. S. Bates, C. W. Macosko, *AIChE J.* **2000**, *46*, 229.

[152] J. Kamp, J. Villwock, M. Kraume, *Rev. Chem. Eng.* **2017**, *33*, 1.

[153] P. M. M. Bapat, L. L. L. Tavlarides, G. W. W. Smith, *Chem. Eng. Sci.* **1983**, *38*, 2003.

[154] M. J. Prince, H. W. Blanch, *AIChE J.* **1990**, *36*, 1485.

[155] M. A. Delichatsios, R. F. Probstein, *J. Colloid Interface Sci.* **1975**, *51*, 394.

[156] G. Kocamustafaogullari, M. Ishii, *Int. J. Heat Mass Transf.* **1995**, *38*, 481.

[157] T. Wang, J. Wang, Y. Jin, *Ind. Eng. Chem. Res.* **2005**, *44*, 7540.

[158] C. A. Coulaloglou, L. L. L. Tavlarides, *Chem. Eng. Sci.* **1977**, *32*, 1289.

[159] A. W. Nienow, *Adv. Colloid Interface Sci.* **2004**, *108–109*, 95.

[160] T. Hibiki, M. Ishii, *Int. J. Heat Mass Transf.* **2000**, *43*, 2711.

[161] F. Lehr, M. Millies, D. Mewes, *AIChE J.* **2002**, *42*, 1225.

[162] T. Wang, J. Wang, Y. Jin, *Chem. Eng. Sci.* **2005**, *60*, 6199.

[163] I. U. Vakarelski, R. Manica, E. Q. Li, E. S. Basheva, D. Y. C. Chan, S. T. Thoroddsen, *Langmuir* **2018**, *34*, 2096.

[164] D. Y. C. Chan, E. Klaseboer, R. Manica, *Soft Matter* **2011**, *7*, 2235.

[165] E. Klaseboer, J. P. Chevaillier, C. Gourdon, O. Masbernat, *J. Colloid Interface Sci.* **2000**, *229*, 274.

[166] K. Guo, T. Wang, Y. Liu, J. Wang, *Chem. Eng. J.* **2017**, *329*, 116.

[167] S. G. Yiantsios, R. H. Davis, *J. Fluid Mech.* **1990**, *217*, 547.

[168] C. Tsouris, L. L. Tavlarides, *AIChE J.* **1994**, *40*, 395.

[169] A. Vrij, *Discuss. Faraday Soc.* **1966**, *42*, 23.

[170] S. Abid, A. K. Chesters, *Int. J. Multiph. Flow* **1994**, *20*, 613.

[171] T. G. M. van de Ven, S. G. Mason, *J. Colloid Interface Sci.* **1976**, *57*, 505.

[172] G. R. Zeichner, W. R. Schowalter, *AIChE J.* **1977**, *23*, 243.

[173] M. Manga, H. A. Stone, *J. Fluid Mech.* **1993**, *256*, 647.

[174] M. Manga, H. A. Stone, *J. Fluid Mech.* **1995**, *300*, 231.

[175] X. Zhang, R. H. Davis, *J. Fluid Mech.* **1991**, *230*, 479.

[176] H. Wang, A. Z. Zinchenko, R. H. Davis, *J. Fluid Mech.* **1994**, *265*, 161.

[177] M. A. Rother, A. Z. Zinchenko, R. H. Davis, *J. Fluid Mech.* **1997**, *346*, 117.

[178] M. A. Rother, R. H. Davis, *Phys. Fluids* **2001**, *13*, 1178.

[179] Y. Liao, D. Lucas, *Chem. Eng. Sci.* **2010**, *65*, 2851.

[180] L. A. Utracki, Z. H. Shi, *Polym. Eng. Sci.* **1992**, *32*, 1824.

[181] S. Lyu, F. S. Bates, C. W. Macosko, *AIChE J.* **2002**, *48*, 7.

[182] A. K. Chesters, I. B. Bazhlekov, *J. Colloid Interface Sci.* **2000**, *230*, 229.

[183] J. Boyd, C. Parkinson, P. Sherman, *J. Colloid Interface Sci.* **1972**, *41*, 359.

[184] A. J. Ramic, J. C. Stehlin, S. D. Hudson, A. M. Jamieson, I. Manas-zloczower, *Macromolecules* **2000**, *33*, 371.

[185] L. Leibler, *Makromol. Chemie. Macromol. Symp.* **1988**, *16*, 1.

[186] M. Mathew, S. Thomas, *Polymer (Guildf).* **2003**, *44*, 1295.

[187] D. Heikens, W. Barentsen, *Polymer (Guildf).* **1977**, *18*, 69.

[188] S. Jouenne, J. A. González-Léon, A. V. Ruzette, P. Lodéfier, L. Leibler, *Macromolecules* **2008**, *41*, 9823.

[189] C. Pagnoulle, R. Jérôme, *Polymer (Guildf).* **2001**, *42*, 1893.

[190] D. Thomas, L. Sperling,, in *Polymer Blends*, (Eds: D. R. Paul, S. Newman), , Academic Press, Inc., New York **1978**.

[191] H. R. Brown, K. Char, V. R. Deline, in *Integration of fundamental polymer science and technology*, (Eds: P. J. Lemstra, L. A. Kleintjens), Elsevier Applied Science, London, New York, **1990**.

[192] J.C. Lepers, B. D. Favis, C. Lacroix, *J. Polym. Sci. Prat B Polym. Phys.* **1999**, *37*, 939.

[193] S. P. Lyu, T. D. Jones, F. S. Bates, C. W. Macosko, *Macromolecules* **2002**, *35*, 7845.

[194] N. C. Beck Tan, S. K. Tai, R. M. Briber, *Polymer (Guildf).* **1996**, *37*,

3509.

[195] S. T. Milner, H. Xi, *J. Rheol. (N. Y. N. Y).* **1996**, *40*, 663.

[196] U. Sundararaj, C. W. Macosko, *Macromolecules* **1995**, *28*, 2647.

[197] X. Luo, X. Huang, H. Yan, D. Yang, P. Zhang, L. He, *Sep. Purif. Technol.* **2018**, *203*, 152.

[198] Y. Liao, D. Lucas, *Chem. Eng. Sci.* **2009**, *64*, 3389.

[199] E. H. Herø, N. La Forgia, J. Solsvik, H. A. Jakobsen, *Chem. Eng. Technol.* **2019**, *42*, 903.

[200] M. Kostoglou, A. J. Karabelas, *Chem. Eng. Sci.* **2005**, *60*, 6584.

[201] J. C. C. Lasheras, C. Eastwood, C. Martínez-Bazán, J. L. Montaes, C. Martínez-Bazán, J. L. Montañés, *Int. J. Multiph. Flow* **2002**, *28*, 247.

[202] J. Baldyga, W. Podgórska, *Can. J. Chem. Eng.* **1998**, *76*, 456.

[203] G. M. Evans, G. J. Jameson, B. W. Atkinson, *Chem. Eng. Sci.* **1992**, *47*, 3265.

[204] A. K. Bin, *Chem. Eng. Sci.* **1993**, *48*, 3585.

[205] X. Y. Fu, M. Ishii, *Nucl. Eng. Des.* **2002**, *219*, 143.

[206] G. Narsimhan, J. P. Gupta, D. Ramkrishna, *Chem. Eng. Sci.* **1979**, *34*, 257.

[207] L. Hagesaether, H. A. Jakobsen, H. F. Svendsen, *Chem. Eng. Sci.* **2002**, *57*, 3251.

[208] F. Lehr, D. Mewes, *Chem. Eng. Sci.* **2001**, *56*, 1159.

[209] C. Y. Wang, R. V Calabrese, *AIChE J.* **1986**, *32*, 667.

[210] T. Wang, J. Wang, Y. Jin, *Chem. Eng. Sci.* **2003**, *58*, 4629.

[211] P. H. M. Elemans, J. M. H. Janssen, H. E. H. Meijer, *J. Rheol.* **1990**, *34*, 1311.

[212] R. Andersson, B. Andersson, *AIChE J.* **2006**, *52*, 2020.

[213] J. Alvarez, J. Alvarez, M. Hernández, *Chem. Eng. Sci.* **1994**, *49*, 99.

[214] P. Chu, J. Finch, G. Bournival, S. Ata, C. Hamlett, R. J. Pugh, *Adv. Colloid Interface Sci.* **2019**, *270*, 108.

[215] H. P. Grace, *Chem. Eng. Commun.* **1982**, *277*, 225.

[216] B. J. Bentley, L. G. Leal, *J. Fluid Mech. Digit. Arch.* **2006**, *167*, 219.

[217] G. I. Taylor, *Proc. R. Soc. London A.* **1932**, *138*, 41.

[218] K. Arai, M. Konno, Y. Matunaga, S. Saito, *J. Chem. Eng. Japan* **1977**, *10*, 325.

[219] S. Wu, *Polym. Eng. Sci.* **1987**, *27*, 335.

[220] P. H. M. Elemans, H. L. Bos, J. M. H. Janssen, H. E. H. Meijer, *Chem. Eng. Sci.* **1993**, *48*, 267.

[221] J. J. Elmendorp, *Polym. Eng. Sci.* **1986**, *26*, 418.

[222] R. A. De Bruijn, *Chem. Eng. Sci.* **1993**, *48*, 277.

[223] S. Tomotika, *Proc. R. Soc. A Math. Phys. Eng. Sci.* **1935**, *150*, 322.

[224] J. O. Hinze, *AIChE J.* **1955**, *1*, 289.

[225] J. S. Lagisetty, P. K. Das, R. Kumar, K. S. Gandhi, *Chem. Eng. Sci.* **1986**, *41*, 65.

[226] C. A. Coulaloglou, L. L. Tavlarides, *AIChE J.* **1976**, *22*, 289.

[227] A. Koshy, R. Kumar, K. S. Gandhi, *Chem. Eng. Sci.* **1989**, *44*, 2113.

[228] H. A. Stone, L. G. Leal, *J. Fluid Mech.* **1990**, *220*, 161.

[229] C. D. Eggleton, T. M. Tsai, K. J. Stebe, *Phys. Rev. Lett.* **2001**, *87*, 48302.

[230] N. Ashgriz, J. Y. Poo, *J. Fluid Mech.* **1990**, *221*, 183.

[231] W. Seifriz, *J. Phys. Chem.* **1924**, *29*, 587.

[232] A. Gilchrist, K. N. Dyster, I. P. T. Moore, A. W. Nienow, K. J. Carpenter, *Chem. Eng. Sci.* **1989**, *44*, 2381.

[233] A. W. Pacek, A. W. Nienow, *Int. J. Multiph. Flow* **1995**, *21*, 323.

[234] F. Jahanzad, G. Crombie, R. Innes, S. Sajjadi, *Chem. Eng. Res. Des.* **2009**, *87*, 492.

[235] E. Sheppard, N. Tcheurekdjian, *J. Colloid Interface Sci.* **1977**, *62*, 564.

[236] T. J. Lin, H. Kurihara, T. Ohta, *J. Soc. Cosmet. Chem.* **1975**, *57*, 353.

[237] D. P. Kessler, J. L. York, *AIChE J.* **1970**, *16*, 369.

[238] S. Matsumoto, Y. Kita, D. Yonezawa, *J. Colloid Interface Sci.* **1976**, *57*, 353.

[239] S. Matsumoto, W. W. Lang, *J. Dispers. Sci. Technol. J. Dispers. Sci. Technol.* **1989**, *10*, 4.

[240] M. Frenkel, R. Shwartz, N. Garti, *J. Colloid Interface Sci.* **1983**, *94*, 174.

[241] M. Ficheux, L. Bonakdar, J. Bibette, *Langmuir* **1998**, *14*, 2702.

[242] L. Y. Chu, A. S. Utada, R. K. Shah, J. W. Kim, D. A. Weitz, *Angew. Chemie - Int. Ed.* **2007**, *46*, 8970.

[243] A. T. Florence, D. Whitehill, *J. Colloid Interface Sci.* **1981**, *79*, 243.

[244] J. M. Morais, O. D. H. H. Santos, J. R. L. L. Nunes, C. F. Zanatta, P. A. Rocha-Filho, *J. Dispers. Sci. Technol.* **2008**, *29*, 63.

[245] W. Seifriz, *J. Phys. Chem.* **1924**, *29*, 738.

[246] J. M. Morais, P. A. Rocha-Filho, D. J. Burgess, *Langmuir* **2009**, *25*, 7954.

[247] R. Pal, *AIChE J.* **1993**, *39*, 1754.

[248] A. W. Pacek, I. P. T. Moore, A. W. Nienow, R. V. Calabrese, *AIChE J.* **1994**, *40*, 1940.

[249] J. Yan, R. Pal, *J. Memb. Sci.* **2004**, *244*, 193.

[250] G. A. Davies, G. V. Jeffreys, D. V. Smith, F. A. Ali, *Can. J. Chem. Eng.* **1970**, *48*, 328.

[251] H. Bararnia, S. M. Seyyedi, D. D. Ganji, B. Khorshidi, *Colloids Surfaces A Physicochem. Eng. Asp.* **2013**, *424*, 40.

[252] J. M. Lee, K. H. Lim, D. H. Smith, *Langmuir* **2002**, *18*, 7334.

[253] A. T. Florence, D. Whitehill, *Int. J. Pharm.* **1982**, *11*, 277.

[254] L. Hong, G. Sun, J. Cai, T. Ngai, *Langmuir* **2012**, *28*, 2332.

[255] A. S. Utada, E. Lorenceau, D. R. Link, P. D. Kaplan, H. A. Stone, D. A. Weitz, *Science* **2005**, *308*, 537.

[256] C. H. Choi, D. A. Weitz, C. S. Lee, *Adv. Mater.* **2013**, *25*, 2536.

[257] S. Okushima, T. Nisisako, T. Torii, T. Higuchi, *Langmuir* **2004**, *20*, 9905.

[258] Y. Liu, E. L. Carter, G. V. Gordon, Q. J. Feng, S. E. Friberg, *Colloids Surfaces A Physicochem. Eng. Asp.* **2012**, *399*, 25.

[259] E. Tyrode, I. Mira, N. Zambrano, L. Márquez, M. Rondón-Gonzalez, J. L. Salager, *Ind. Eng. Chem. Res.* **2003**, *42*, 4311.

[260] S. Sajjadi, F. Jahanzad, M. Yianneskis, *Colloids Surfaces A Physicochem. Eng. Asp.* **2004**, *240*, 149.

[261] L. K. Saw, B. W. Brooks, K. J. Carpenter, D. V Keight, *J. Colloid Interface Sci.* **2003**, *257*, 163.

[262] L. Nielsen, R. Landel, *Mechanical properties of polymers and composites*, 2nd ed, CRC Press, **1993**.

[263] G. P. Leal, J. M. Asua, *Polymer (Guildf).* **2009**, *50*, 68.

Figure captions

FIGURE 1 Ambivalent ranges for toluene(O)-water(W) (solid lines), CCl4(O)-water(W) (dashed lines) and heptane(O)-acetonitrile(W) (dotted lines). Lines were drawn from available experimental data[12,21]

FIGURE 2 Ambivalence diagram as a function of phase viscosity ratio (built from Selker and Sleicher[10])

FIGURE 3 Comparison of predicted phase inversion (PI) points with viscosity ratio. For simplification, the stress ratio was considered equal to the apparent viscosity ratio when necessary

FIGURE 4 Interfacial tension of petroleum sulfonate aqueous solutions with different organic phases (replotted from the original figure found in Morgan et al[46])

FIGURE 5 Water-cyclohexane-nonylphenol ethoxylates (NPE) inversion map for different hydrophilic-lipophilic balance (HLB) values

FIGURE 6 Qualitative evolution of emulsion interfacial tension with temperature (taken from Kunieda and Shinoda[82]). Here, D stands for the dispersion phase

FIGURE 7 Phase inversion map as a function of temperature for water-cyclohexane-polyoxyethylene nonylphenylether (built from the original figure by Shinoda and Saito[75]). Surfactant load is 7 wt%

FIGURE 8 Effect of emulsifier concentration on surface tension (redrawn from the data by Saien and Akbari[90])

FIGURE 9 Effect of Span concentration on phase inversion (PI) of O/W to W/O systems (redrawn from the data found in Becher[91]). Values in parentheses represent the hydrophilic-lipophilic balance (HLB) of the emulsifier

FIGURE 10 Effect of Tween concentration on PI of W/O to O/W systems.

Values in parentheses indicate hydrophilic-lipophilic balance (HLB) of emulsifier

FIGURE 11 Delayed phase inversion (PI) with increasing surfactant concentration for a W/O emulsion (Groeneweg et al[92]).

FIGURE 12 Evolution of mixture viscosity with reaction time for high-impact polystyrene (HIPS) bulk process (redrawn from Freeguard and Karmarkar[114])

FIGURE 13 Storage modulus and loss factor of a polypropylene-polystyrene blend as a function of PS content (built from the data in Omonov et al[115])

FIGURE 14 Phase inversion detected with different emulsification methods (Bouchama et al[14])

FIGURE 15 Qualitative comparison of collision frequency of equal drops according to published models as a function of particle diameter

FIGURE 16 Deformable drops with different interface mobility: A, immobile interface; B, partially mobile interface; and C, fully mobile interface

FIGURE 17 A, rigid drop; and B, deformable drop

FIGURE 18 Coalescence rate as a function of surfactant's hydrophilic-lipophilic balance (HLB) (built form the data by Boyd et al[183])

FIGURE 19 Coalescence suppression by copolymer steric repulsion (Sundararaj and Macosko[196])

FIGURE 20 Effect of dispersed phase viscosity on maximum stable drop size before break-up (Arai et al[218])

FIGURE 21 Deformation process of a polyamide 6 thread surrounded by a polystyrene matrix (taken from Elemans et al[220])

FIGURE 22 Tipstreaming breakup mechanism (reproduced from de Bruijn[222])

FIGURE 23 Two possible outcomes of drop-drop collisions: coalescence

(above) and separation (below). Evolution of the process is from right to left. Taken from Ashgriz and Poo[230]

FIGURE 24 Outcome after collision map for equal size drops (Ashgriz and Poo[230])

FIGURE 25 Example of a drop-in-drop structure (reproduced from Jahanzad et al[234])

FIGURE 26 Inclusion of continuous phase by drop deformation (reproduced from Yan and Pal[249])

FIGURE 27 Entrapment mechanism proposed by Kumar[12]

FIGURE 28 Two-step method to produce a multiple emulsion (Florence and Whitehill[253])

FIGURE 29 Catastrophic phase inversions at the vicinity of the transitional threshold for a cyclohexane/water emulsion with 2 wt% NPE5/NPE12 at 22ºC (taken from Sajjadi et al[260]). Solid curve shows the threshold of transitional inversion and the dotted lines are the boundary of the catastrophic inversion from abnormal to normal morphology. In each case, white symbols represent a catastrophic inversion and black symbols transitional inversion. The approach direction is given always from white to black, as represented by the A and B examples

FIGURE 30 Effect of initiator concentration on the drop-in-drop structure. Upper figures: low concentration; lower figures: higher concentration. Reproduced from Leal and Asua[263]

TABLE 1 Models for the phase inversion point as a function of viscosity (or viscous stress)

Model	Author	Physical system
$\frac{\phi_d}{1-\phi_d} = \left(\frac{\eta_d}{\eta_c}\right)^{0.5}$	Yeh et al[22]	O/W (Nitrobenzene, benzene, cyclohexanol, etc. in water)
$\frac{\phi_d}{1-\phi_d} = \frac{\eta_d}{\eta_c}$	Jordhamo et al[11]	PS/PB. Castor oil + PS-U/PS.
$\frac{\phi_d}{1-\phi_d} = 1.22\left(\frac{\tau_d}{\tau_c}\right)^{0.29}$	Ho et al[27]	PP/EPR. PS/SBR.
$\frac{\phi_d}{1-\phi_d} = 1.2\left(\frac{\tau_d}{\tau_c}\right)^{0.3}$	Chen and Su[28]	PPS/PE.
$\frac{\phi_d}{1-\phi_d} = 0.887\left(\frac{\eta_d}{\eta_c}\right)^{0.29}$	Kitayama et al[29]	Nylon 6/Styrene-Acrylonitrile
$\frac{\phi_d}{1-\phi_d} = \left(\frac{\eta_d}{\eta_c}\right)^{0.3}$	Everaert et al[30]	PP/(PS/PE)
$\phi_d = 0.5 + \log\left(\frac{\eta_d}{\eta_c}\right)^{0.1108}$	Arirachakaran et al [31]	W/O systems, for which η_d = 1 cP and $[\eta_c]$=cP.
$\phi_d = 1 - \frac{1}{1 + \frac{\eta_d}{\eta_c}\left(1 + 2.25\log\left(\frac{\eta_d}{\eta_c}\right) + 1.81\left(\log\left(\frac{\eta_d}{\eta_c}\right)\right)^2\right)}$	Metelkin and Blekht[32]	Polymer blends in general.
$\phi_d = 0.5 + \log\left(\frac{\eta_d}{\eta_c}\right)^{5/19}$	Utracki[33]	EPDM/PB. Polymer blends in general.
$\phi_d = 0.52 + \log\left(\frac{\eta_d}{\eta_c}\right)^{3/25}$	Steinmann et al[34]	PMMA/PS. PMMA/P(SA)

ratio

TABLE 2 Effect of main operating variables on the phase inversion mechanism as a general rule

Effect on / An ↑ in	Break-up frequency (ω_b)	Coalescence frequency (ω_c)	Average particle diameter (d_{32})		Number of (stable) occlusions	φ_d at PI
Stirring speed (N)	↑	↑	↓ if ω_b↑> ω_c		↓	↑
			↑ if ω_b↑< ω_c		↑	↓
Continuous phase density (ρ_c)	↑ considering turbulent break-up	↓	↓		↓	↑
Dispersed phased density (ρ_d)	↑	↑	↓ if ω_b↑> ω_c		↓	↑
			↑ if ω_b↑< ω_c		↑	↓
Continuous phase viscosity (η_c)	↓ if turbulent break-up	↓	↓ if ω_b↓< ω_c		↓	↑
			↑ if ω_b↓> ω_c		↑	↓
	↑ if viscous shear break-up	↓	↓		↓	↑
Dispersed phase viscosity (η_d)	↓	↓	↓ if ω_b↓< ω_c		↓	↑
			↑ if ω_b↓> ω_c		↑	↓
Interfacial tension (γ)	↓	↑	↑		↑	↓
Surfactant concentration	↑	↓	↓		↓	↑
Surfactant's HLB	∩	∪	∪		∪	∩
Relative permittivity (ϵ)	↓	↑	↑		↑	↓

Abbreviations: PI: phase inversion; HLB: hydrophilic-lipophilic balance.

Note: ∩ and ∪ symbols indicate that the variable reaches a maximum or minimum value, respectively.

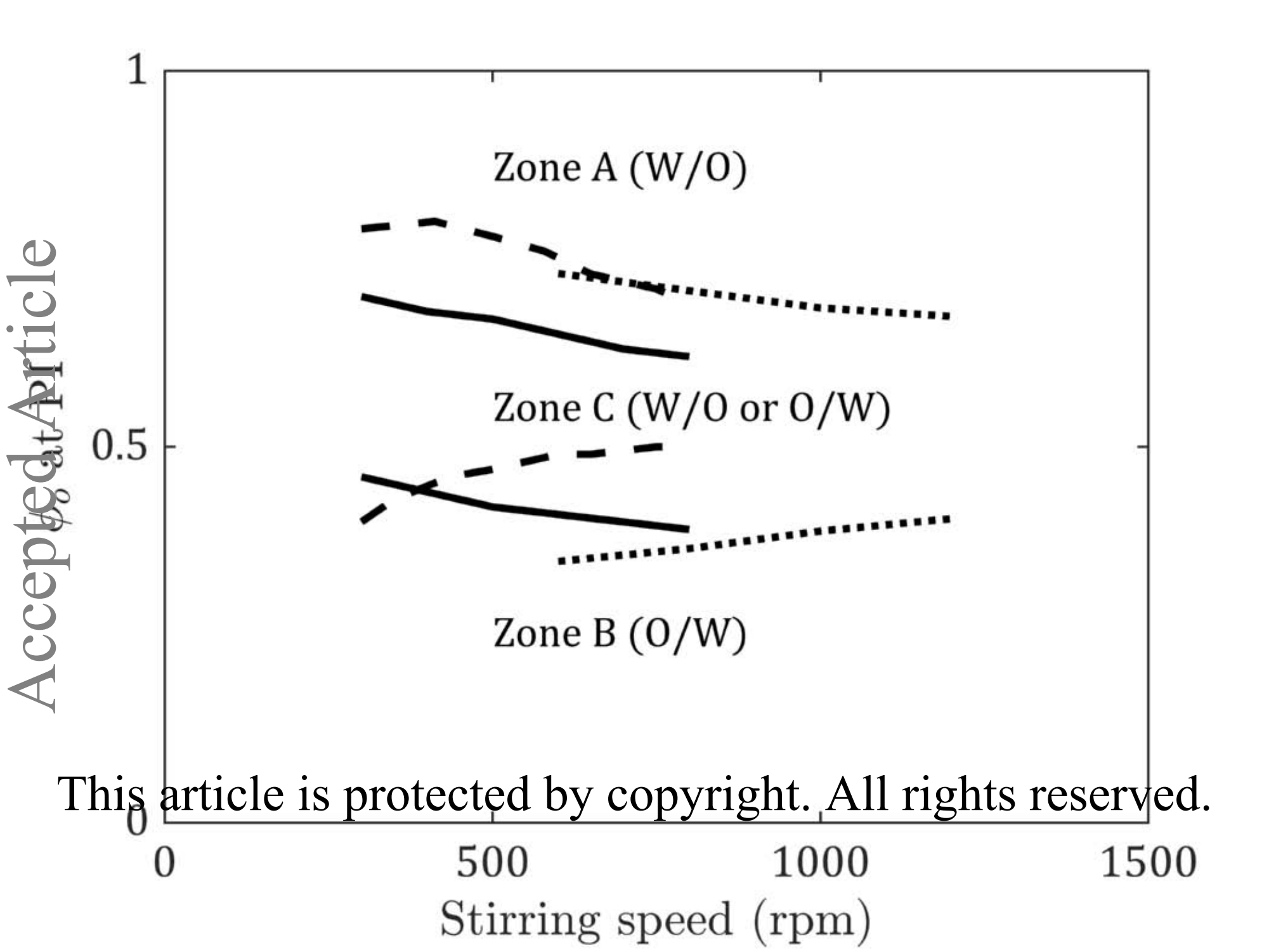

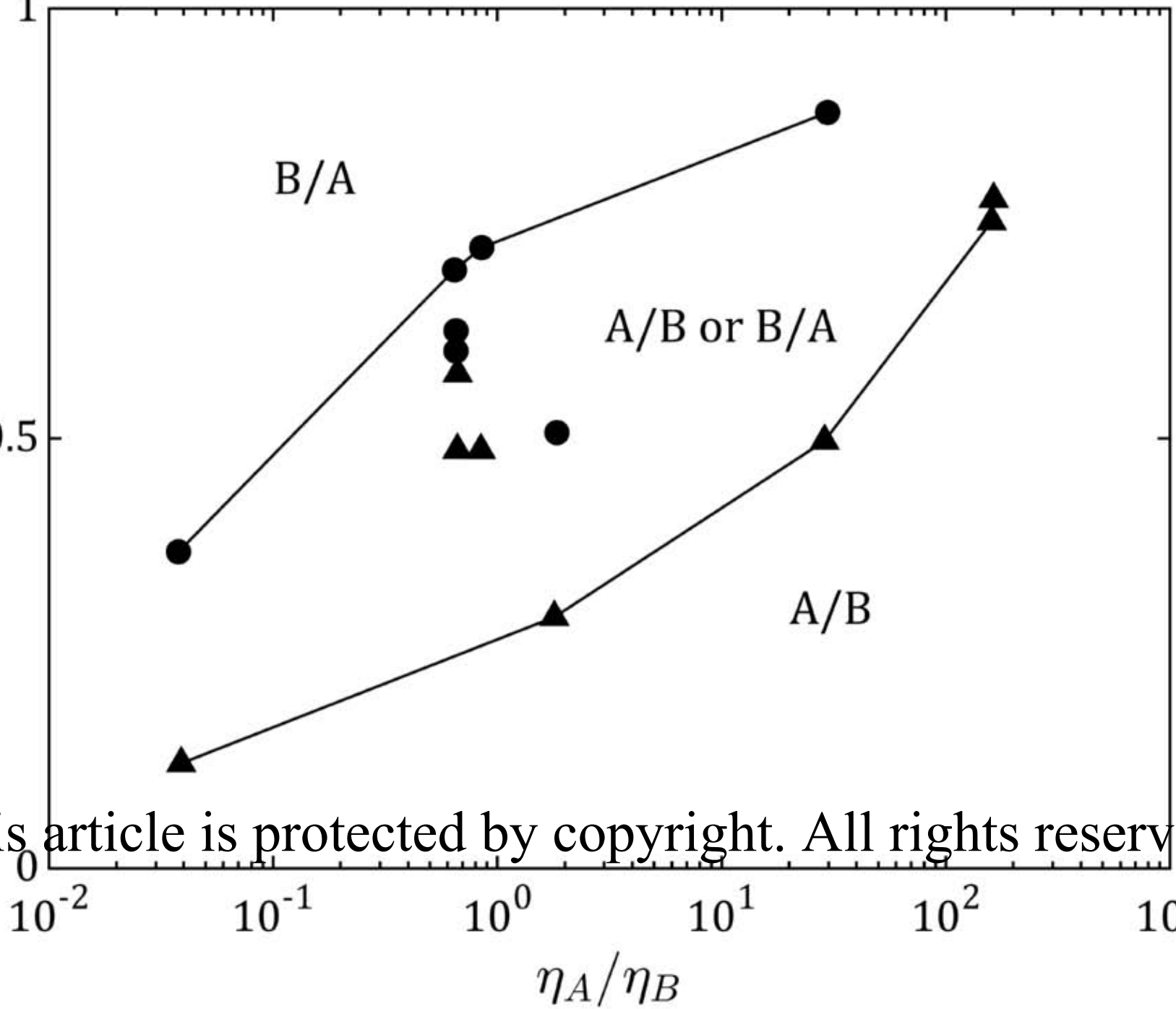

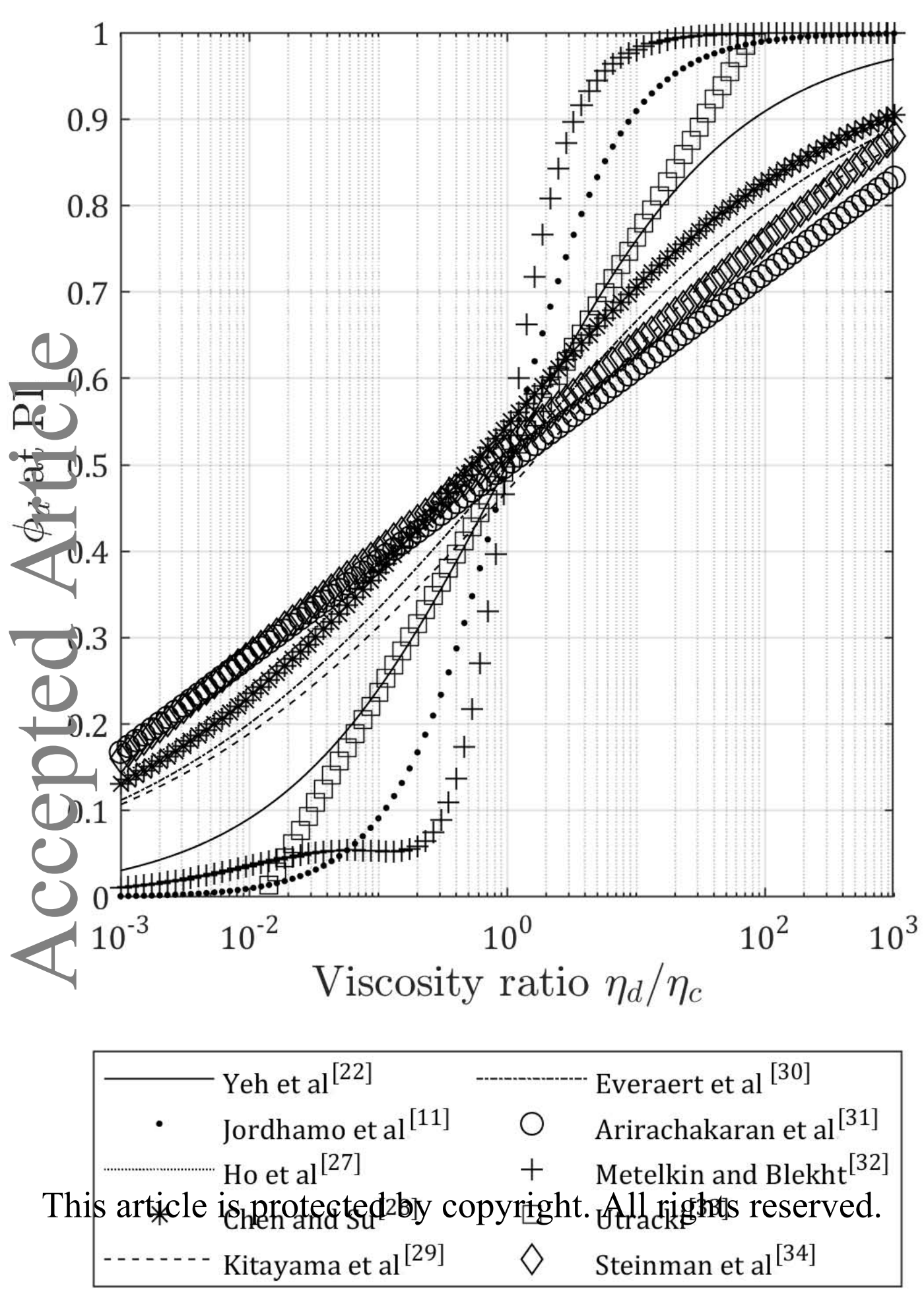

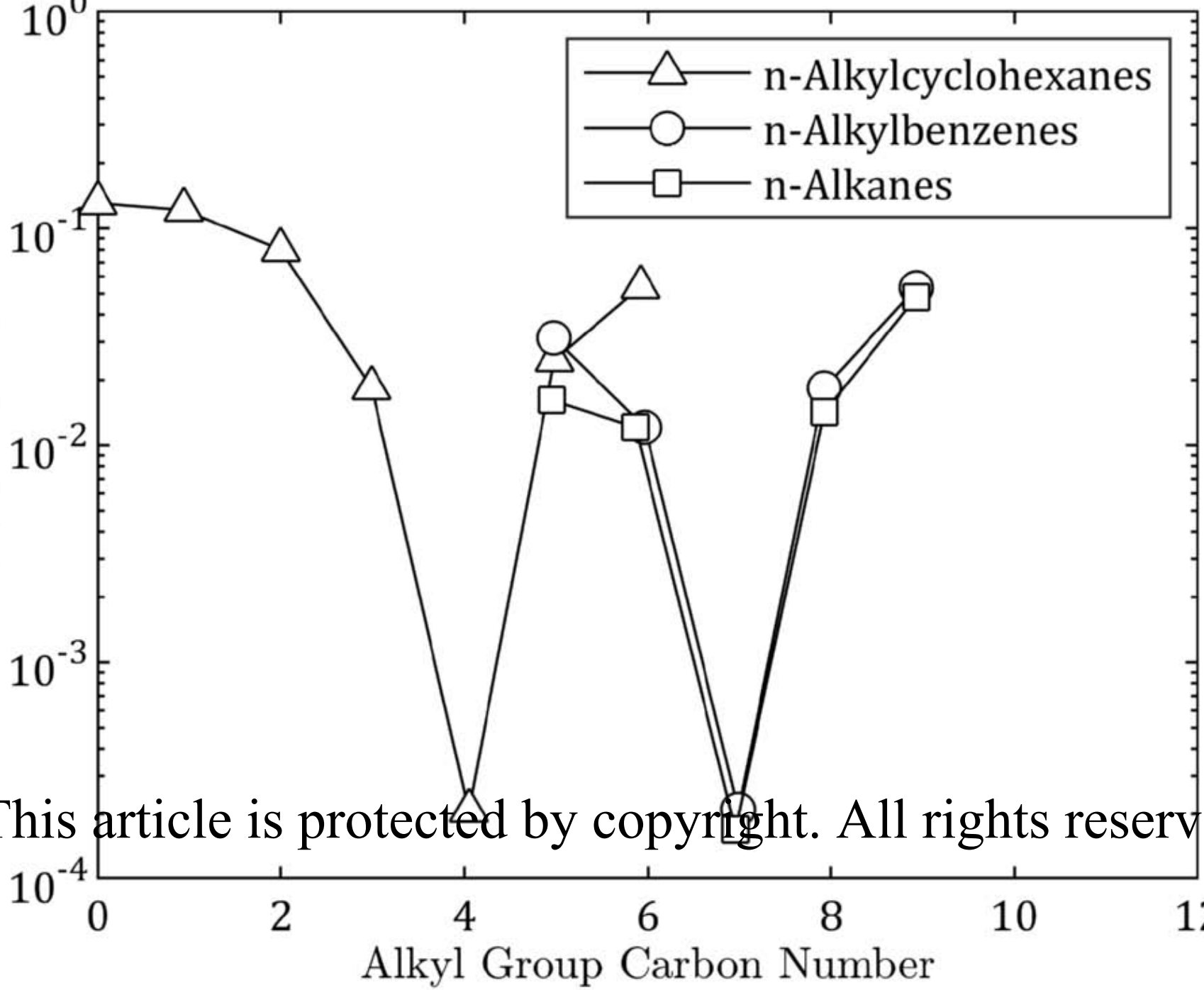

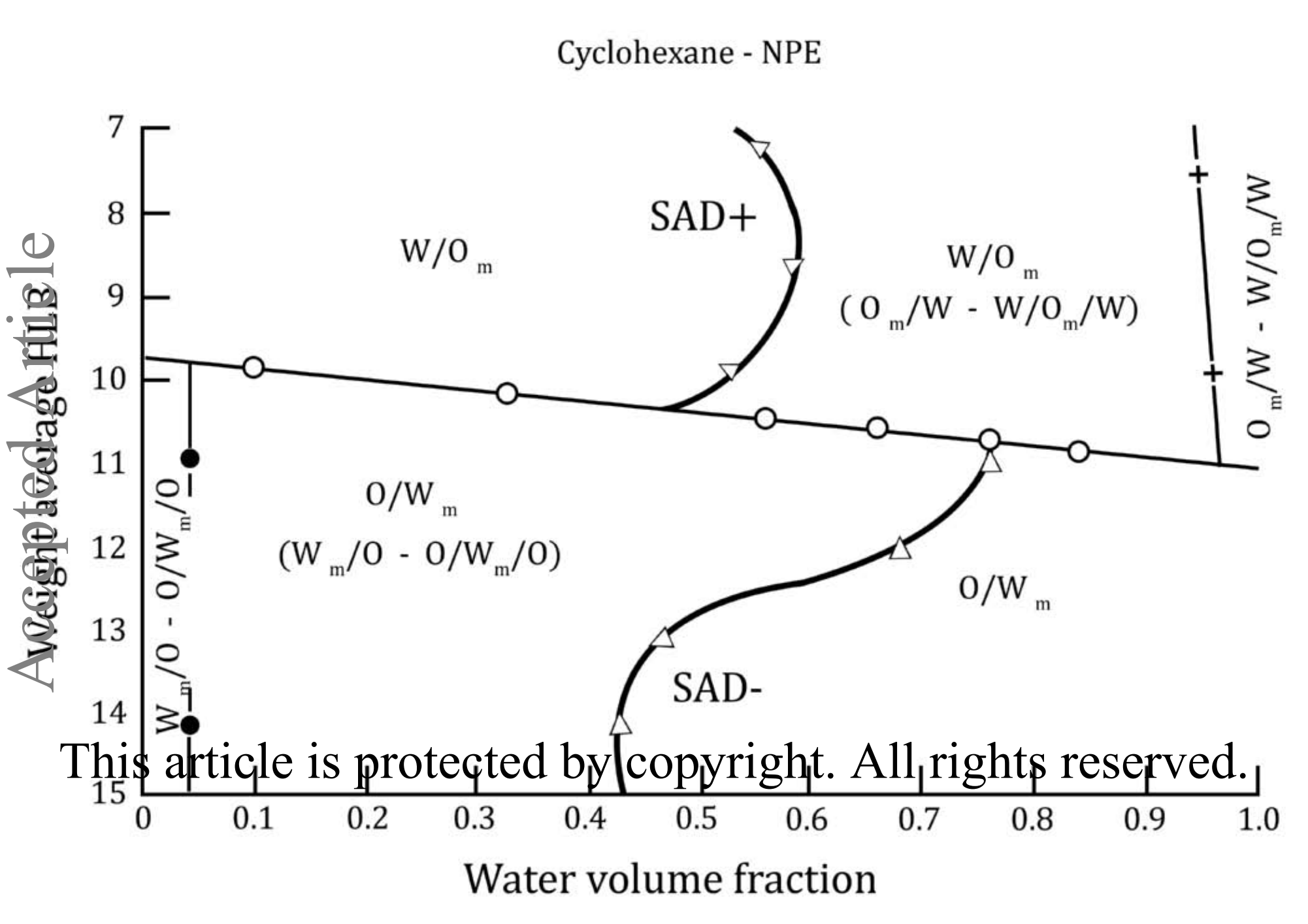

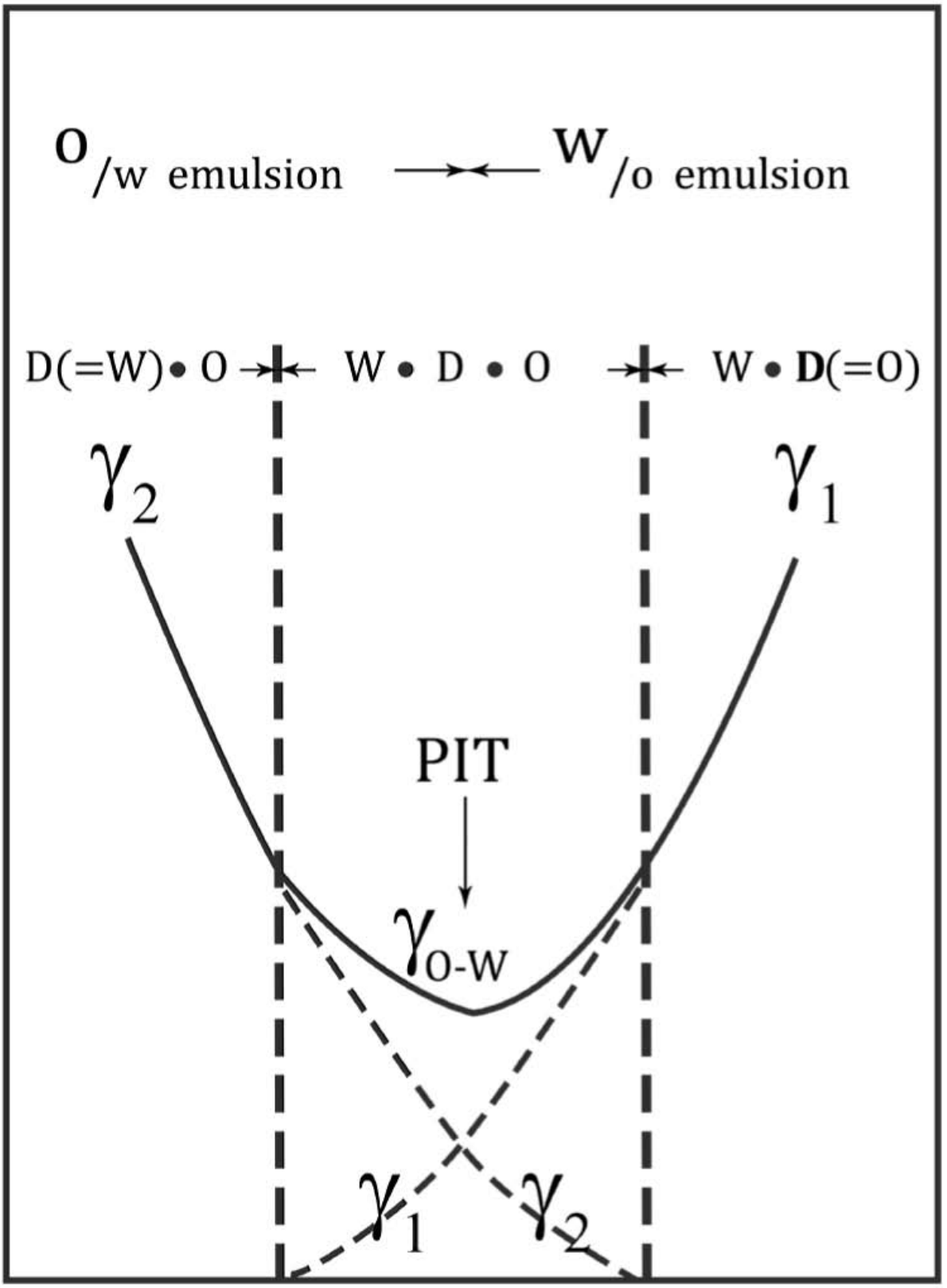

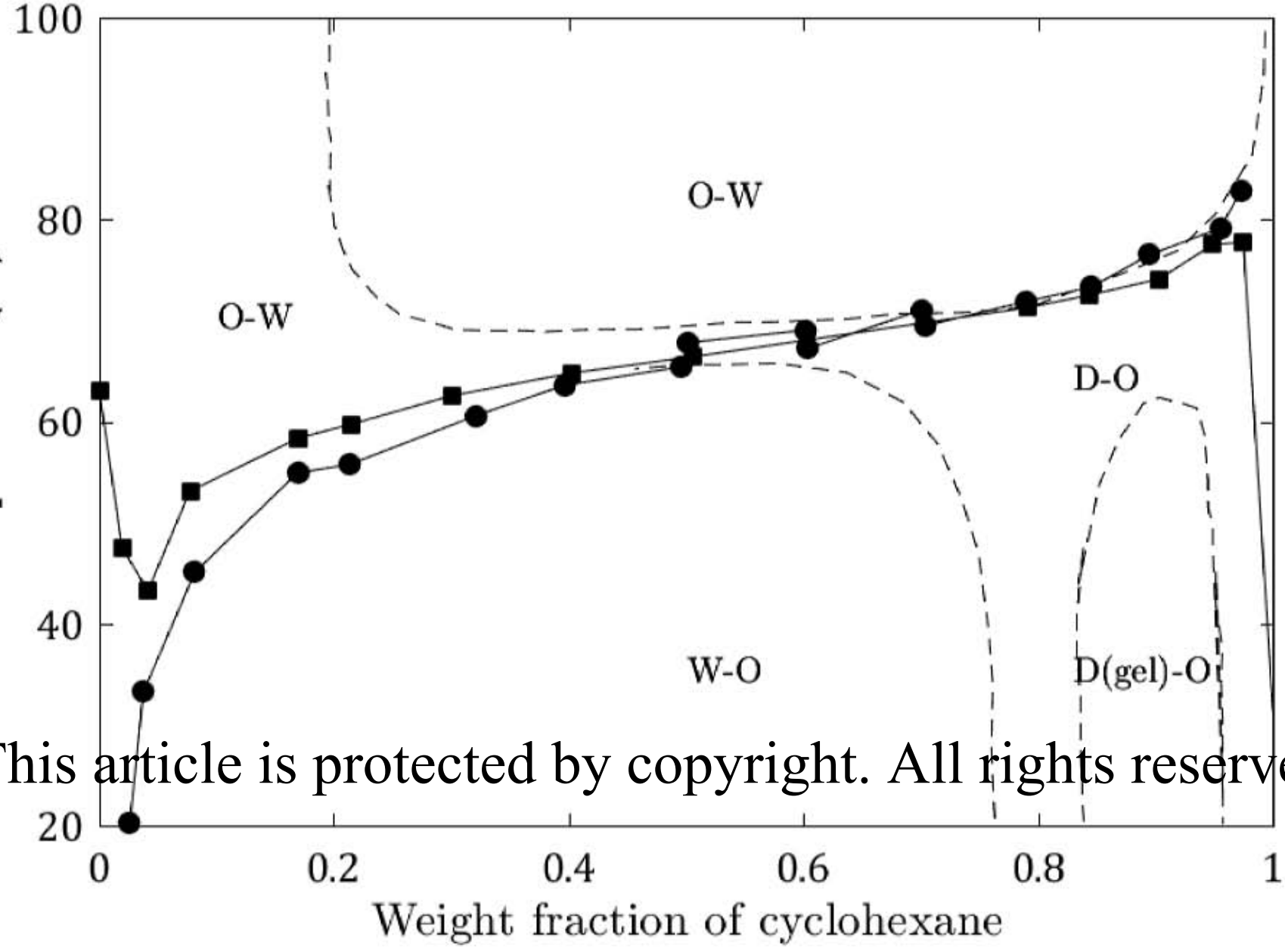

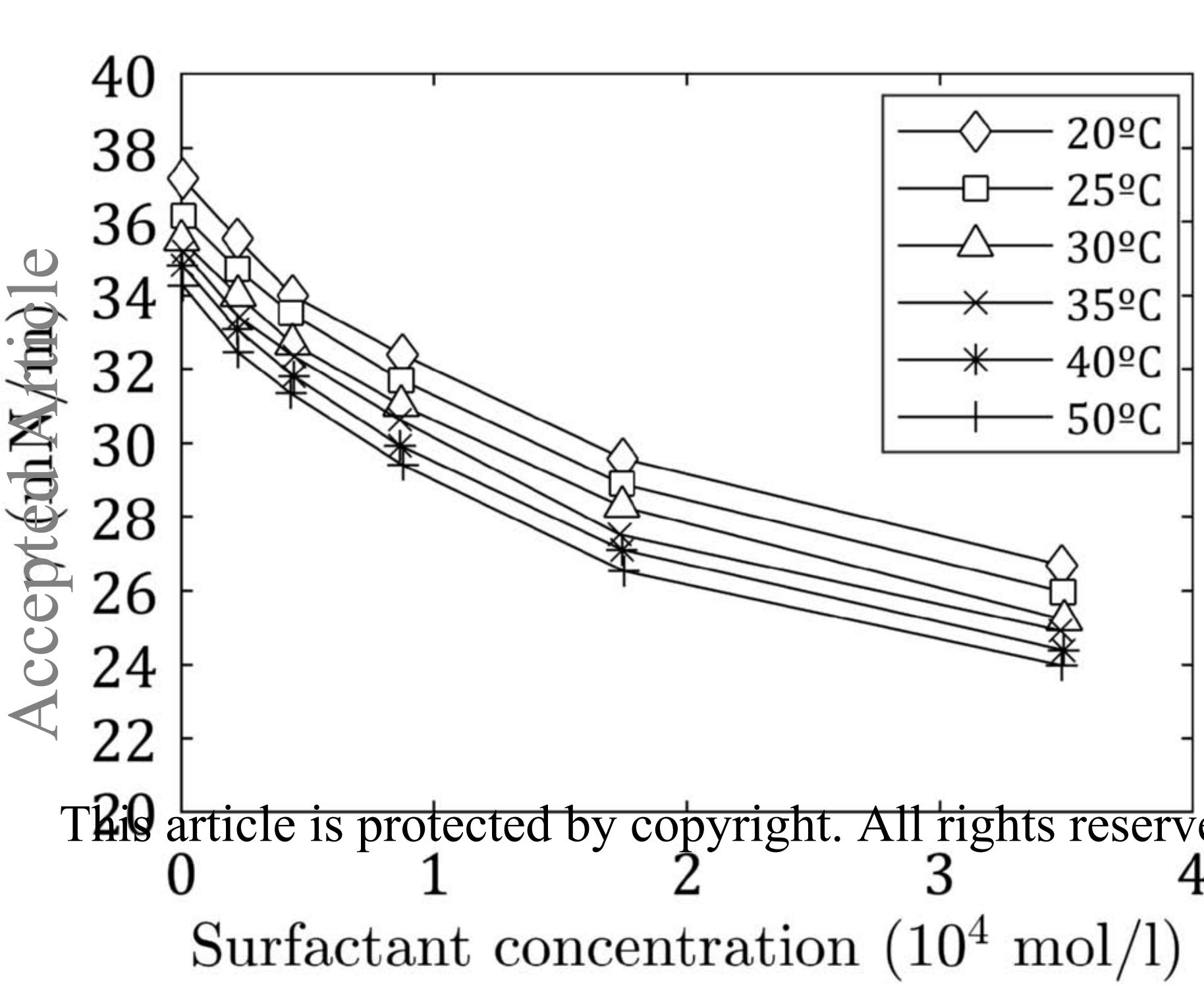

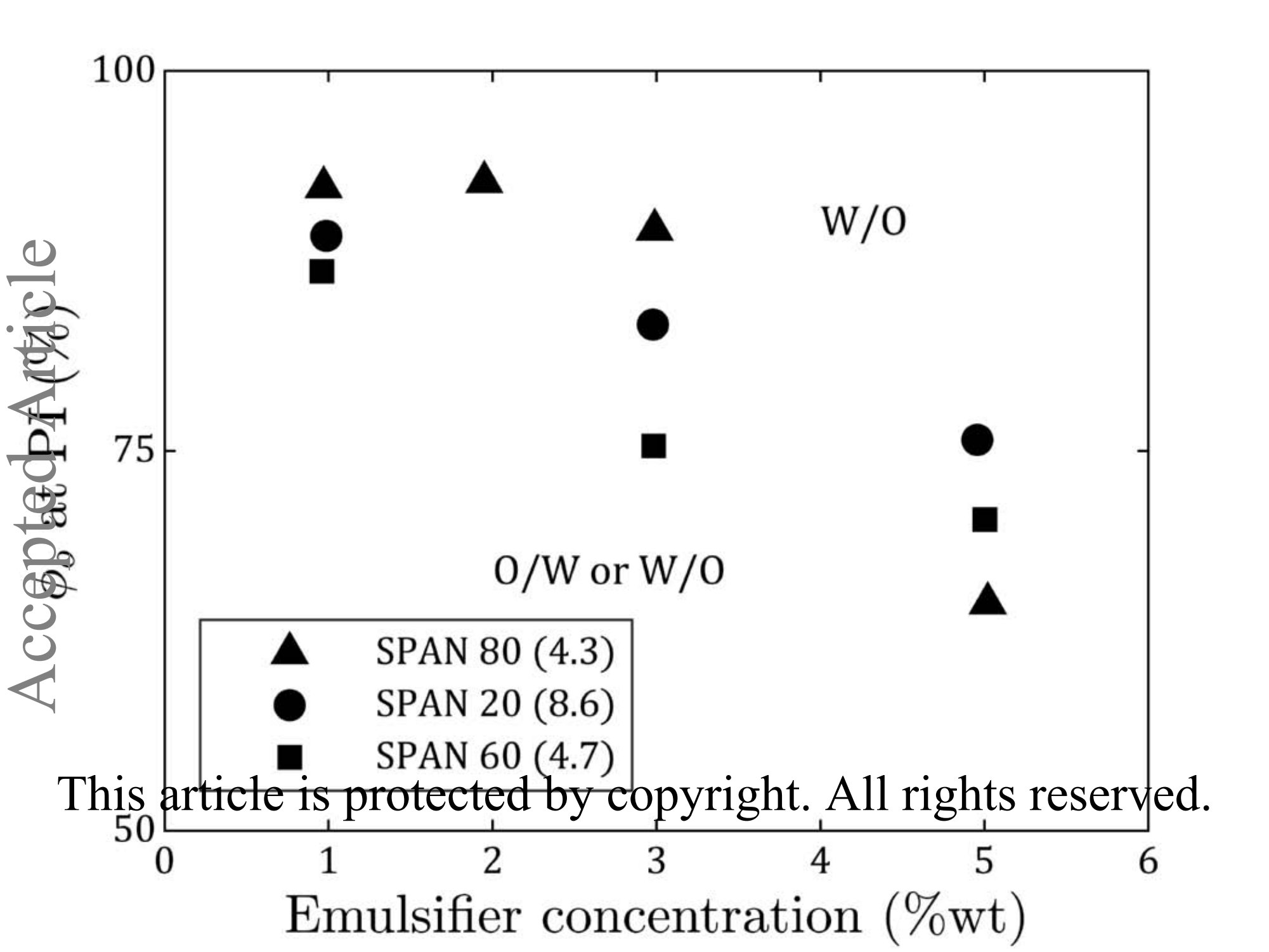

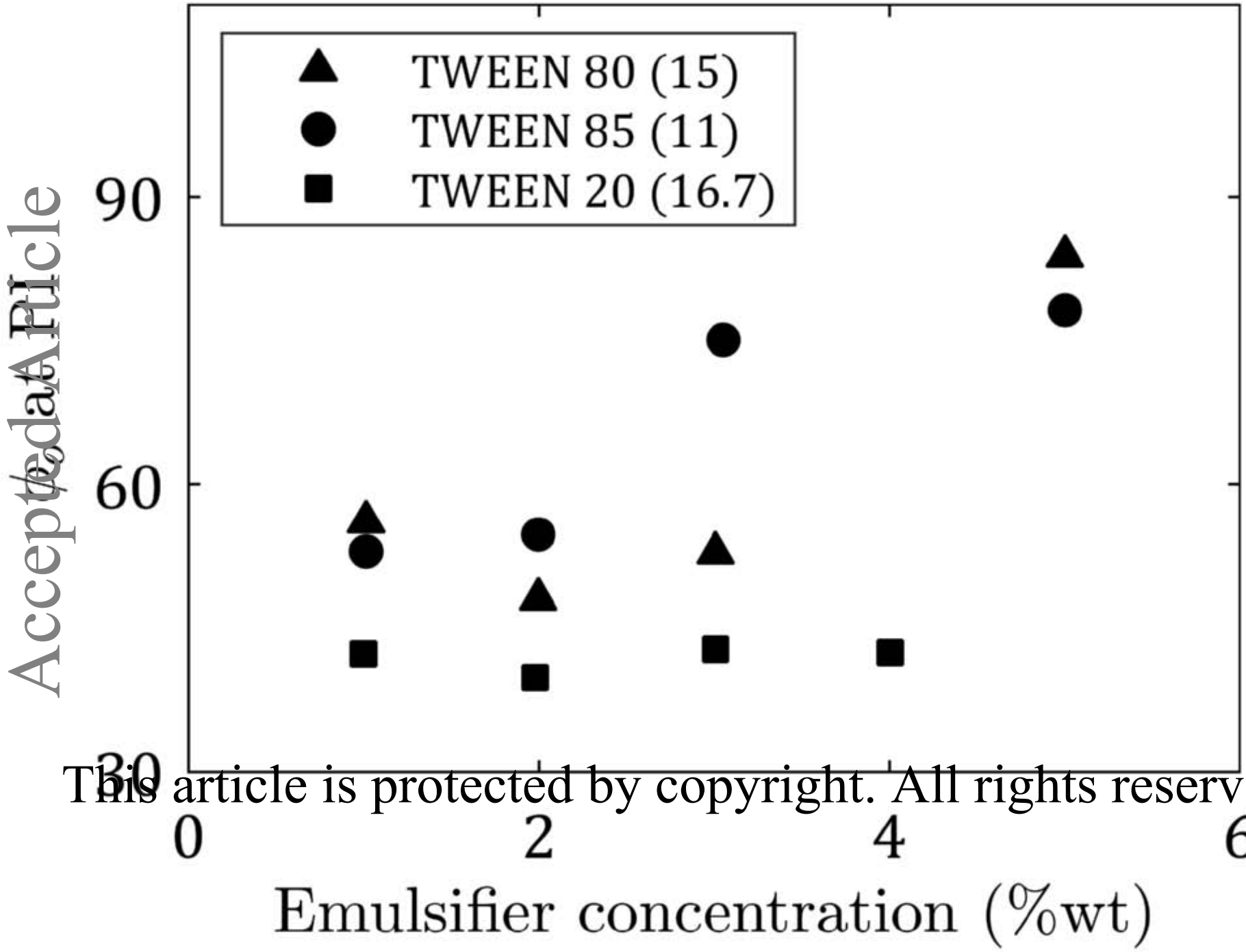

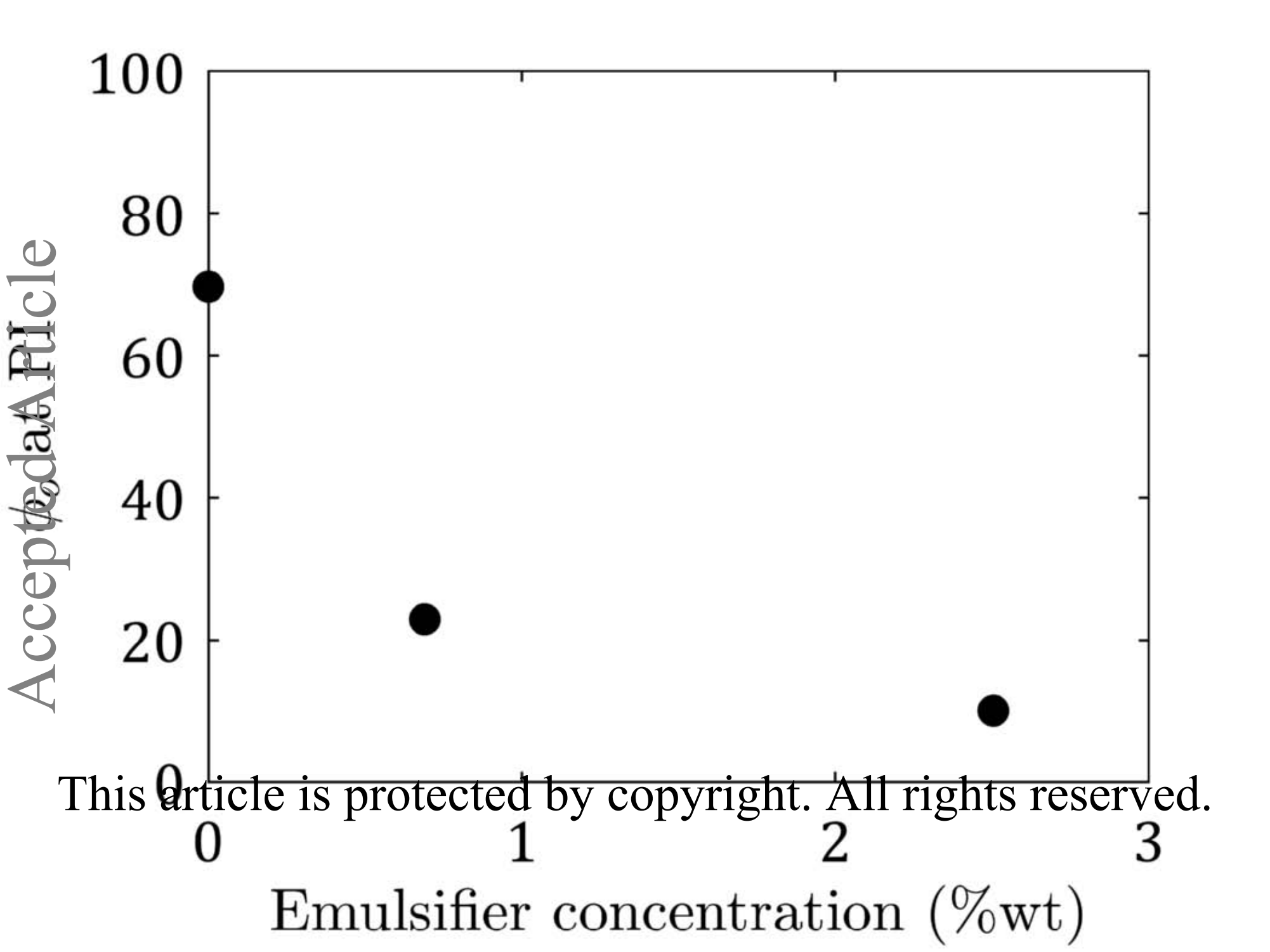

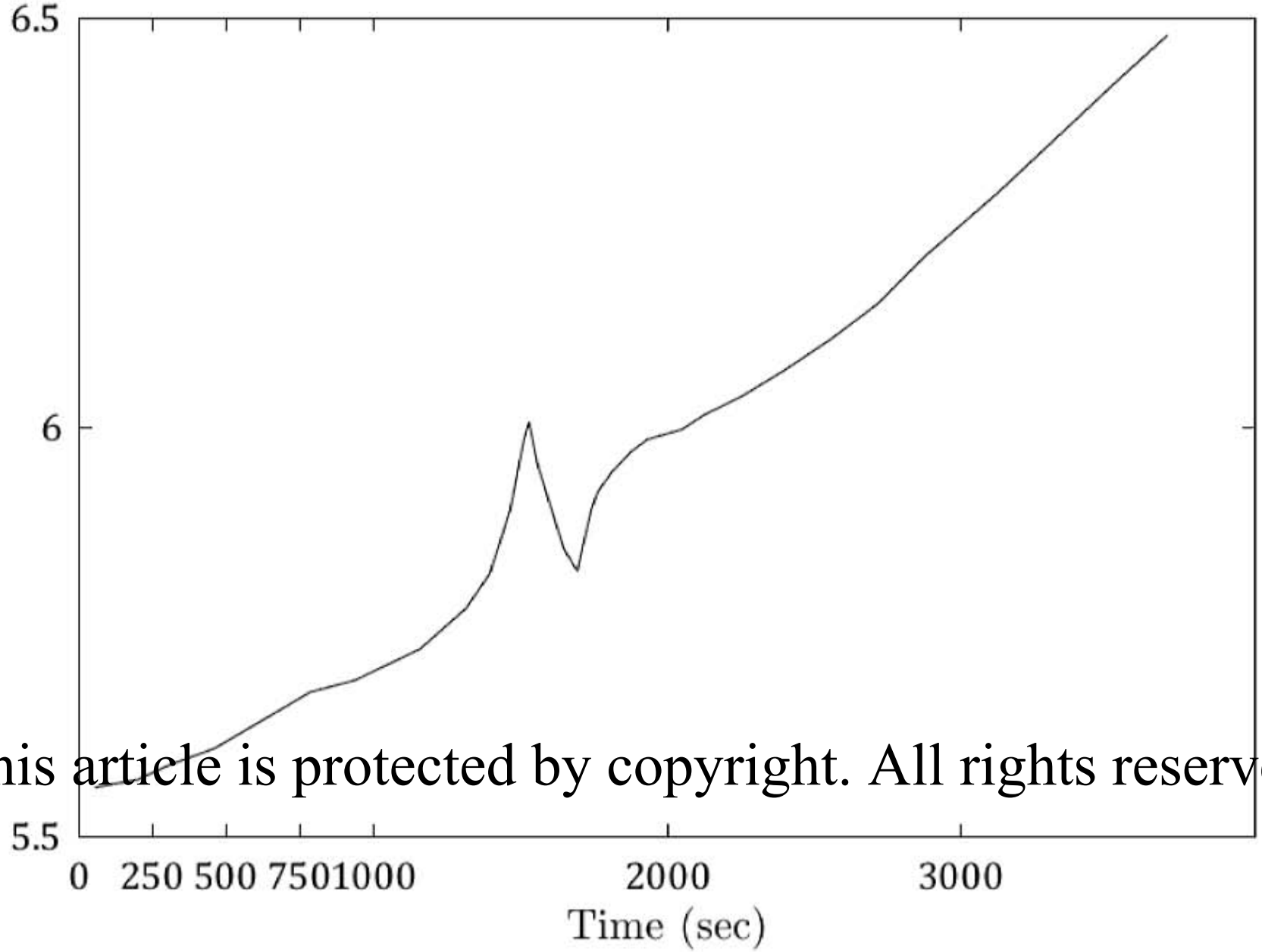

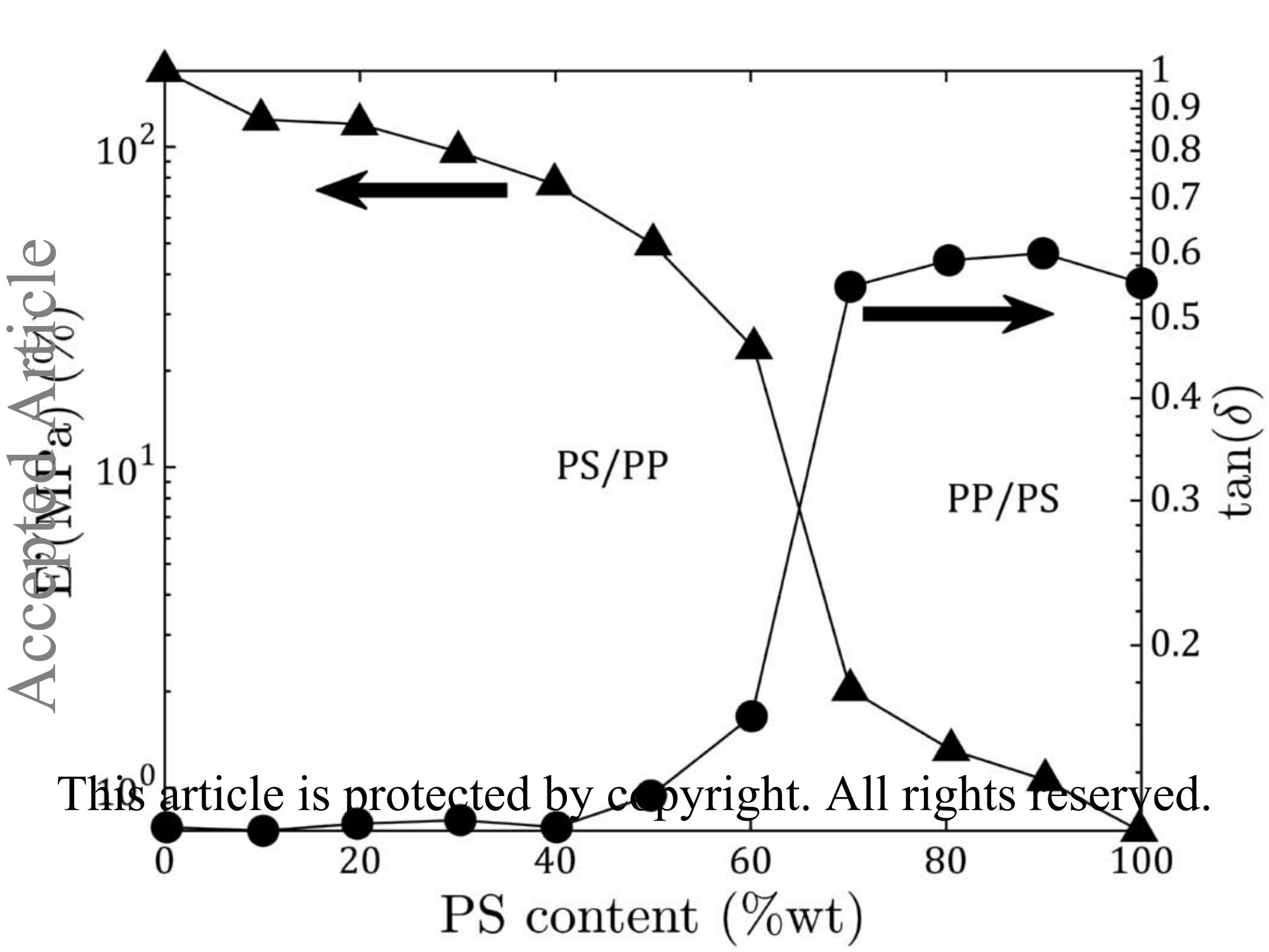

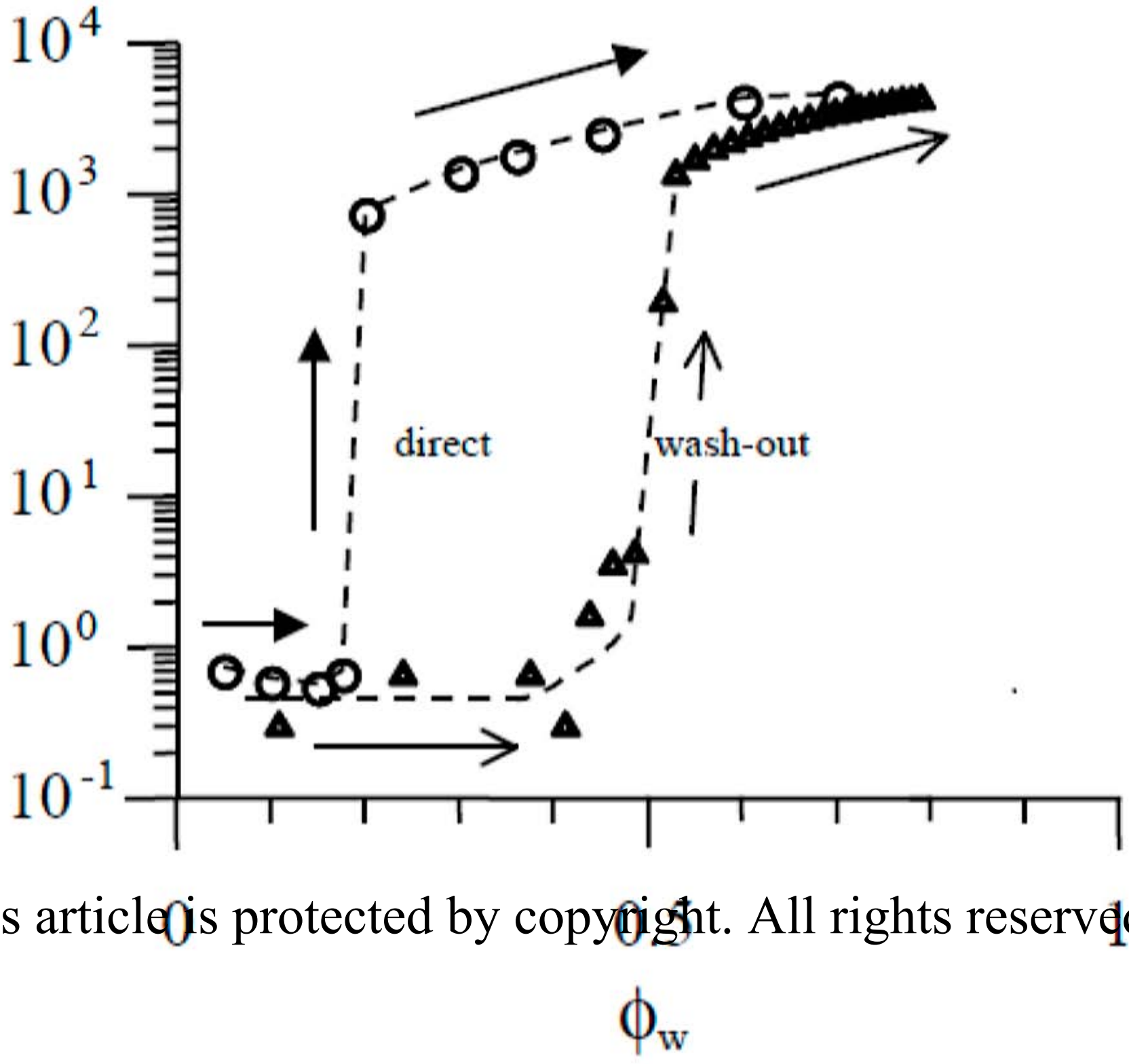

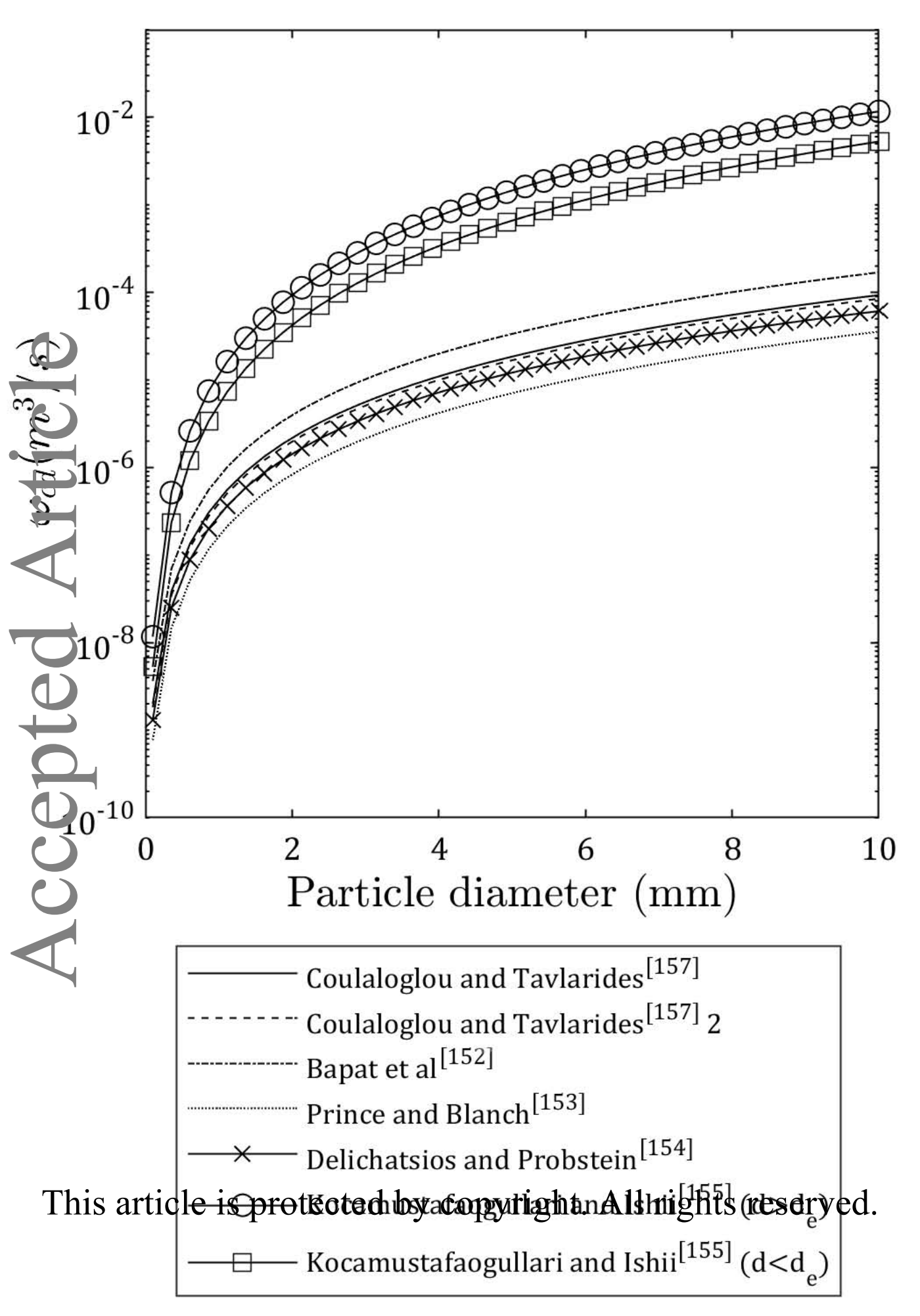

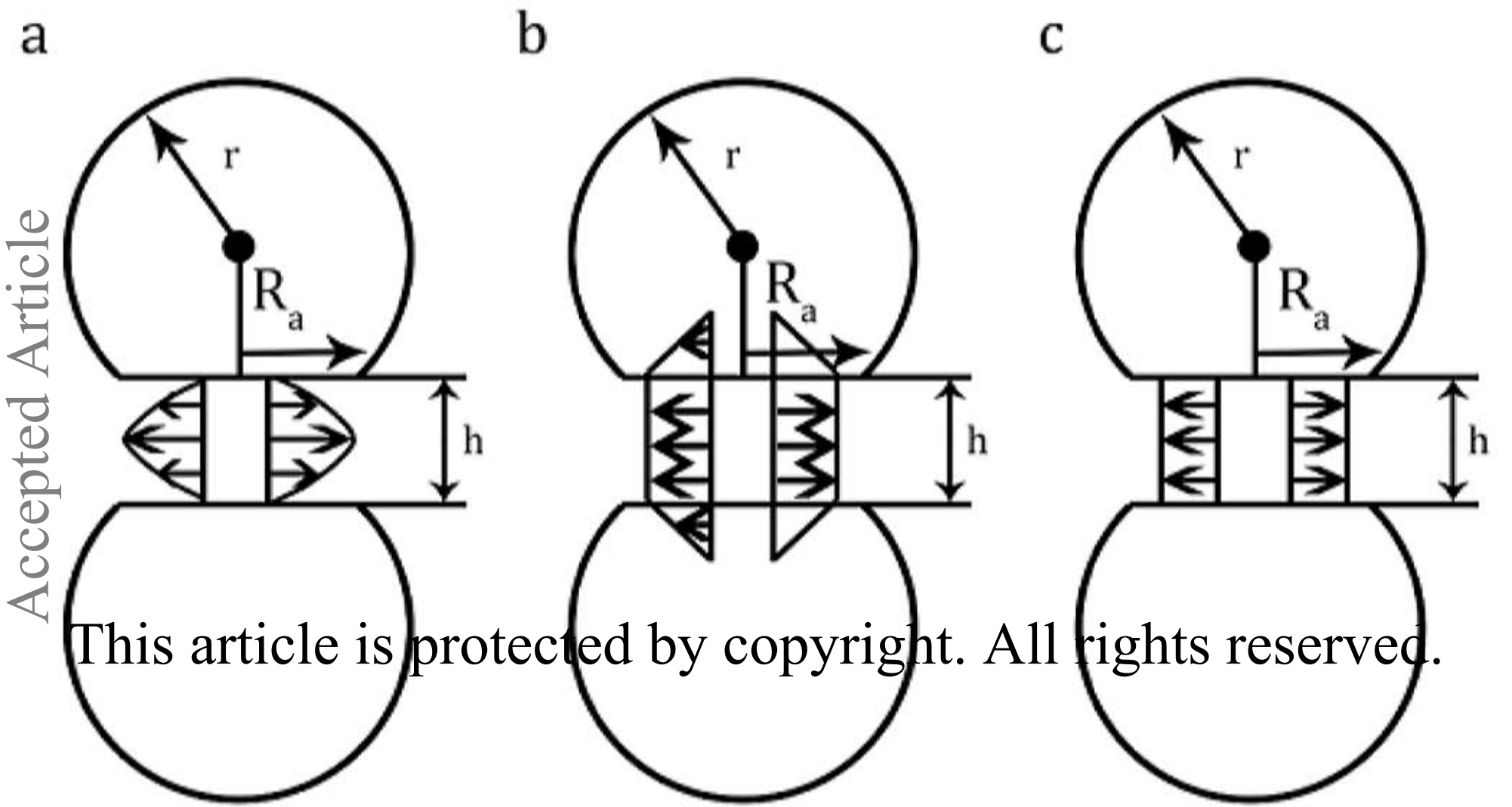

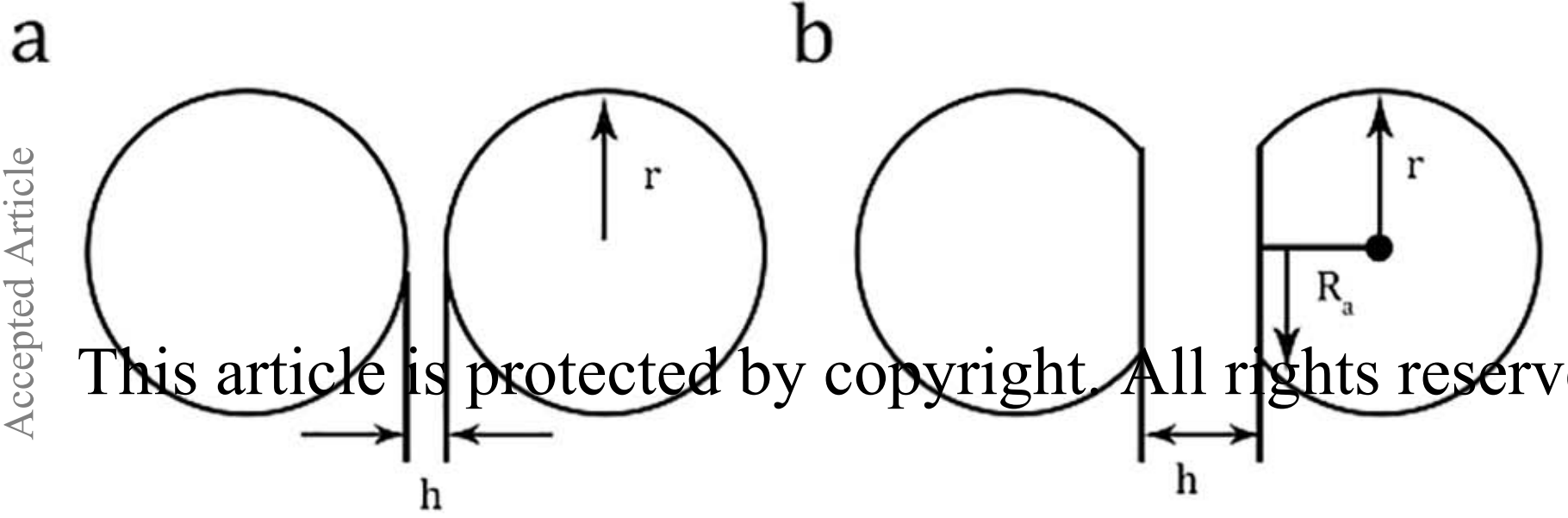

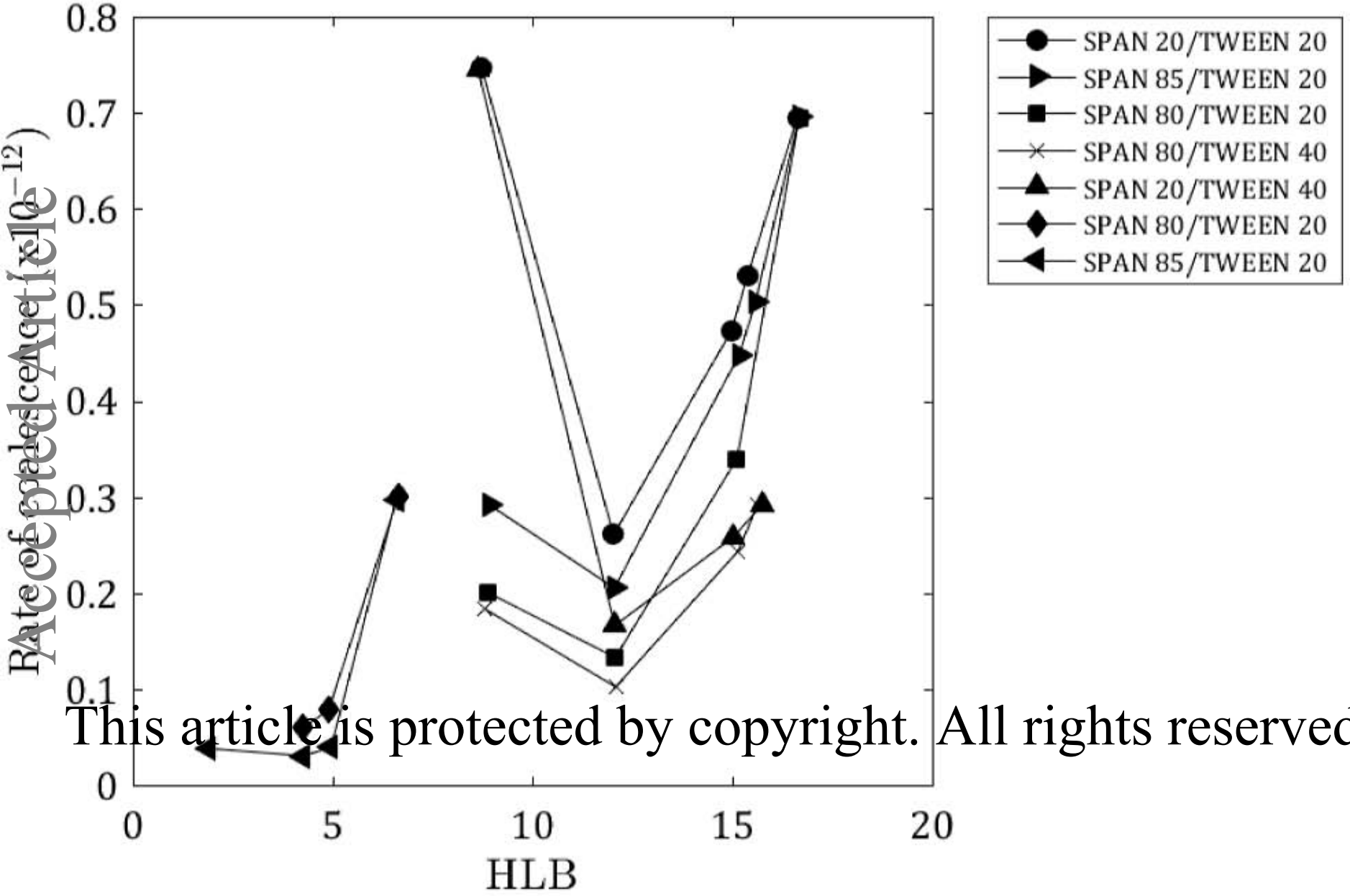

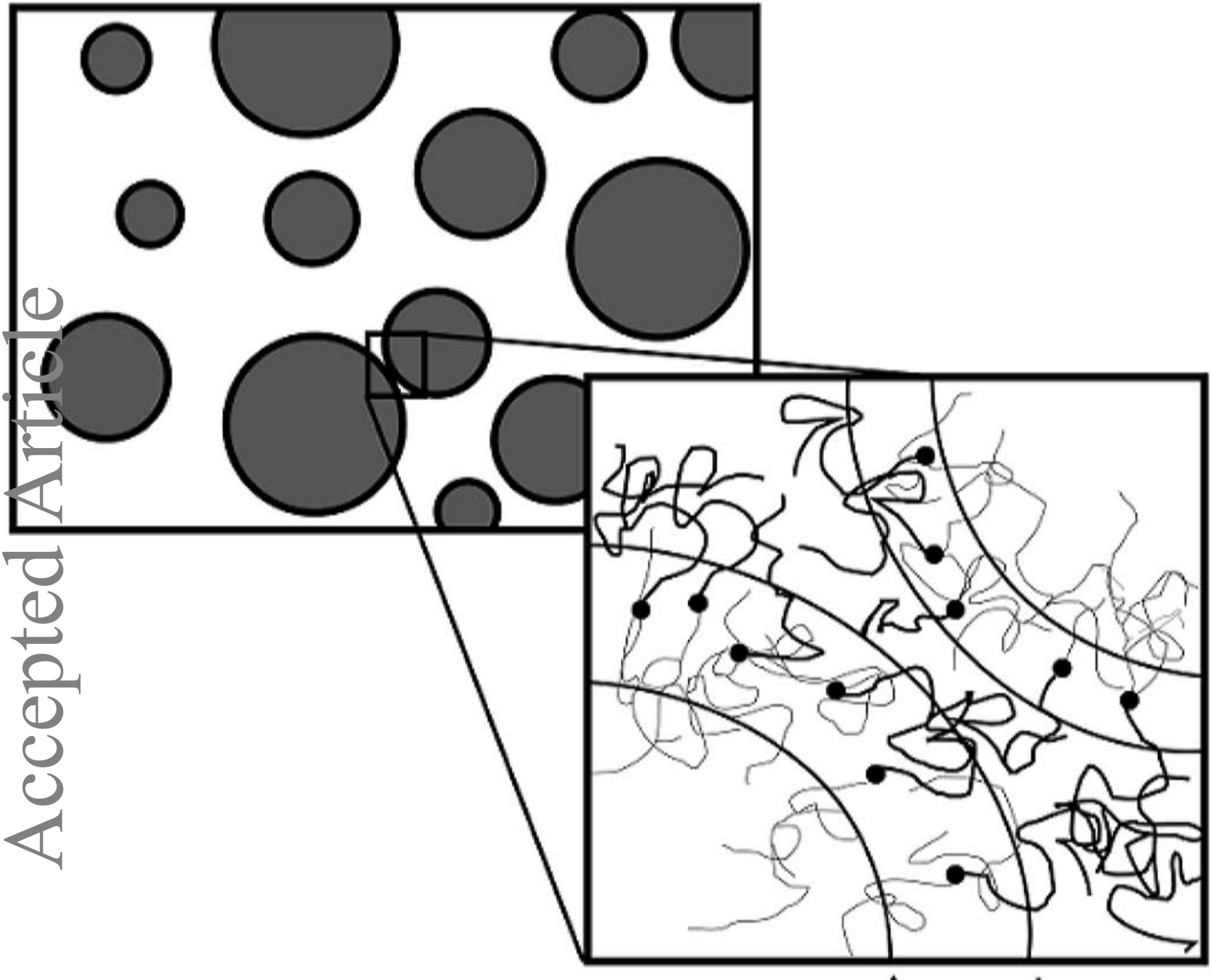

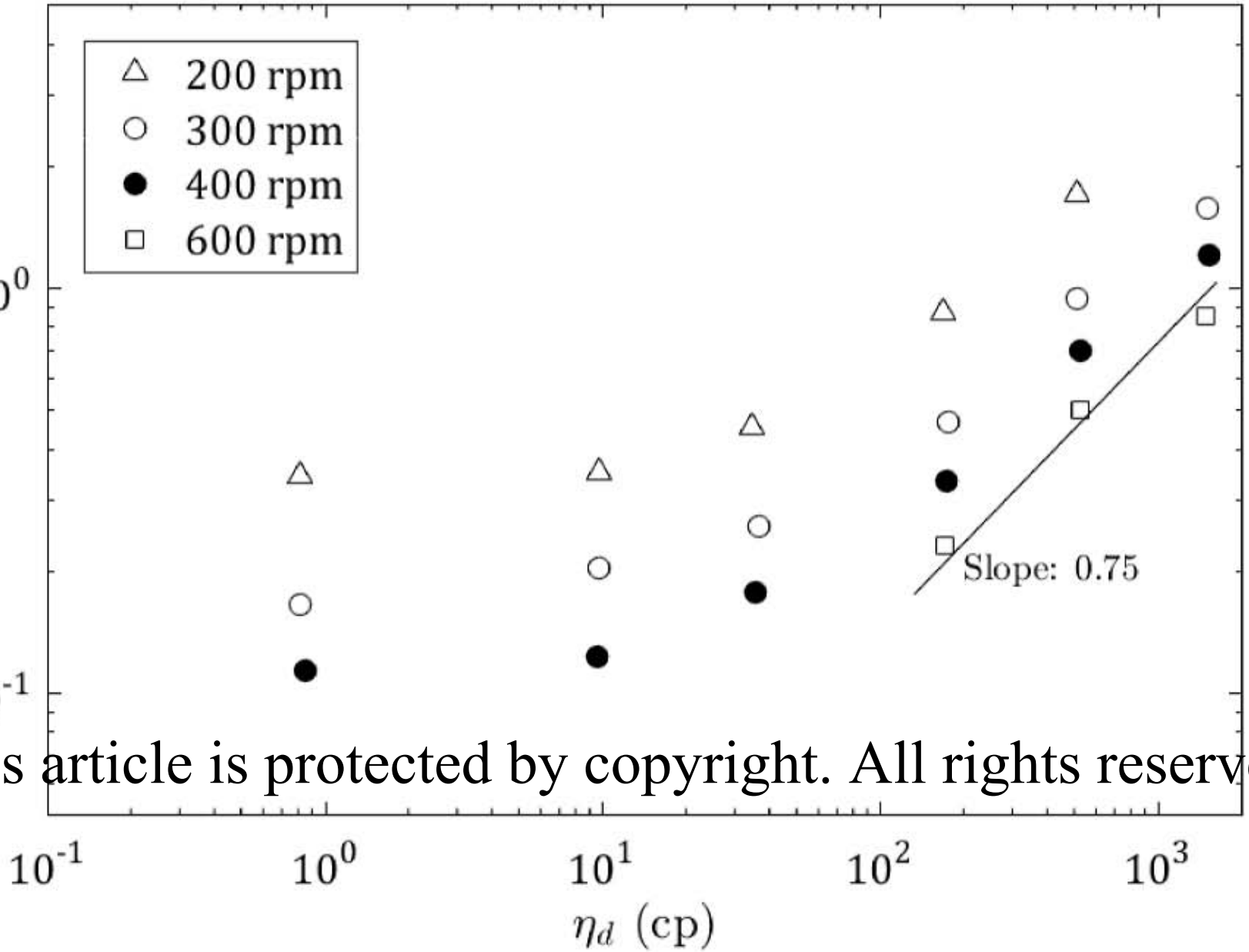

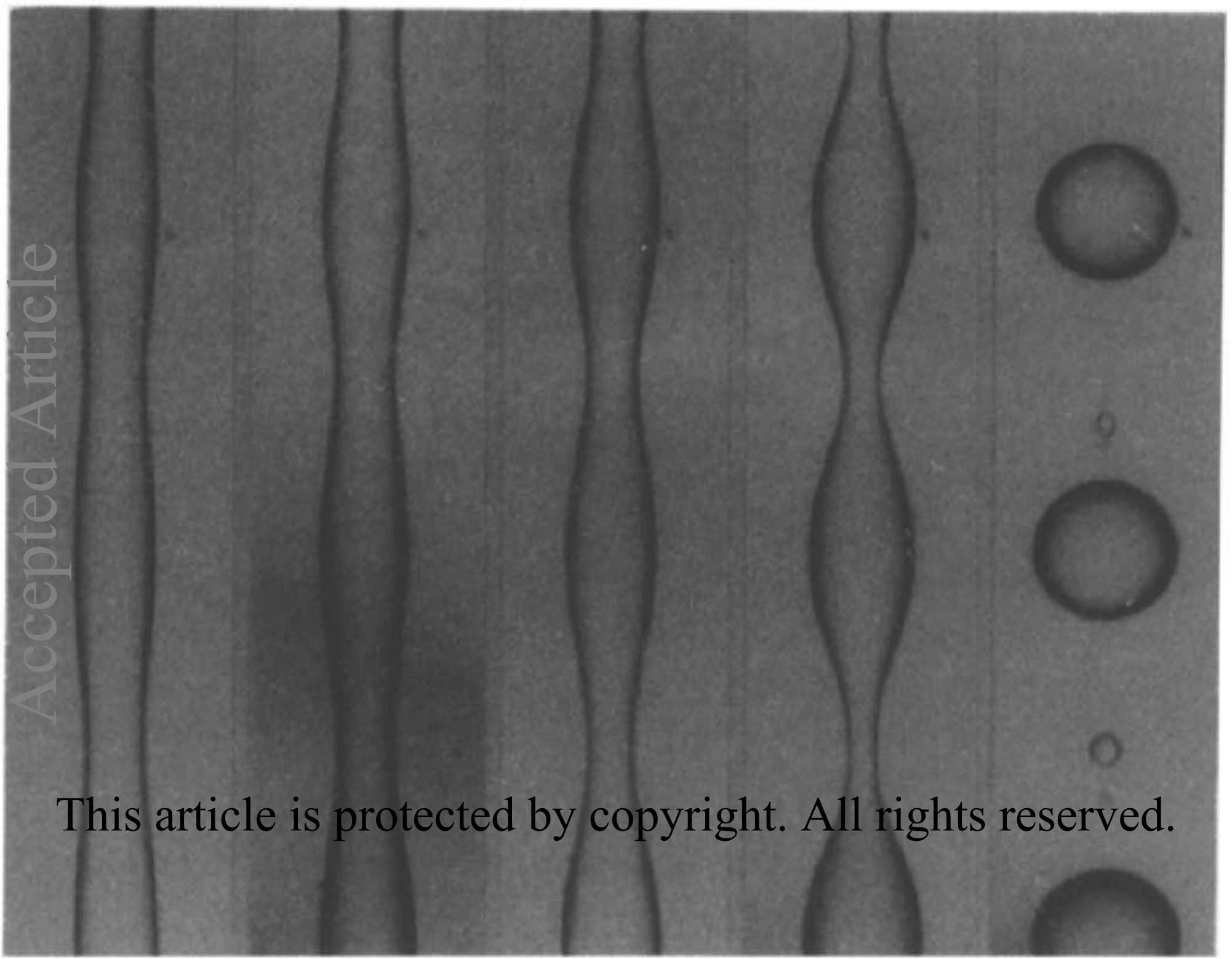

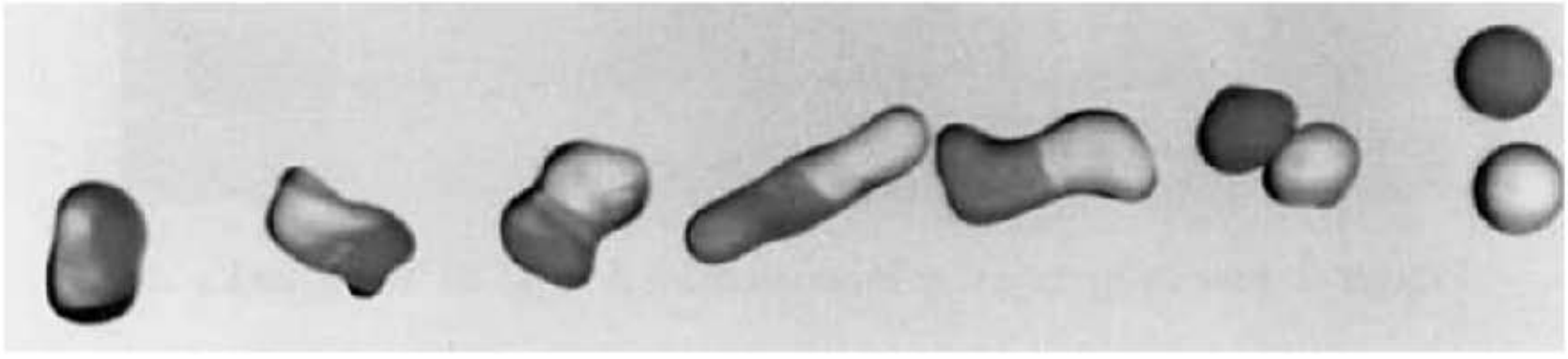

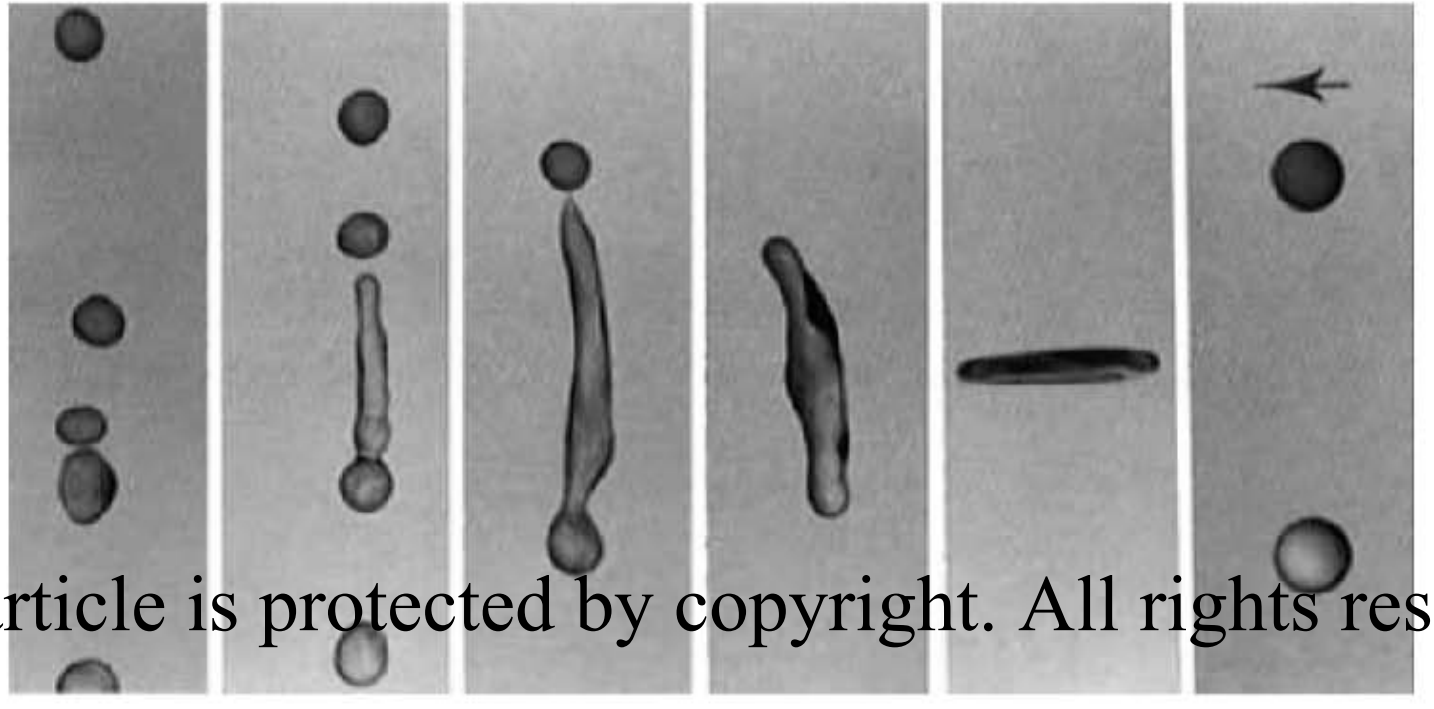

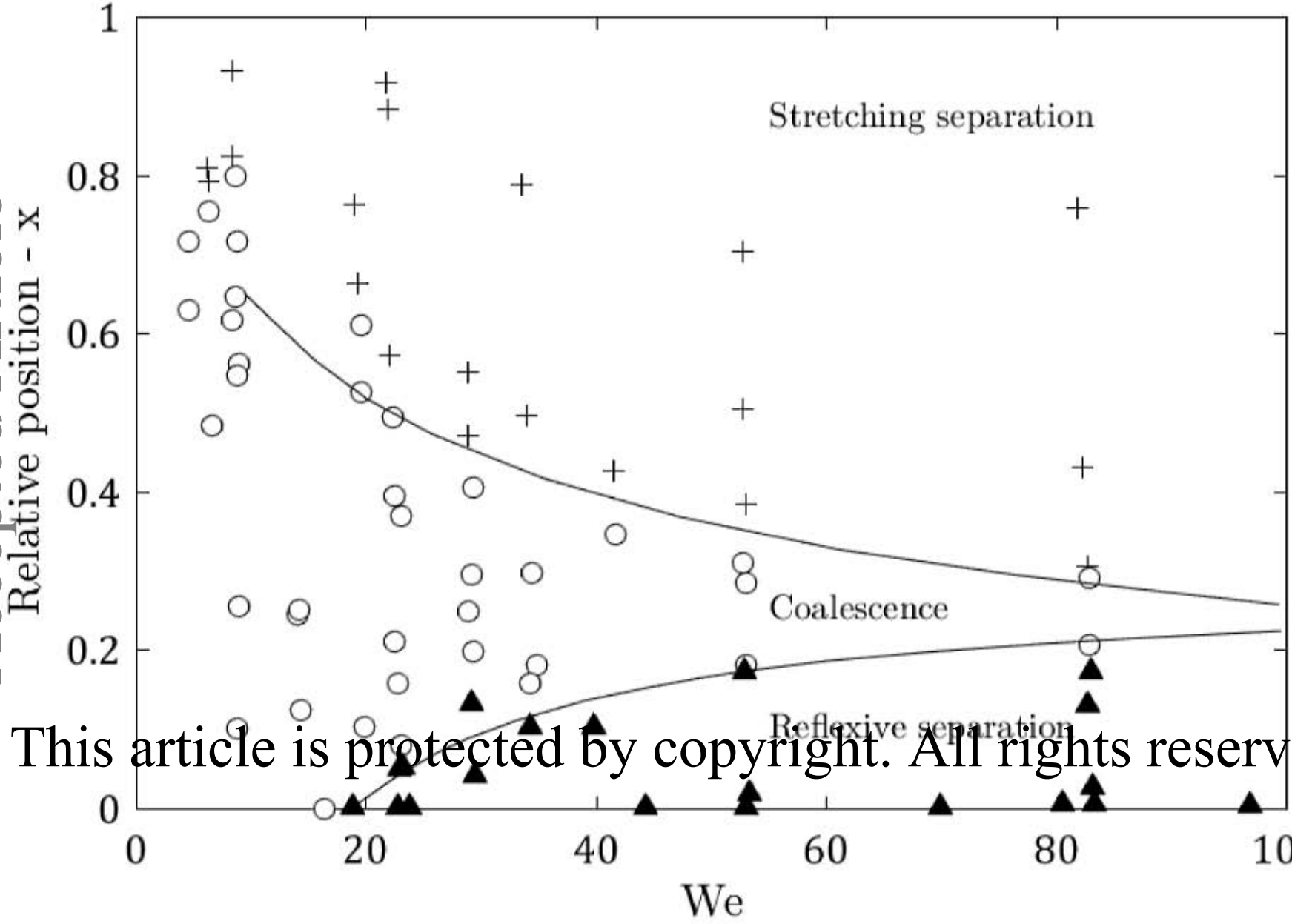

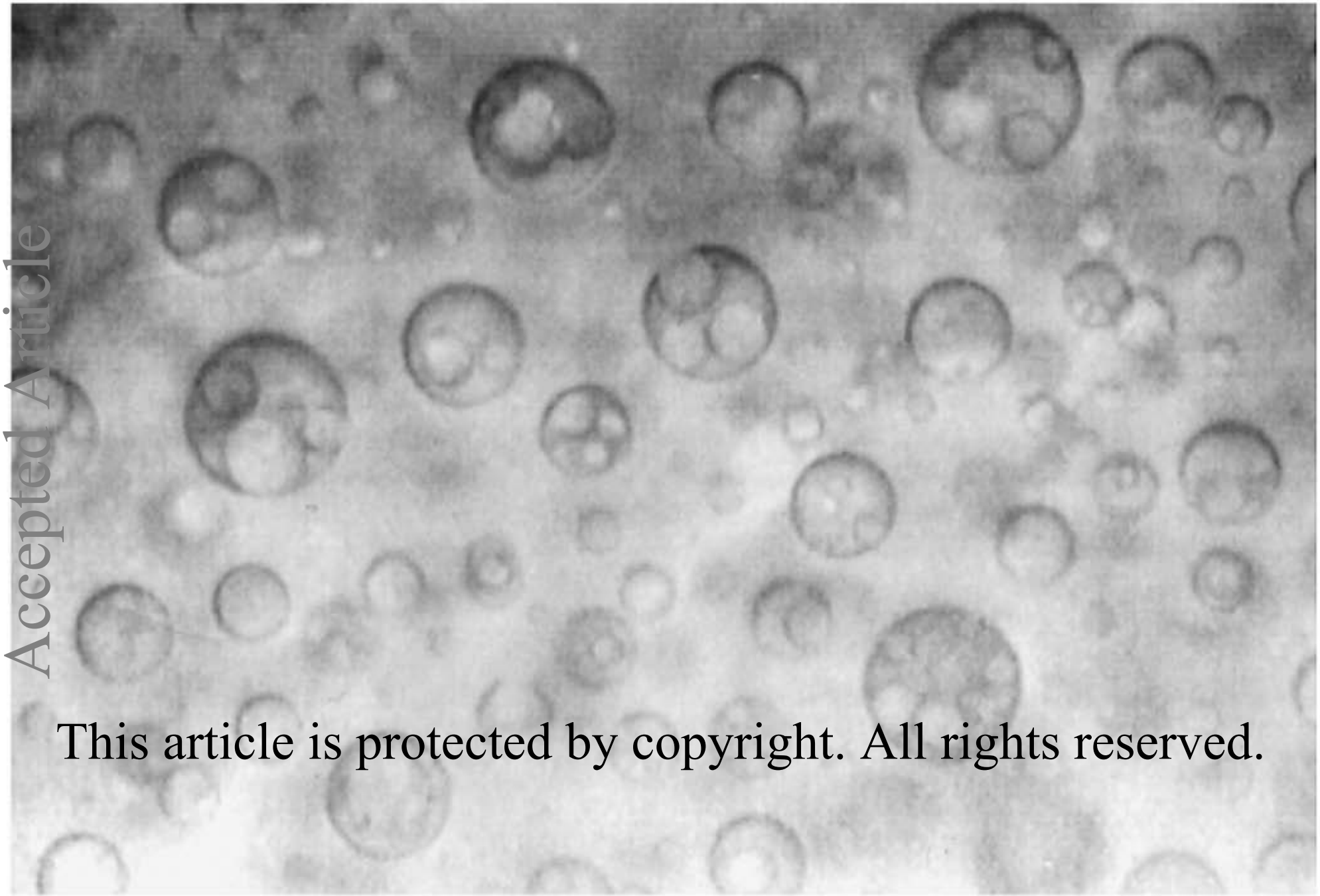

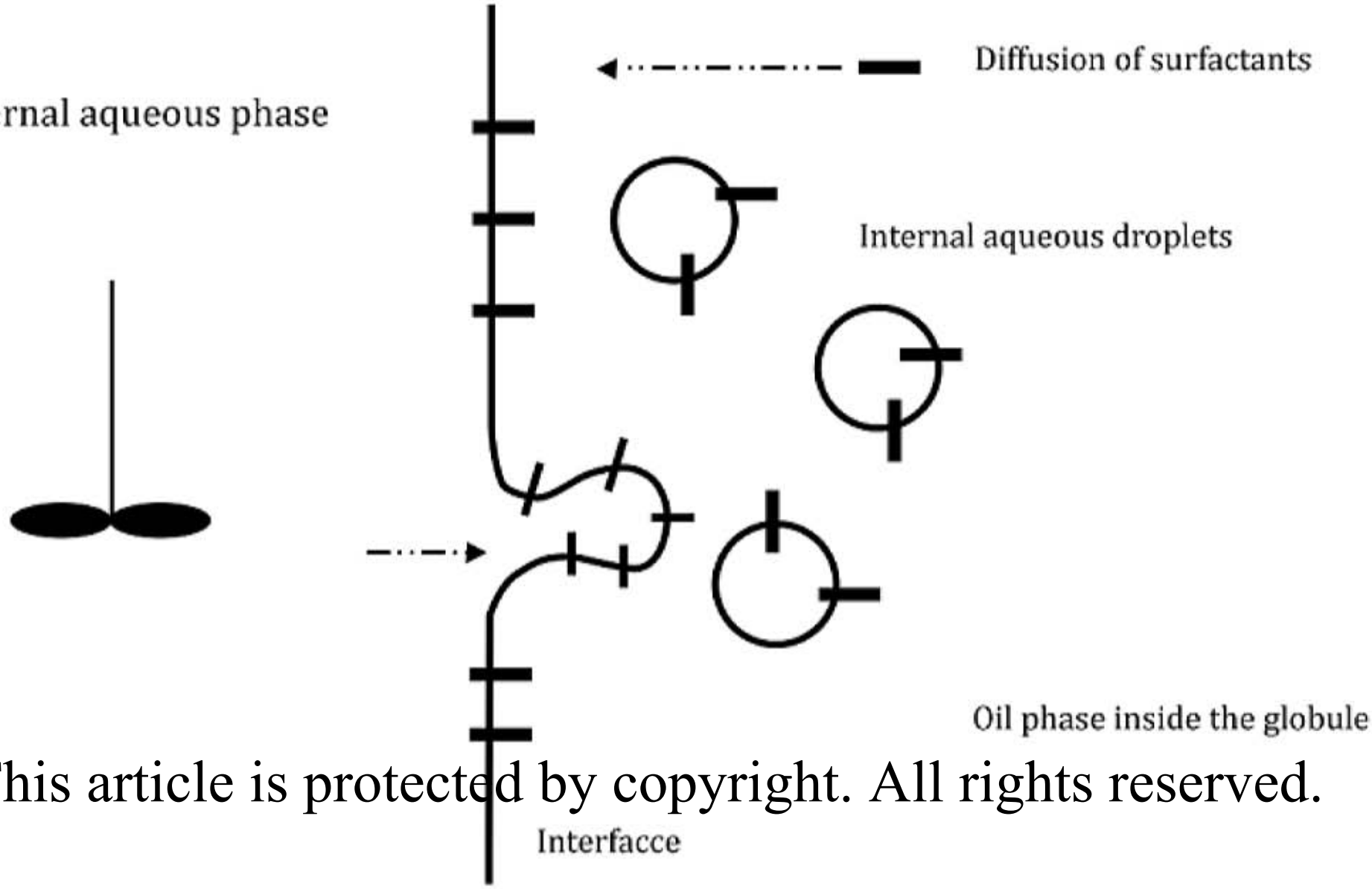

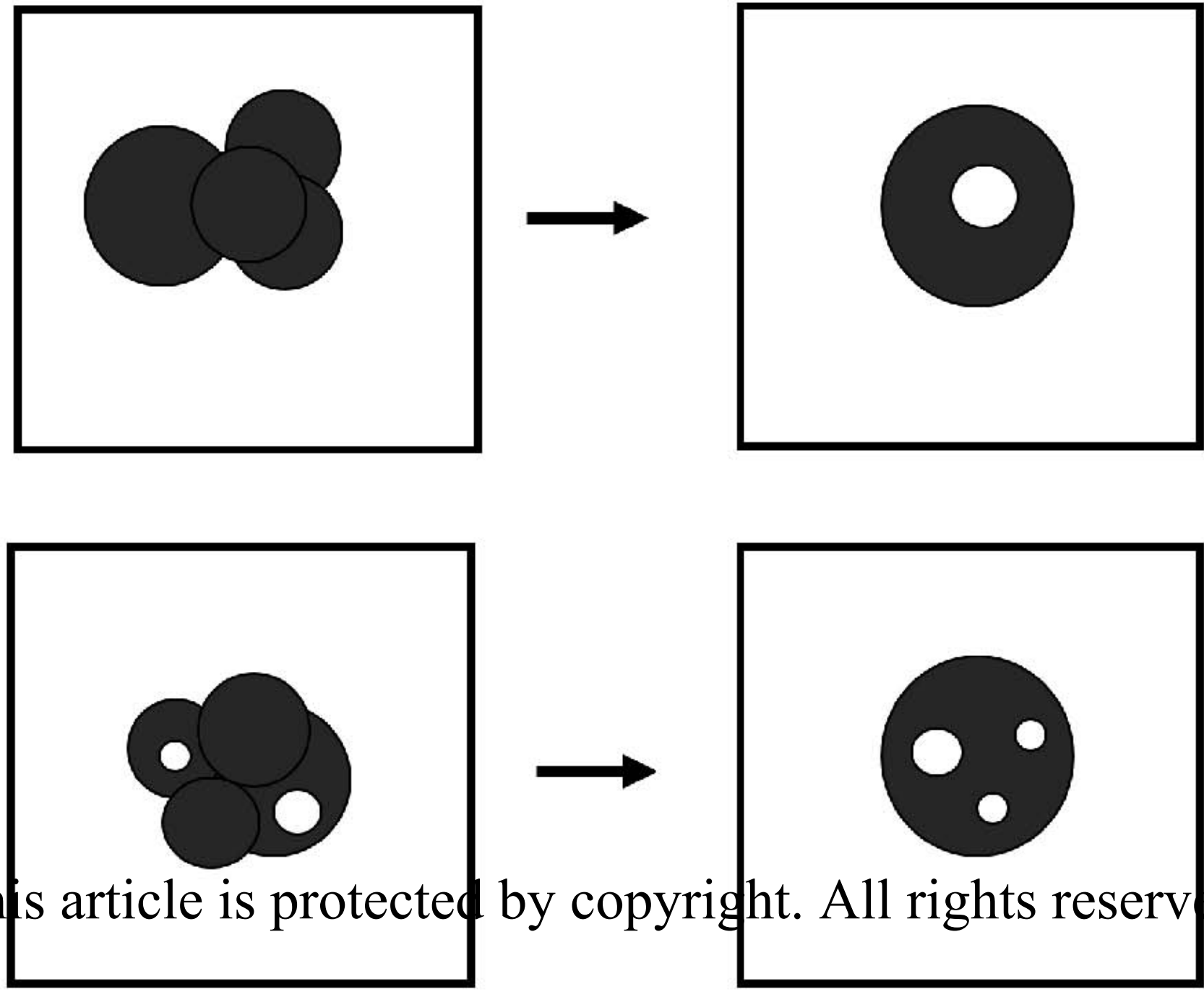

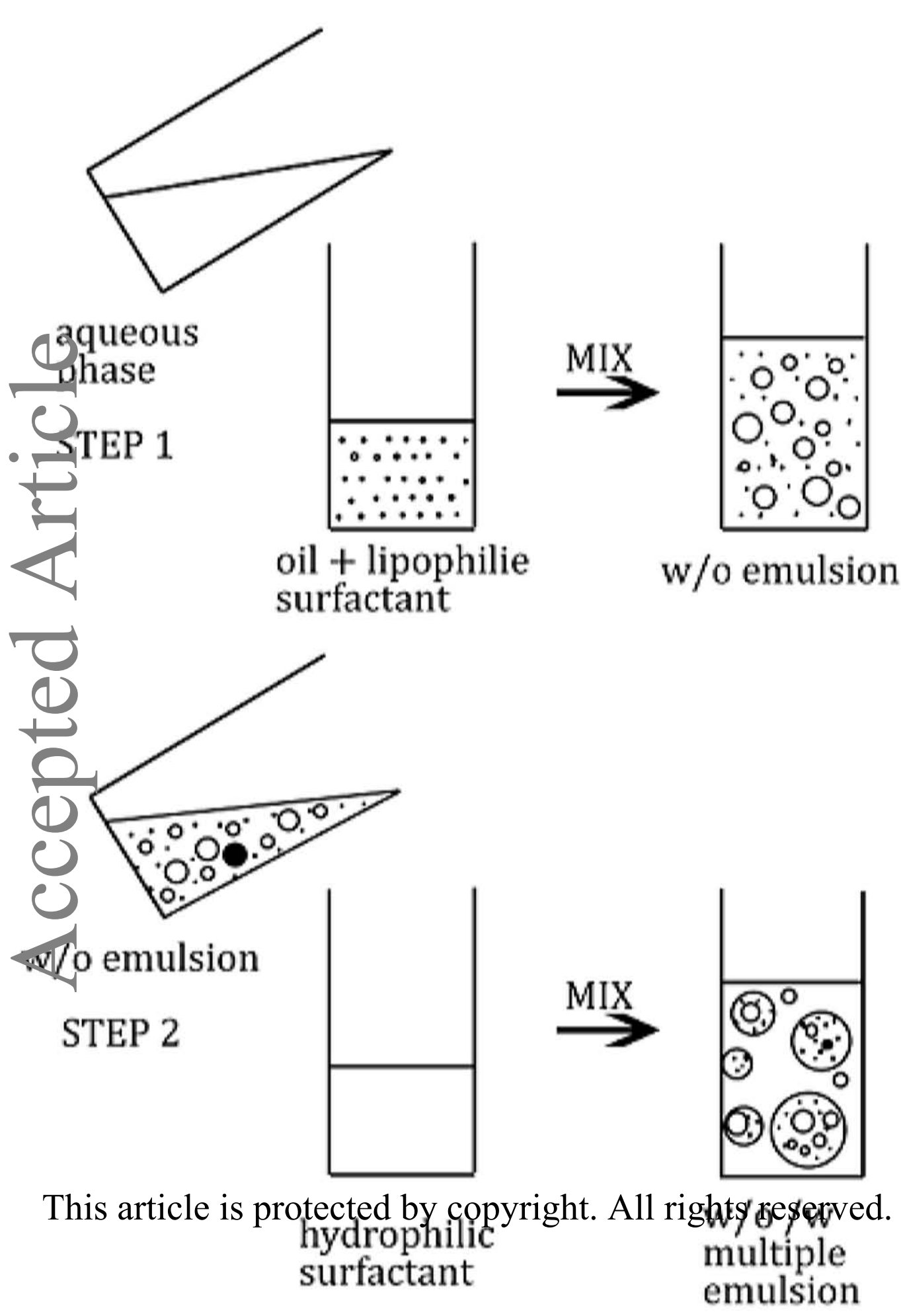

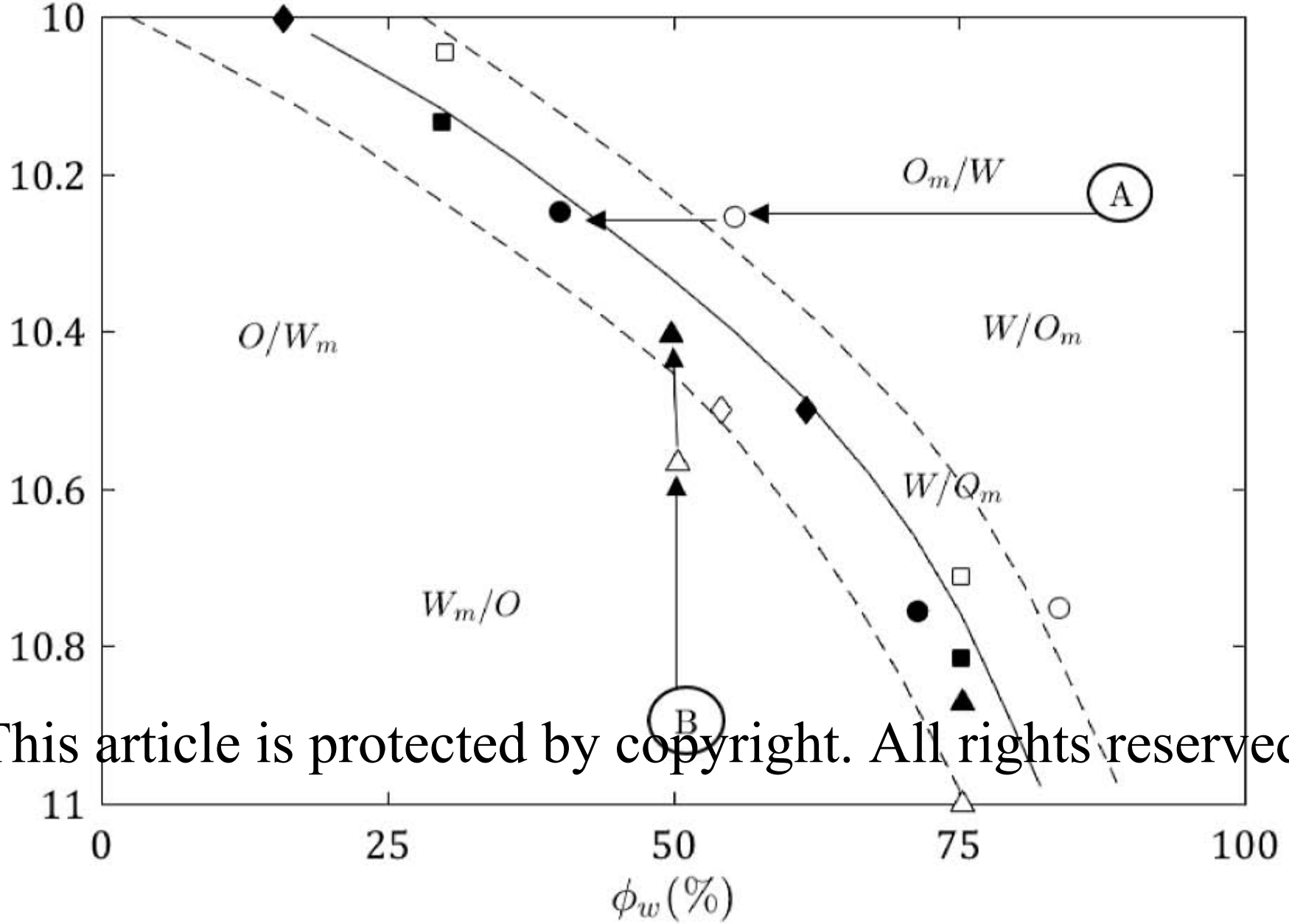

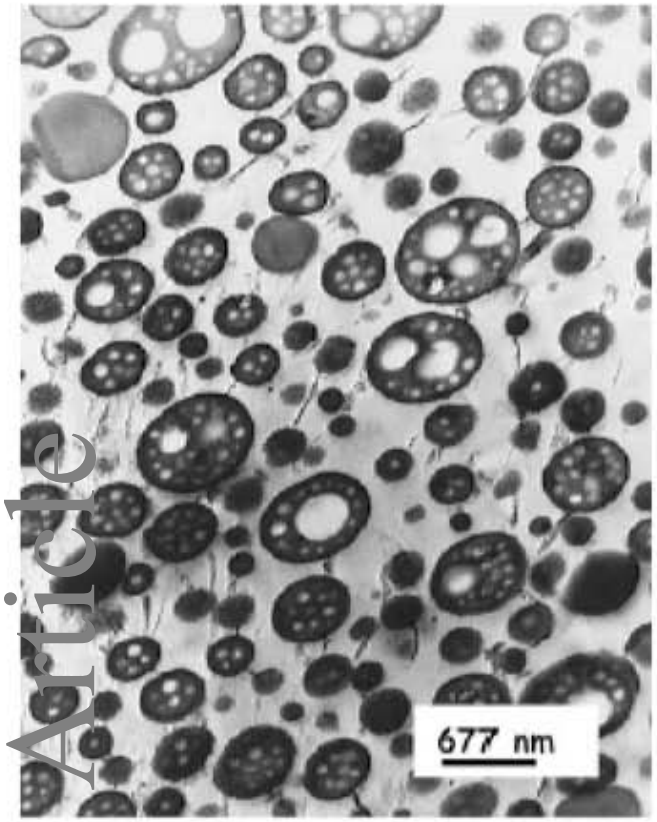

24.7 % solids

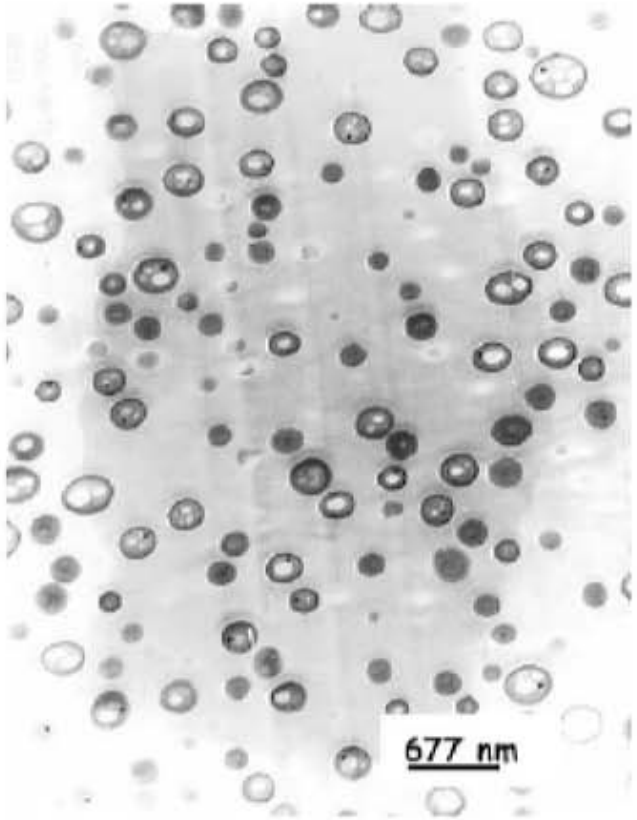

72.4 % solids

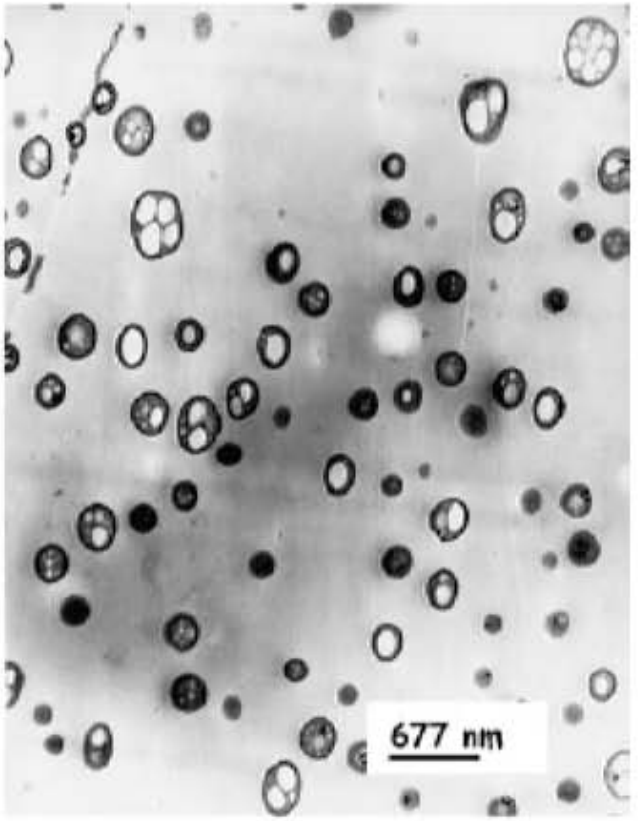

100 % solids

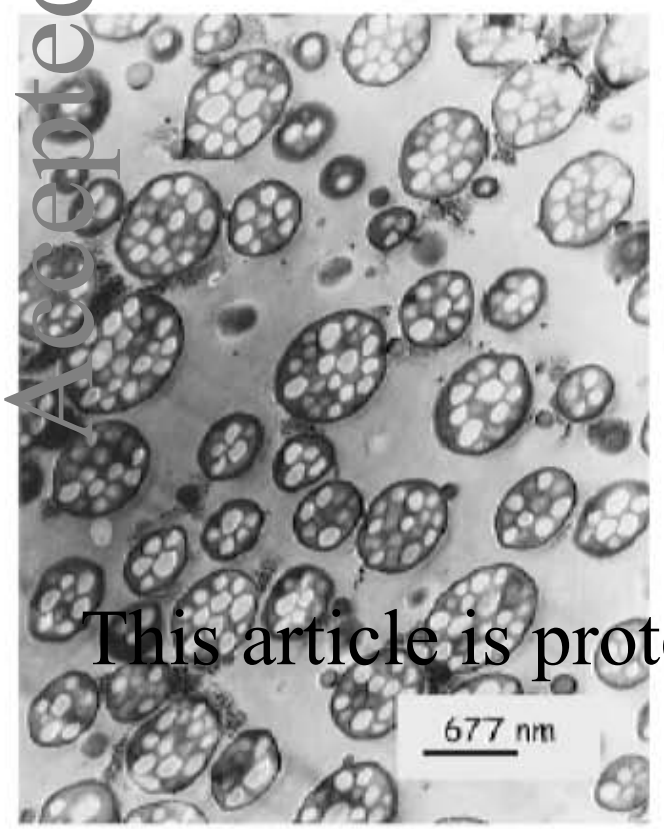

29.3 % solids